



Reshaping EV load profiles
at a workplace by adopting
smart charging strategies

Roeland in 't Veld

TU/e



Department of the Built Environment
Building Services Research Group

Reshaping EV load profiles at a workplace by adopting smart charging strategies

Master Thesis

Roeland in 't Veld

Supervisors:
Prof. ir. W (Wim) Zeiler
Ir. W. (Waqas) Khan
Dr. ir. S.S.W. (Shalika) Walker

Final version

Eindhoven, April 2023

Reshaping EV load profiles at a workplace by adopting smart charging strategies

Master Thesis

Author:

R.R.T. in 't Veld

1236072

General information:

University: Eindhoven University of Technology

Department: Built Environment

Master program: Architecture, Building and Planning

Track: Building Physics and Services

Course information:

Course code: 7S45M0

Study Load: 45 EC

Date of graduation: 13-04-2023

Graduation supervision committee:

Chair of Committee:

Prof. ir. W (Wim) Zeiler

Second Committee Member:

Dr. ir. P. (Pieter-Jan) Hoes

Third Committee Member:

Ir. W. (Waqas) Khan

Fourth Committee Member:

Ir. J. (Joep) van der Velden

This thesis is open to the public and has been carried out in accordance with the rules of the TU/e Code of Scientific Integrity

Signature Chairperson

Abstract

Electric vehicles (EVs) are becoming increasingly popular to reduce greenhouse gas emissions from the transportation sector. However, the increasing number of EVs also leads to an ever-growing peak power load on the electricity grid, which can cause stability issues and increase costs necessary for grid expansion. To address this problem, smart charging solutions have been proposed, which aim to distribute EV charging in a way that reduces the peak load on the grid. This research presents a versatile smart charging controller design for small EV fleets based on optimization modelling, which successfully redistributes EV loads to allow for peak-shaving and valley-filling.

To achieve this goal, an online form to acquire EV charge related data is utilized, which can be used as an input for an optimization model along with building load and PV power data. By using this online form, user-specific information is collected, and avoids the necessity of State of Charge (SOC) values for redistributing EV loads more efficiently. The smart charging method used in this research, optimization modelling, has proven successful for planning and controlling EV charging during a workday.

The optimization model is tested using different variations (linear and bilinear models with different weight factors and sampling intervals), and the performance has been found to be better with linear optimization models in terms of computational time. Furthermore, adding a penalty function to the cost function greatly improves the control performance by alternating charging between the cars at higher current values, resulting in higher charging efficiency.

The simulation study showed that the peak power reduction is significant on the main simulation days, and the model allows for peak-shaving and valley-filling. The optimization model is versatile, as it can be adapted by changing the parameters, such as the total charging efficiency, the maximum voltage, power, and current, for different types of EV chargers.

In conclusion, this research provides a solution to the ever-growing peak power loads due to uncontrolled EV charging by offering a smart charging controller design. The design successfully redistributes EV loads to allow for peak-shaving and valley-filling.

Preface

I hereby present my graduation project at the TU/e, which involves the development of smart charging at the office of Kropman Breda. The graduation project is part of work package 2 (WP2) of the Brains for Building's Energy Systems (B4B) multi-stakeholder project. WP2 addresses "the development of smart control models to increase energy flexibility (heat, cold and electricity) within buildings" (Brains 4 Buildings, n.d.). Although electrical vehicle (EV) charging is not within buildings, it can be part of the building load, and the smart control of EV charging can help increase the electricity flexibility of the aggregated building load. EV smart charging is a relatively new topic. This challenged me to look at the problem with a new perspective, applying my existing knowledge and broadening it by researching this new field.

I would like to express my gratitude to Prof. W. (Wim) Zeiler of the TU/e and Ir. J.A.J. (Joep) van der Velden from Kropman for giving me the opportunity to do my graduation project at the living lab of Kropman Breda. Working on a case study with real building data allowed me to apply my theoretical knowledge in practice. Furthermore, I would like to thank ir. W. (Waqas) Khan for supervising my graduation project, assisting me in defining the scope of my research, and offering constant feedback and suggestions. I would like to express my gratitude to Dr. Ir. S.S.W. (Shalika) Walker, for her guidance and feedback throughout my graduation project. Her introductions to other students and employees of Kropman not only facilitated my research, but also made me feel welcome and supported throughout the project. Furthermore, I would like to thank Jan-Willem Dubbeldam and Dennis Fontein for setting up necessary data connections and developing the online form.

I would also like to thank Ir. R. (Redouane) Edeanne and Dr. Ir. J.H.A. (Jobert) Ludlage of Avans University of Applied Physics for allowing me the opportunity to perform my research at the Smart Energy Lab. Special thanks to Redouane for assisting me with performing my emulations, next to his busy schedule.

Furthermore, I would like to thank Koen Reinders for helping at the start of my project, including giving a clear introduction to MPC. I would like to thank Ward Somers and Bram Hermans for taking the time to give suggestions and discuss solutions for my problems during the project.

Roeland in 't Veld

Eindhoven, April 2023

Contents

Abstract	v
Preface	vii
Contents.....	ix
List of Figures	x
List of Tables.....	xii
List of Abbreviations.....	xiv
1. Introduction.....	1
2. Literature study.....	3
3. Case study	10
3.1. Overview	10
3.2. Smart charging controller	11
4. Methods	14
4.1. Data pre-processing	14
4.2. Data analysis.....	15
4.3. KPIs	16
4.4. Algebraic model	17
4.5. Optimization model.....	21
4.6. Simulation scenarios	23
5. Results.....	24
5.1. Data analysis.....	24
5.2. Optimization models	26
5.3. Simulation Scenario's.....	31
5.4. PHIL-testbed.....	39
6. Discussion	40
7. Conclusion	42
References	44
Appendices	47

List of Figures

Figure 3.1: Overview of the building systems and data collection	10
Figure 3.2: The EV charging form in the Welkom Kropman application (in Dutch).....	11
Figure 3.3: The smart charging process	12
Figure 3.4: Illustration of the prediction horizon in MPC (Miyazaki et al., 2019)	12
Figure 3.5: Visualization of the batch-type prediction horizon	13
Figure 4.1 Schematic overview of the micro grid of the office building	15
Figure 4.2 Simplified microgrid of the Office at Breda.....	17
Figure 4.3: The PHIL testbed at Avans SEND Lab.....	21
Figure 4.4: Diagram showing the PHIL simulation process in Simulink	22
Figure 4.5: The roof of the office with an area of approximately 70m ² in red	23
Figure 5.1: Valley-filling and peak-shaving potential in March	24
Figure 5.2: Valley-filling and peak-shaving potential in June	25
Figure 5.3: Valley-filling and peak-shaving potential in December	25
Figure 5.4: EV data on March 21st for bi-linear_15 min optimization model (in the second top graph the red line indicates the minimum of 6A)	28
Figure 5.5: EV data on March 21st for bilinear_penalty_15min optimization model.....	29
Figure 5.6: Historic data vs optimization data on March 21 st for linear_penalty_5min_0.4	31
Figure 5.7: Historic data vs optimization data on June 20th for linear_penalty_5min_0.4	32
Figure 5.8: Historic data vs optimization data on December 12th for linear_penalty_5min_0.4.....	32
Figure 5.9: Historic data vs optimization data on July 6th for linear_penalty_5min_0.4.	33
Figure 5.10: Uncontrolled charging of 10 EVs vs optimization model on March 21 st	34
Figure 5.11: Uncontrolled charging of 20 EVs vs optimization model on March 21st.....	35
Figure 5.12: Historic data vs optimization model for 9 to 13 January	38
Figure 5.13: Charging on December 12th in the optimization model vs EV emulator.	39
Figure C.1: EV data on March 21 st for bi-linear_15min optimization model	48
Figure C.2: EV data on March 21st for linear_15min optimization model.....	48
Figure C.3: EV data on June 20 th for bi-linear_15min optimization model.....	49
Figure C.4: EV data on June 20 th for linear_15min optimization model	49
Figure C.5: EV data on December 12 th for bi-linear_15min optimization model	50
Figure C.6: EV data on December 12th for linear_15min optimization model	50
Figure C.7: EV data on March 21st for bi-linear_penalty_15min optimization model.....	51
Figure C.8: EV data on March 21 st for linear_penalty_15min optimization model.....	51
Figure C.9: EV data on June 20th for bi-linear_penalty_15min optimization model	52
Figure C.10: EV data on June 20th for linear_penalty_15min optimization model	52
Figure C.11: EV data on December 12th for bi-linear_penalty_15min optimization model	53
Figure C.12: EV data on December 12th for linear_penalty_15min optimization model.	53
Figure C.13: EV data on March 21st for bi-linear_penalty_5min optimization model.....	54
Figure C.14: EV data on March 21st for linear_penalty_5min optimization model.....	54
Figure C.15: EV data on June 20th for bi-linear_penalty_5min optimization model	55
Figure C.16: EV data on June 20th for bi-linear_penalty_5min optimization model	55

Figure C.17: EV data on December 12th for bi-linear_penalty_5min optimization model	56
Figure C.18: EV data on December 12th for linear_penalty_15min optimization model.	56
Figure C.19: EV data on March 21st for linear_penalty_15min_0.4 optimization model	57
Figure C.20: EV data on March 21st for linear_penalty_15min_0.6 optimization model	57
Figure C.21: EV data on June 20th for linear_penalty_15min_0.4 optimization model ...	58
Figure C.22: EV data on June 20th for linear_penalty_15min_0.6 optimization model	58
Figure C.23: EV data on December 12th for linear_penalty_15min_0.4 optimization model	59
Figure C.24: EV data on December 12th for linear_penalty_15min_0.6 optimization model	59
Figure C.25: EV data on March 21st for linear_penalty_5min_0.4 optimization model...	60
Figure C.26: EV data on March 21st for linear_penalty_5min_0.6 optimization model...	60
Figure C.27: EV data on June 20th for bi-linear_penalty_5min_0.4 optimization model .	61
Figure C.28: EV data on March 21st for linear_penalty_5min_0.6 optimization model...61	61
Figure C.29: EV data on December 12th for linear_penalty_5min_0.4 optimization model	62
Figure C.30: EV data on December 12th for linear_penalty_5min_0.6 optimization model	62

List of Tables

Table 2.1 Relevant references and their optimization methods	5
Table 4.1: Example of user-specific data from the online form	14
Table 4.2: Example of pre-processed EV data.....	14
Table 4.3: Dates used for the data analysis.....	15
Table 4.4 Tested optimization models and their specifications	20
Table 4.5 Hardware specifications of the simulation computer.....	21
Table 4.6: The hardware on the PHIL-testbed.....	21
Table 5.1 Computational times of different optimization models for March 21st	26
Table 5.2 Computational times of different optimization models for June 20 th	27
Table 5.3 Computational times of different optimization models for December 12 th	27
Table 5.4: SS and SC on the three simulations dates	29
Table 5.5 PPR on the three simulation dates	30
Table 5.6: KPIs of historic data vs optimization data on July 6th.....	33
Table 5.7: Amount of energy charged for 10 EVs	34
Table 5.8: Amount of energy charged for 20 EVs	35
Table 5.15: Computational times for different numbers of EVs on March 21st	35
Table 5.16: KPIs for different numbers of EVs on March 21 st	36
Table 5.17: KPIs for different amounts of PV on March 21 st	36
Table 5.18: KPIs for different amounts of PV and EVs on July 6 th	37
Table 5.13: Welkom Kropman EV data for 9 to 13 January.....	38
Table 5.14: EV data for 9 to 13 January after the feasibility check.....	38
Table 5.15: Amount of energy charged at different stages in the PHIL-testbed simulation	39
Table A.1: Simulation EV data for 10 EVs	47
Table A.2: Simulation EV data for 20 EVs	47
Table B.1 Computational times of different optimization models for March 21st.... Error! Bookmark not defined.	
Table B.2 Computational times of different optimization models for June 20 th Error! Bookmark not defined.	
Table B.3 Computational times of different optimization models for December 12 th	
..... Error! Bookmark not defined.	
Table B.4 Computational times of different penalty weightfactors for March 21st.. Error! Bookmark not defined.	
Table B.5 Computational times of different penalty weightfactors for June 20 th Error! Bookmark not defined.	
Table B.6 Computational times of different penalty weightfactors for December 12 th	
..... Error! Bookmark not defined.	
Table D.1: KPIs for different optimization models on March 21 st Error! Bookmark not defined.	
Table D.2: KPIs for different optimization models on June 20 th Error! Bookmark not defined.	
Table D.3: KPIs for different optimization models on December 12 th ... Error! Bookmark not defined.	

Table D.4: KPIs for optimization models with different weight values on March 21 st	Error! Bookmark not defined.
Table D.5: KPIs for optimization models with different weight values on June 20 th	Error! Bookmark not defined.
Table D.6: KPIs for optimization models with different weight values on December 12 th	Error! Bookmark not defined.

List of Abbreviations

AC	Alternating current
ACN	Adaptive charging network
BESS	Battery energy storage system
CDR	Charge detail record
CMS	Continuous monitoring system
DC	Direct current
EV	Electric Vehicle
GHG	Greenhouse gas
KPI	Key performance indicator
LP	Linear programming
MILP	Mixed-integer linear programming
MPC	Model predictive control
PHIL	Power Hardware-in-the-loop
PPR	Peak power reduction
PV	Photovoltaic
QP	Quadratic programming
SC	Self-consumption
SOC	State of Charge
SS	Self-sufficiency
TOU	Time-of-use
VRES	Variable renewable energy sources

1. Introduction

1.1. Background

To limit global warming and meet the goals of the Paris agreement, greenhouse gas (GHG) emissions need to be reduced (United Nations Framework Convention on Climate Change (UNFCCC), 2016). The transport sector accounts for 23.3% of all the European Union (EU) GHG emissions in 2020, and 76.7% is from road transport, which is made up of 59.4% by cars (European Commission & Directorate-General for Mobility and Transport, 2022). To reduce GHG emissions due to the transport sector, the use of electrical vehicles (EVs) is rapidly increasing. In the Netherlands, the percentage of EVs in newly registered vehicles has increased from 5.8% in 2016 to 29.8% in 2021 (Netherlands Enterprise Agency, 2022). In Europe, the share of EVs in new car registrations has increased from 1% in 2016 to 17.8% in 2021 (European Environment Agency, 2022). However, the sustainability of these EVs depends on the mix of generation types used to charge them (Van Der Meer et al., 2018). Furthermore, the mass-scale deployment of EVs introduces a large increase in the electricity demand potentially larger than current power systems and generation capacity are capable of handling (Mangipinto et al., 2022). Currently, EVs are mostly charged uncontrolled at high charging loads, in increasingly shorter times with the introduction of fast charging, resulting in high peak load demands (Chadha et al., 2022).

1.2. Research motivation

At workplaces, EVs usually arrive in the morning (6 – 9 am) and depart late in the afternoon (Sadeghianpourhamami et al., 2018). Charging takes place mostly in the morning, while PV-generated electricity is available in the afternoon. This can result in both a high peak demand in the morning and a surplus of sustainably generated electricity, or valleys, in the afternoon. By adopting smart charging strategies to shift EV loads, peak loads can be reduced, and charging can occur when sustainably generated electricity is available. (Heilmann & Wozabal, 2021) Both, increasing the self-use of sustainably generated electricity and reducing the necessity for large-scale grid infrastructure investments.

1.3. Problem statement

This research concerns a case study of the office of Kropman in Breda in the Netherlands. The office has a small fleet of EVs, where currently charging is uncoordinated. This results in EVs being charged directly when plugged in, often at the same time, resulting in a large power peak demand in the morning. Contrarily, in the middle of the day there can be a surplus of energy due to an overabundance of PV-generated electricity. Since charging times are often shorter than the dwell time, the time an EV is plugged in, there is a potential to shift the charging loads by delaying or scheduling charging. This can be used to reduce the power peaks and increase the self-consumption of PV-generated electricity. In previous research by Somers (2022), the

application of machine learning models to predict the individual EV charging load was explored, to create accurate predictions for robust smart charging control applications. In the case of a small EV fleet, such as at the office of Kropman Breda, it is difficult to identify load patterns and make accurate predictions, unless the presence of EVs is known. Furthermore, at the moment state of charge (SOC) values, such as the amount of energy at arrival, are not yet shared by EVs.

1.4. Research aim

In this research, considering the above-mentioned problems, a solution is being explored which does not rely on EV load predictions or the availability of SOC values. To provide the smart charging controller with the necessary input, a web application is created to obtain user-specific information, such as the departure time and desired amount of energy in kWh. The user-specific information is used as input for an optimization model. The model determines the best time and charging current for each EV to charge based on the input variables and PV- and building load predictions. The goal of EV charging scheduling is reducing peak loads and timing of charging with the availability of renewable (solar) energy. Furthermore, reducing the cost of charging by using available solar energy and taking into consideration variable energy prices. Therefore, the research question of this project is as follows:

How to implement smart charging to shift EV loads, increase the self-use of PV and reduce peak loads, without the use of SOC values and EV load predictions?

To answer this research question, the following sub-questions are answered in this research:

- *What method of smart charging is best applicable to solve the research problem?*
- *To what extent does the smart charging solution improve energy flexibility, PV self-use and decrease peak loads?*

1.5. Thesis outline

This thesis starts with literature research on exploring smart charging and recent methods used for smart charging and optimization modelling in Chapter 2. An overview of the case study is given in Chapter 3. This is followed by a description of the research methods used in Chapter 4, which includes: optimization modelling, simulation, the use of a power hardware-in-the-loop (PHIL) testbed and key-performance indicators (KPIs). In Chapter 5 the results of the data analysis and simulations are presented and discussed. Finally, Chapter 6 presents the conclusions drawn from the research and recommendations for future research.

2. Literature study

2.1. Smart charging

Smart charging involves “adapting the charging cycle to best meet both the restrictions and conditions of the power system and the needs of electric vehicle (EV) users” (International Renewable Energy Agency, 2019). Smart charging is a general term for various methods of intelligently controlling the charging of electric vehicles (EVs). The goal of smart charging is to reduce the peak demand and overall load on the grid, reduce the economic impact on the EV owner by reducing charging costs and increase the sustainability of EVs by utilizing renewable energy (Sadeghian et al., 2022). Smart charging has potential benefits for the EV owner, grid operators and the environment.

Increase renewable energy utilization

According to (Fachrizal et al., 2020), the sustainability of an EV depends on the generation type of electricity used to charge it. Well-to-wheel (WTW) emissions of an EV charged with coal-based power are comparable to gasoline-based combustion engine vehicles. If recharged with PV or wind-generated energy the WTW emissions can be close to zero. Increasing EV load flexibility allows for higher renewable energy utilization, by allowing the loads to be shifted to when sustainably generated electricity is available.

Reduce grid infrastructure investments

Both high electric load from charging EVs and generation from variable renewable energy sources (VRES), put stress on the existing electricity systems that necessitate the costly upgrade of lines and transformers in voltage grids (Heilmann & Wozabal, 2021). Across Europe, the transmission grid expansion is expected to cost between 30 billion to 93 billion by 2050 (Egerer et al., 2013). Coordinated smart charging of EVs is a way to reduce stress on distribution grids and reduce grid expansion investments. According to Heilmann & Wozabal (2021), uncontrolled charging results in peak loads, while VRES results in valleys, shifting loads by smart charging potentially reduces stress on the grid from both.

Reduce charging costs

As mentioned before, increased EV load flexibility allows for higher utilization of renewably generated electricity. This potentially lowers the charging costs for instance by using PV-generated electricity compared to electricity from the grid. Furthermore, if Time of Use (TOU) pricing is in place, EVs can be charged considering the overall demand on the grid and electricity prices (Chadha et al., 2022).

2.1.1. Keywords

The purpose of this literature review is to research recent smart charging methods. First smart charging in general and its potential benefits are described. Then recent charging methods from 2018 to the present are reviewed. The goal is to show

similarities, variations, and shortcomings of previous work to make recommendations for a future application of smart charging.

This review will examine EV smart charging approaches from the year 2018 to the present. This time-period is chosen to focus on recent smart charging methods only. General keywords used to search for literature and complete this review are *smart charging*, *EV smart charging*, *EV smart charging workplace*, *EV smart charging office*, *vehicle smart charging*, *EV smart scheduling*, *EV scheduling*, *EV load balancing*, *electric vehicle “load balancing”*, *flexible charging*, *EV valley filling & V2G*.

2.1.2. State-of-the-art

In this section, various smart charging methods as proposed in recent literature (2018 – present) are described. Limited to smart charging methods which involve controlling EV charging with the focus on residential or workplace applications.

Load balancing

Dynamic load balancing monitors the power load on the grid, limiting the power output to prevent overloading the circuit. This also applies when there are multiple chargers connected to one power network. Although not all EV chargers have dynamic load balancing, chargers connected to the internet can often be upgraded (Tüzes & van Barlingen, 2022).

Unidirectional and bidirectional smart charging

Smart charging can be done in the form of unidirectional power flow management during EV charging, known as V1G. The charging load is shifted over time to better fit the grid conditions and availability of sustainably generated energy. This is also referred to as “valley filling” (Wang et al., 2019). Additionally, the implementation can include bidirectional charging, known as vehicle-to-grid (V2G), that enables energy to be stored in the battery of the EV and later discharged back to the grid. Alternatively, the energy can also be exported to a building, known as Vehicle-to-home (V2H) and Vehicle-to-building (V2B) (He et al., 2022). One of the benefits of bidirectional charging is increased load flexibility (Wei et al., 2022). However bidirectional charging introduces a much higher degree of difficulty. For example, additional costs due to battery degradation need to be considered. Should EV owners be compensated for the additional wear of their EV’s battery and if yes how much? Furthermore, bidirectional charging can increase the charging time, which with unpredictable user behavior can introduce additional inconvenience and difficulty.(Gschwendtner et al., 2021; Spencer et al., 2021)

Flexible charging

One of the methods for smart charging involves using time of day set points for charging current. A recent paper by Bons et al. (2021) paper describes a large-scale project called “Flexpower”. It describes a method called flexible charging, which controls EV charging speed to reduce peak loads and match charging loads with the availability of sustainably generated energy. Time-dependent charging profiles are applied to public charging

2. Literature study

stages in Amsterdam. During household peak consumption hours charging current is reduced, increased during the night-time, and linked to solar intensity levels during the day. The results showed that the peak loads from EVs can be reduced with limited user impact. Although this project focuses on publicly available charging stations, there is a possibility of applying this method at a workplace. The use of time-dependent charging profiles is limited compared to other papers that propose elaborate optimization models, especially when applied at a workplace. Limiting the charging speed with set-points can result in longer charging times, which can reduce energy flexibility rather than increase it. A more dynamic smart charging solution would offer more energy flexibility, cost benefits and user convenience (Bons et al., 2019).

Optimization modelling

Recent studies with similar research objectives often make use of optimization modelling for scheduling EV charging. Compared to the methods mentioned previously in this chapter, this smart charging method is more complex and allows for a wider range of applications and inputs. For example, a wide range of chargers and EVs or the inclusion of PV predictions.

The optimization models often make use of a form of convex programming or integer programming. Both include only unidirectional charging (V1G) or also bidirectional charging (V2G). In the table below relevant references are presented, including their main objective, inputs, optimization model and limitations.

Table 2.1 Relevant references and their optimization methods

References	Main Objective	V2G	Time-scaled	Inputs	Optimization model	Predictions	Numb. of chargers	Limitations
Van der Meer et al. (2018)	Decreasing charging costs by optimizing power flows between PV systems, grid and BEVs.	yes	15-min	Arrival time, departure time and desired energy content	MILP CPLEX solver	Weather (ARIMA)	1 and 2	Only 1 and 2 chargers were tested. Only case study with "realistic" inputs and no implementation.
Fridgen et al. (2021)	Allocating a limited available power at one coupling point in a way that maximizes the resulting utility of EV drivers in bottleneck situations.	no	1-min	departure time and the required amount of energy for the expected travel time	MILP	No	1 to 3	The model is evaluated with "exemplary cases" and is not suitable for real-world application
(Wang et al., 2019)	"Valley filling" to match the charging of EVs at a workplace with peak PV production.	no	15-min	Arrival time, layover time and energy demand assuming a full charge by the departure time	QP	PV	31	Simulation only with realistic data.

2. Literature study

(Ramos Muñoz & Jabbari, 2020)	Shift PEV charging to fill the overnight demand valley	no	-	"Flexibility ratio" calculated from the dwell time, desired charging demands and maximum charge rate	LP	No	500	The assumption is made that each driver knows their driving patterns for the entire workday with reasonable accuracy Simulation of parking structures with 500 BEV only.
(Lee et al., 2018)	Defer costly infrastructure upgrades while also meeting operator objectives, such as minimizing charging delay, maximizing revenue, or following demand response signals	no	10-min	Expected departure time and energy demand	Convex optimization MPC algorithm	No	-	Only simulation using real historical data. Real-life implementation limited (Heredia et al., 2020)

The optimization model for EV charging described by Fridgen et al. (2021), uses mixed-integer linear programming (MILP). The output of the model is an EV charging schedule that takes the expected travel time of the owner into consideration. The input variables are the departure time and the required amount of energy for the expected travel time. The model is evaluated using "exemplary cases". This means the model is evaluated for the occurrence of bottlenecks by using selected input data for the different parameters. A limitation is that the current model is programmed in a hard class of optimization problems and adequate mathematical solutions for real-world applications need to be developed. The problem with hard class optimization problems is that they "cannot be solved to optimality or within a reasonable integrality gap by any standard MIP solver within a reasonable time limit" (Kallrath, 2009).

Wang et al. (2019), propose unidirectional EV charging scheduling based on short-term solar forecasts. The paper describes a typical valley-filling problem that focuses on workplace charging of EVs during regular business hours coinciding with times of peak PV production. Control parameters, including charge power, are optimized using quadratic programming. To allow for a corrective approach, control actions are modified by a receding horizon algorithm. The research by Wang et al. (2019), is limited to simulation with realistic input data and therefore might lack real-world variability.

In the work of (Ramos Muñoz & Jabbari, 2020), a smart charging protocol for a workplace is proposed. The protocol uses an ordering strategy based on the vehicles' load-shifting ability to develop a charging order. A decentralized smart charging strategy is used that generates a charging profile for each EV via linear programming (LP). This is based on the drivers' "expected driving patterns". This includes the dwell time, desired charging demands and maximum charge rate. From these values, a "Flexibility ratio" is calculated, which is to create a charging order for the EVs. Cost optimization is used to generate a parking structure demand load with desirable characteristics. An algorithm assigns EVs to chargers in calculated time slots. A

2. Literature study

limitation of the study is that the assumption made that each driver knows their driving patterns (i.e., periods between dwell times and distances travelled during these periods) for the entire workday with reasonable accuracy, which might not be the case in practice. Furthermore, the research is limited to simulation only.

One of the papers with the most similar objective is the work by Van der Meer et al. (2018), which presents a promising design for an energy management system (EMS) that uses PV forecasting to optimize power flow between PV, grid and EVs at a workplace. The design uses mixed-integer linear programming (MILP), which determines at what time the charging results in the lowest overall cost. In this case, both the arrival and departure times are considered as variables for each EV as well as the BEV owners' desired energy content upon departure. This allows for the charging of multiple EVs to be best allocated during the day. The research includes case studies, with one and two chargers. The case studies are performed by running the EMS with selected "realistic" input variables. The study is limited to one and two EV chargers. Furthermore, the input variables are currently selected and not based on actual data. Translating these promising results to practice is challenging since some values can be more variable in practice.

Lee et al. (2018), describe an online scheduling system for EV charging. It uses an adaptive charging network (ACN), which computes charging rates using model predictive control (MPC) and convex optimization. A mobile application is used to collect user input. This collects the expected departure time and the energy demand of the EV owner. The model can operate based on various utility functions. Two examples are given: a utility function that maximizes profit and one that encourages charging as quickly as possible. Optimization is done based on a utility function and set infrastructure constraints such as a maximum power draw.

Research by (Heredia et al., 2020) includes a real-world implementation of the smart charging technology described by Lee et al. (2018). The study took place at a workplace with sixteen EV chargers. The ACN calculates charging power limits for each charger, taking into consideration the requested energy and power demand of the owner, while keeping the aggregate power under the capacity of the transformers serving the EV charging stations and below a power peak threshold to lower electricity costs.

The papers mentioned use a varying range of optimization model programming methods. Depending on the use case different methods are used. Firstly, convex optimization, which is used in the paper by Leet et al. (2018), is a term for a broad range of problem classes. A convex optimization problem is an optimization problem for which the objective function is convex, and the problem can reach a global optimal point. A linear optimization problem, used by Ramos Muñoz & Jabbari (2020) is very much like a convex optimization problem, however, the objective and all constraint functions are all linear. In the case of quadratic programming (QP), the optimization problem involves quadratic functions (Boyd & Vandenberghe, 2004).

The papers by Van der Meer et al. (2018) and Fridgen et al. (2021), make use of mixed-integer linear programming (MILP), which is a form of integer programming. These are forms of optimization problems in which the function uses integers as well. One

mathematical optimization model is not necessarily better than another, their suitability depends on its use case.

2.1.3. Research gaps and research focus

Recent smart charging methods that involve controlling charging current range from relatively simple to complicated solutions. This seems to be related to whether it includes a real-life implementation. For example, the research by Bons et al. (2021), involves a large-scale project. However, the use of time-dependent charging profiles is limited compared to other papers that propose elaborate optimization models.

Other smart charging solutions that involve optimization modelling with multiple input parameters, many constraints and an elaborate objective function are often limited to simulation. For example, the paper by van der Meer et al. (2018), describes a promising cost optimization model, which is evaluated using case studies with realistic input data. Similarly, the papers by Wang et al. (2019), Lee et al. (2018) and Fridgen et al. (2021), evaluate their models by simulating with realist values or historical data.

When the research does involve a real-life implementation the smart charging controller is limited. In the research of Heredia et al. (2020) for the test deployment, the user input variables are set to a default constant value of 8h and 8 miles. Furthermore, the number of constraints is limited, since only the maximum power draw allowed by the charging infrastructure and a power peak threshold are considered. To be able to deploy an optimization model smart charging method some form of simplification is required when the timescale is limited. However, addressing the variability of EV owner behavior is an intrinsic part of the smart charging problem. With the inclusion of more input variables and constraints, the elaborate smart charging controller proposed by Lee et al. (2018) can be greatly improved.

The input parameters for the optimization models of the smart charging controllers in the previously described literature are similar. Most papers make use of the departure time and requested energy or aim for a full charge at the departure time. Research by Ramos Muñoz & Jabbari (2020) describes a performance indicator called the “Flexibility ratio”, which is based on various factors including the dwell time, desired charging demands and maximum charge rate. In practice, these values might not be available.

In the papers by van der Meer et al. (2018), Fridgen et al. (2021) and Wang et al. (2019), the optimization model makes use of state-of-charge (SOC) or the energy content at arrival. In all papers presented in Table 2.1, the maximum charging power of the EV is used in the model. In practice, these values are unknown since they are not shared by the EV. For the SOC and maximum charging rate often realistic values or historical data are used. In the paper by Heredia et al. (2020), the maximum power draw is ignored which results in different power draw calculated by the model compared to in practice, resulting in a lower final SOC.

V2G is excluded from the smart charging solution in most papers found since it increases the complexity of the solution. Additionally, according to the study by van der Meer et al. (2018) that did implement V2G, it is currently not economically viable due to the battery degradation costs.

2. Literature study

In this research, the focus is on the implementation of a state-of-the-art smart charging solution for an office. The goal is to increase the self-use of PV and reduce peak loads while meeting the requests of the EV owner. As opposed to changing the real-world uncertainty by setting user input to default values, the difficulty of the optimization problem is reduced by focusing on unidirectional charging (V1G) only. This is done to reduce the complexity of the smart charging problem to allow for a real-world implementation of a smart charging controller within the timescale of this research. The goal of a real-world implementation is detecting problems that might occur in practice, which are not found when using simulation to evaluate smart charging solutions. The input parameters for the optimization model are limited to the departure time and requested energy by the EV owner, which are acquired through a digital form. The research is performed using these two input parameters to reduce the amount of information required from the EV owner. This is done to ensure convenience for the EV owner and to avoid requiring the user to fill in a large amount of information. Instead of making use of SOC values for the model, the requested energy will be used to determine optimum charging rates. The minimum charging rate is set to a default value, determined by the minimum charging speed of the EV charger. The maximum charging rate is determined by looking at the maximum charging current drawn when an EV is plugged in or set to a default value when retrieving this information is not possible. This information together with PV data and electricity prices is used to develop an optimization model which schedules EV charging. This optimization model is a key component of the smart charging controller designed for the office. Similarly, to the research by Lee et al. (2018), the charging controller makes use of MPC, which uses prediction models to control a system with constraints (Miyazaki et al., 2019).

3. Case study

3.1. Overview

To answer the research question of this research a case study is performed at the office of Kropman in Breda, The Netherlands. The office is built in 1993 and has a total floor area of approximately 1500 m². The maximum occupancy count of the office is 35 people (Reinders, 2022). The building is equipped with a building management system that allows for continuous monitoring of the building installations, battery energy storage system, EVs and PV. Furthermore, weather measurement data is collected with equipment on the roof. Using the weather measurement data, weather predictions are made by an external party (Solargis). All the data is stored within a database. An overview of the building systems and data collection is presented in Figure 3.1. The data is processed within the continuous monitoring system (CMS) InsiteSuite and stored in the historical database called InsiteReports. Whereas InsiteSuite allows for real-time monitoring of the building systems, InsiteReports allows for requesting historic building, charging and weather data. The historic data is processed using Python for data analysis and for developing prediction models.

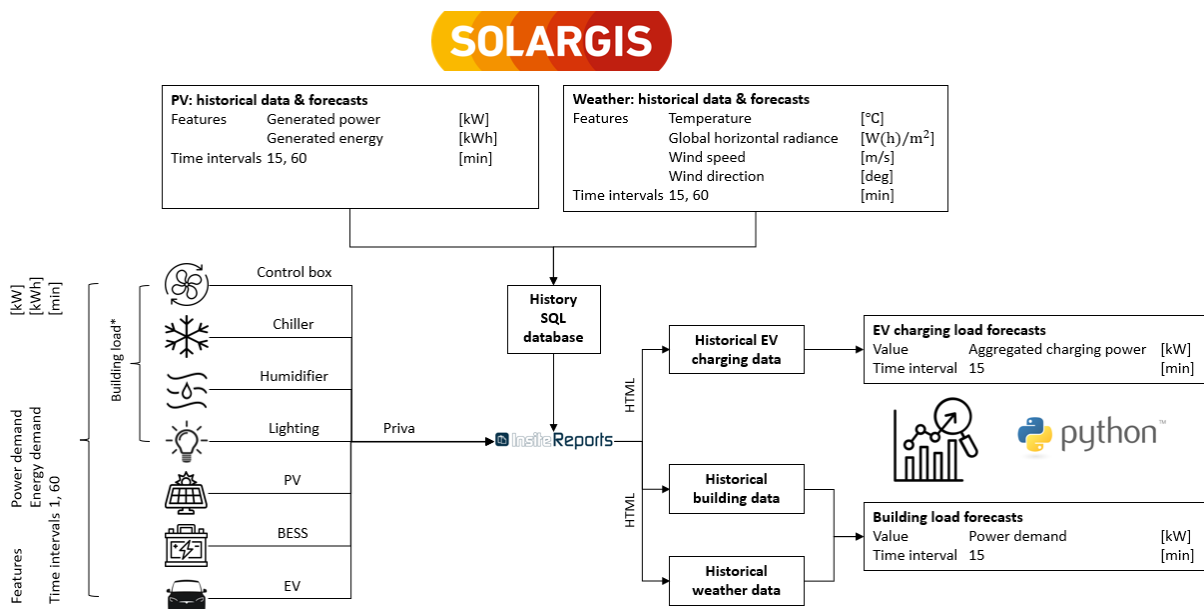


Figure 3.1: Overview of the building systems and data collection

On the roof, 65 PV panels are located, which have a combined maximum capacity of 16.9 kW (Reinders, 2022). When there is a surplus of solar energy, the electricity is fed back into the grid. At the office 4 type 2 EV chargers are available. These chargers allow for charging at a maximum of 7.4 kW (1 phase/32 A) or 22 kW (3 phase / 32 A) depending on the vehicle type (de Bont, 2019). Aggregated charging power data is available from the InsiteReports database. Individual charging detail records (CDR) are available through an external partner called Last Mile Solutions (LMS). Additionally, there is an application for employees to fill in their attendance called Welkom Kropman. Within the application, there is a form for EV charging, which collects user-specific information, such as the arrival time, desired amount of EV charging energy in kWh and expected

3. Case study

departure time. This data is processed through InsiteSuite and can be collected using an RPC-call. The form is presented in Figure 3.2.

Vul uw gegevens in

Laadpuntnummer	Minimaal gewenst bereik (kWh)	Verwachte vertrektijd
<input type="text"/>	<input type="text"/>	17:17 <input type="button" value=""/>
Indien onbekend: selecteer 0		
Mag uw gepseudonimiseerde data gebruikt worden door Kropman Installatietechniek B.V. en derden?		
<input type="checkbox"/>		
<input type="button" value="Annuleren"/>	<input type="button" value="Bevestigen"/>	

Figure 3.2: The EV charging form in the Welkom Kropman application (in Dutch)

3.2. Smart charging controller

After discussing the various methods for smart charging and describing the case study, a design for the smart charging controller is made. Based on the literature study in Section 2.1.2, optimization modelling can offer a fitting solution to the smart charging problem at the office of Kropman Breda. It allows for optimizing the distribution of energy between EVs during office hours, taking into consideration several constraints.

- The main input for the model is the user-specific information from the online EV charging form, which includes: the arrival time of the employee, the expected departure time, and the requested amount of energy in kWh.
- The second part of the input is the disturbances, which include: the predicted amount of PV-generated electricity, the predicted building load and electricity prices. Although the latter is considered when developing the optimization model, it is not used in this research since time of use pricing is not yet in place in the Netherlands.

MPC is used to control the EV chargers based on predictions and constraints for a specified horizon (Miyazaki et al., 2019). All the inputs described are used by the optimization model to minimize a cost function. Minimizing the cost function results in optimal current values for each EV over time. These current values are then sent to the EV charging stations. After a specified time, new data is loaded, and the optimization model is re-run. A diagram showing the smart charging process is presented in Figure 3.3.

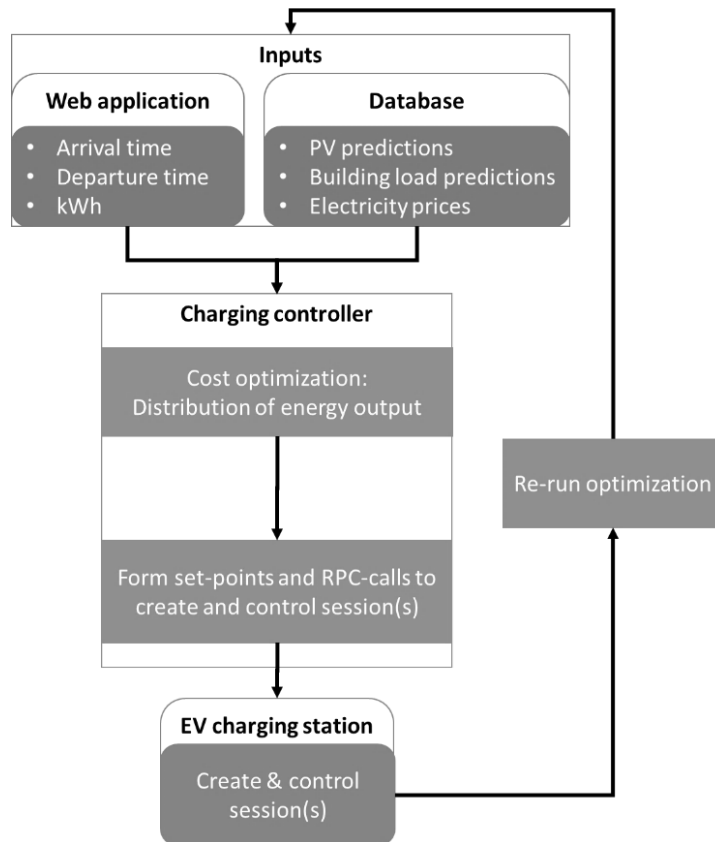


Figure 3.3: The smart charging process

Prediction horizon

The prediction horizon relates to how far the model looks into the future. For each time step into the future, the optimum current value is calculated. The prediction horizon is determined by determining how much time into the future should be considered to get an optimal control input for the present, see Figure 3.4.

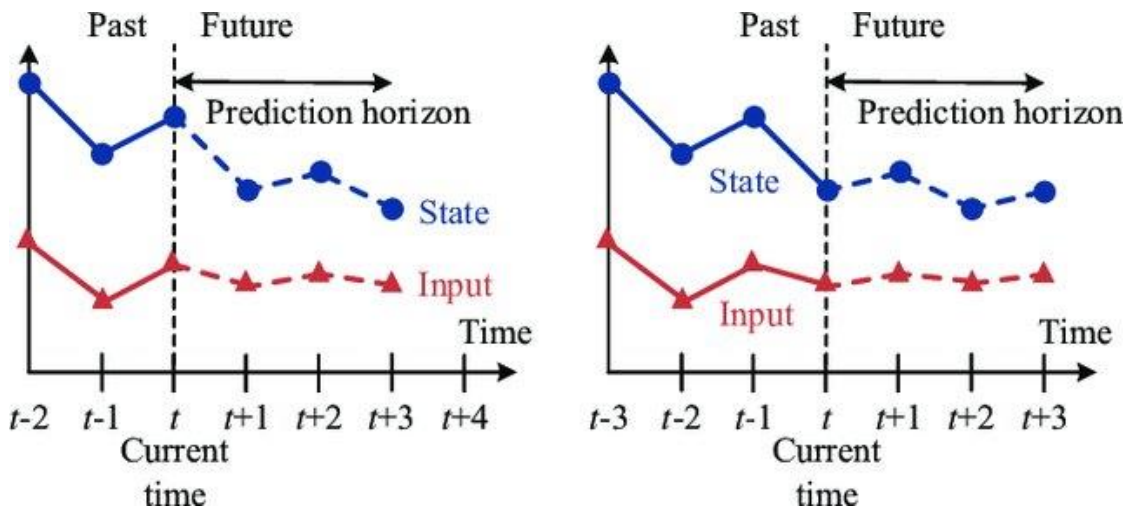


Figure 3.4: Illustration of the prediction horizon in MPC (Miyazaki et al., 2019)

3. Case study

For example, for this case study, the smart charging controller is only active during office hours, from 6 am to 6 pm. When an EV arrives at 6 am, the user-specific data is collected. Using the user-specific data, the predicted building load and PV-generated electricity for the next 12 hours, the charging of the EV can be planned optimally during office hours. If another EV arrives at 1 pm, only the next 5 hours need to be taken into consideration. Since after 6 pm, the smart charging controller is not active as it is outside office hours. This causes the prediction horizon to decrease during the day from 12 to 0 hours. On the next day at 6 am, the length of the prediction horizon is set to 12 hours again. Therefore, a batch-type prediction horizon is used as visible in Figure 3.5.

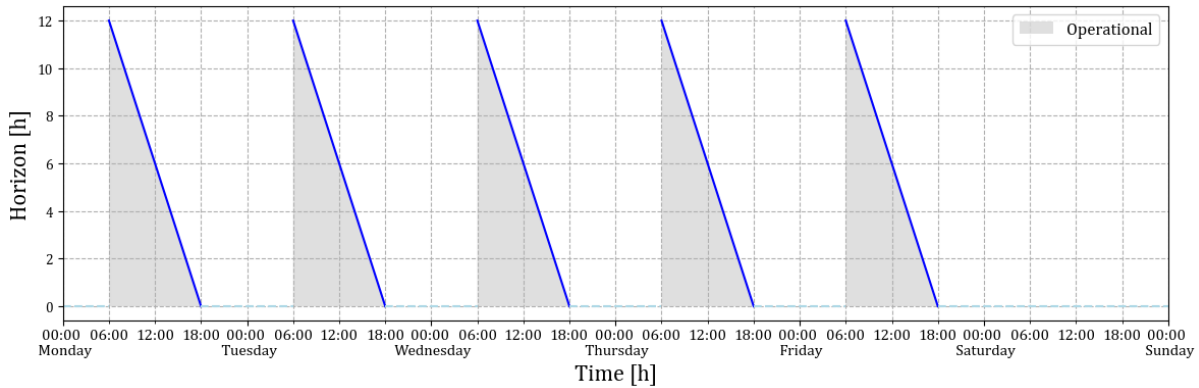


Figure 3.5: Visualization of the batch-type prediction horizon

Time resolution

How often the model is re-run depends on several factors. Firstly, the time resolution of the input data. If the model is re-run when no new data is available, the outcome remains the same. In the case of the office of Kropman, data with a time resolution of one minute is available. Therefore, the model theoretically can be re-run every minute. However, this introduces problems concerning the second factor. For the model to be able to be re-run every minute, the computational time of the optimization model should be less than one minute. However, processing data with a granularity of one minute introduces a large amount of data which can increase the computational time significantly. In this research time resolutions of 15 and 5 minutes are tested. A lower time resolution, for instance, 5 minutes, is preferred. Since this reduces the reaction time between when an EV arrives and when the model is updated. Furthermore, the model can react more quickly to changing building load or PV power.

Charging constraint

Next to the maximum charge power described in Section 3.1. There are other constraints when it comes to charging. The EV should receive a minimum of 6 A, otherwise charging stops (De Herdt, 2020). Therefore, the smart charging controller should not send values between 0 A and 6 A.

4. Methods

4.1. Data pre-processing

EV data

The user-specific data collected using the Welkom Kropman application is stored in the following format, as presented in Table 4.1:

Table 4.1: Example of user-specific data from the online form

Location Name	Charger ID	Minimum desired range [kWh]	Arrival time	Expected departure time
Breda	1	36	2022-12-22 06:25	2022-12-22 15:00
Breda	0	10	2022-12-22 13:13	2022-12-22 14:13

This data is pre-processed for the model to be able to handle it. The location name is dropped before inputting the data into the optimization model. The table is sorted by the charger ID in ascending order. Since the time resolution of the model is 15 minutes the arrival times are rounded up to 15 minutes and the departure times are down to 15 minutes. If the time resolution is 5 minutes the data is rounded to 5 minutes. Since the linear optimization model is not able to process date-time objects, the arrival and departure time are converted to integers. The minimum desired range is checked to see whether or not it is feasible within the expected dwell time. The EV charging model only allows for charging either single-phase 32 A or triple-phase 32 A. Since not all EVs can charge triple phase, the model is limited to single-phase 32 A. This can result in a difference in total energy that can be charged within the dwell time, compared to in practice. To prevent the optimization problem from being unsolvable, the amount of energy is replaced, when it is larger than the dwell time multiplied by the maximum power draw of 7.36 kW. However, since the amount of energy being drawn from the charger is not equal to the energy going into the battery of the EV, the desired amount of energy is multiplied by the total charging efficiency as well. Finally, the energy at arrival is added to the table. This is assumed to be 0 at arrival since SOC values are not available. However, when the optimization model is re-run after 15 minutes the energy at arrival is set to the amount of energy calculated by the model at the previous iteration. An example of the pre-processed EV data is presented in Table 4.2:

Table 4.2: Example of pre-processed EV data

Charger ID	E_requested	T_arrival	T_departure	I_arrival	I_departure	E_arrival
0	6.624	2022-12-22	2022-12-22	16717149000000	16717185000000	0
		13:15	14:15	00000	00000	
1	36	2022-12-22	2022-12-22	16716906000000	16717212000000	0
		06:30	15:00	00000	00000	

For the simulations historic CDR data is used as EV input data. From the historic database, the arrival time, departure time and amount of energy delivered by the charging pole are available. Therefore, the amount of energy is multiplied by the total

4. Methods

charging efficiency to obtain the minimum desired range. Similarly, to processing the data from the Welkom Kropman application the amount of energy historically charged is replaced when it is larger than the dwell time multiplied by the maximum power draw and the total charging efficiency. The total energy charged in practice and the total energy charged in the optimization model is presented to allow for comparison.

Building load data

Before being able to use the building load for data analysis and as input for the optimization model the actual building load needs to be determined. In Figure 4.1, a schematic overview of the metered building installations is presented. The total electricity going to and from the grid is composed of the main power line and the lights. To the main power line, the BESS, PV, EVs, HVAC and power outlets are connected. Of these the BESS, PV, EV and HVAC are metered separately.

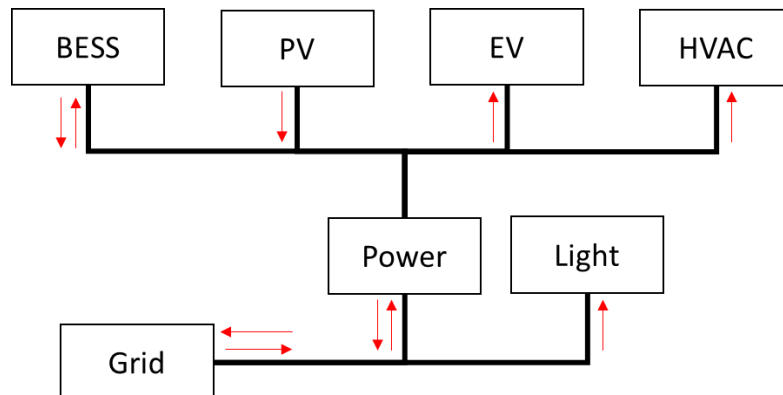


Figure 4.1 Schematic overview of the micro grid of the office building

To calculate the actual building load, the EV power needs to be subtracted from the power from the main power line and the power of the PV and lights needs to be added.

$$P_{Building} = P_{Power} - P_{EV} - P_{BESS} + P_{PV} + P_{Light}$$

Additionally, the power from the BESS is removed from the building load. This is done since the control of the BESS is still under development.

4.2. Data analysis

Data analysis is performed to research the potential for shifting EV-loads to reduce peak loads and increase PV-self use. These EV load shifts are called peak-shaving and valley-filling, respectively. This is done by looking at historic building load, PV and EV power data. The data analysis is performed for the following dates as presented in Table 4.3:

Table 4.3: Dates used for the data analysis.

	From	To
Winter solstice	December 12th 2022*	December 16th 2022
Equinox	March 21st 2022	March 25th 2022
Summer solstice	June 20th 2022	June 24th 2022

December 12th is chosen since in the week of December 21st no CDR data was available

4. Methods

4.3. KPIs

The performance of the optimization model is evaluated with various KPIs relating to energy performance(Li et al., 2021). This allows for accurately comparing the performance of uncontrolled to controlled charging and the performance difference between the different cost functions.

Power Peak Reduction (PPR)

The power peak reduction is an indication of how much the maximum power peak has reduced due to applying load shifting. The period for which the maximum peak is selected is from 6:00 to 18:00. Since this is when the charging controller will be active.

$$\Delta P [-] = P_{Peak_{ref}} - P_{Peak_{flexible}} \quad (1)$$

Units: [kW/kWh] Ideal value: as high as possible

Self-sufficiency (SS)

Self-sufficiency is related to the percentage of the daily solar-generated electricity that is used for compensating the daily electricity load.

$$SS [\%] = \frac{\text{daily generation directly consumed}}{\text{net daily load}} \quad (2)$$

Units: [%] Ideal value: 100

Self-consumption (SC)

The SC is the percentage of solar-generated electricity that is consumed by the building.

$$SC [\%] = \frac{\text{daily generation directly consumed}}{\text{net daily generation}} \quad (3)$$

Units: [%] Ideal value: 100

Both the SS and SC are good indicators of whether shifting the EV loads results in valley-filling. However, where the SC only corresponds to the percentage of generated solar energy used. The SS also indicates how much of the daily load can be compensated with solar-generated electricity by shifting EV loads.

4.4. Algebraic model

Electricity balance

The diagram below in Figure 4.2, shows the simplified microgrid of the office at Breda. The loads are the aggregated building loads, and the aggregated EV charging loads. The EV load is separated from the building load as it will be controlled by the smart charging controller. PV is the energy produced by solar energy. Energy is either drawn or delivered back to the grid based on the total electricity loads and PV production.

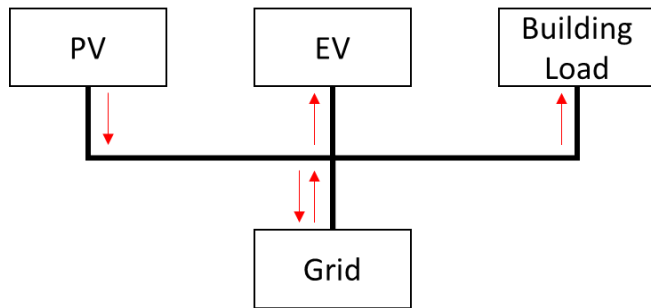


Figure 4.2 Simplified microgrid of the Office at Breda

This results in an electricity balance as shown in Equation 4, where the sum of all loads and electricity production is equal to the electricity drawn from the grid:

$$P_{Grid} = P_{Load} + P_{PV} + P_{EV}^{Aggregated} \quad (4)$$

When electricity is drawn from the grid; P_{Grid} is positive and when it is delivered back to the grid P_{Grid} is negative. This can also be written out by a negative and a positive variable, as shown in Equation 2:

$$P_{Grid} = P_{Grid^+} + P_{Grid^-} \quad (5)$$

The positive component P_{Grid^+} and the negative component P_{Grid^-} are later used in the cost function. As visible in Equations 4 and 5, when P_{Grid} is positive P_{Grid^-} is 0 and vice versa:

$$P_{Grid_t^+} \begin{cases} 0 & \text{if } P_{Grid} \leq 0 \\ P_{Grid} & \text{if } P_{Grid} > 0 \end{cases} \quad (6)$$

$$P_{Grid_t^-} \begin{cases} 0 & \text{if } P_{Grid} \geq 0 \\ P_{Grid} & \text{if } P_{Grid} < 0 \end{cases} \quad (7)$$

Since modelling an if statement is not possible in linear programming, the logic is written out in the following linear equations:

$$P_{Grid^+} \geq 0 \quad (8)$$

$$P_{Grid^-} \leq 0 \quad (9)$$

$$P_{Grid^+} \cdot P_{Grid^-} = 0 \quad (10)$$

4. Methods

Charging model

The aggregated EV load is the sum of all the charging power sent to each charging port:

$$P_{EV}^{Aggregated} = \sum_{c=1}^C P_{Charge_c} \quad (11)$$

Due to charging losses the actual charging power going to each EV, $P_{EV_{c,t}}$, is lower than the charging power drawn from the charging port. The total charging efficiency for level 2 charging ranges from around 87.2% to 90.6%, depending on temperature and power draw (Sears et al., 2014). The assumption is made that the total charging efficiency $\eta_{P_{Charge}}$ is 0.9.

$$P_{EV_{c,t}} = \eta_{P_{Charge}} \cdot P_{Charge_{c,t}} \forall c, t \quad (12)$$

Using the power going to each EV, the energy content of each EV is calculated (Van Der Meer et al., 2018):

$$E_{c,t} = \begin{cases} E_{c,t-1}^{arrival} & \text{if } t \leq t_{arrival_i} \forall c \\ E_{c,t-1} + P_{EV_{c,t-1}} \cdot \Delta t & \text{if } t_{arrival_i} < t < t_{departure_i} \forall c \\ E_{c,t}^{departure} & \text{if } t \geq t_{departure_i} \forall c \end{cases} \quad (13)$$

At arrival, the energy content is considered to be 0. However, when the optimization model is rerun for the same EV the energy content at arrival is set to the energy content calculated at that time point. This is to prevent the optimization model from starting with an energy content of 0 again, while the EV in practice has already charged. An important modification of the original EV energy model by Van der Meer et al. (2018) is changing $P_{EV_{c,t}}$ to $P_{EV_{c,t-1}}$. This results in the power and current being calculated one iteration before the energy content is calculated. For the first iteration of the optimization process, the energy content is 0 and the current and power are the values needed to achieve the desired energy content in the next iteration step.

Constraints

The charging power drawn from the EV charger is the charging current multiplied by the maximum charging voltage of the EV. The maximum voltage V_{Max} is set to a constant value of 230V. The charging current $I_{Charge_{c,t}}$ is the control value, which is taken after running the optimization model and sent to the charging pole.

$$P_{Charge_{c,t}} = I_{Charge_{c,t}} \cdot V_{Max} \forall c, t \quad (14)$$

The charging current and maximum power draw is limited by the maximum current and power draw allowed by the EV charger. The chargers at the office of Kropman Breda are type 2 chargers. Which can charge up to a maximum power of 7.4 kW at single-phase 32 A or 22 kW at triple-phase 32 A (de Bont, 2019). Since it is currently not possible to detect whether an EV allows for triple-phase charging, the maximum current and power are set to 32 A and 7.4 kW, respectively.

$$I_{Charge_{c,t}} \leq I_{Max} \quad (15)$$

4. Methods

$$P_{charge_{c,t}} \leq P_{Max} \quad (16)$$

When the time is before the arrival time or below the departure time of the EV, the charging current of the respective charger is equal to 0.

$$I_{charge_{c,t}} = 0, \quad \text{if } t < t_{arrival_c} \text{ or } t > t_{departure_c} \forall c \quad (17)$$

Objective function

The objective of the optimization model is minimizing the total charging cost, which is calculated using the cost function presented in Equation 19:

$$obj = \min(C_{tot}) \quad (19)$$

$$C_{tot} = \left(\sum_{t=1}^T (\lambda_{Grid_t} \cdot P_{Grid_t^+})^2 - \sum_{t=1}^T (\lambda_{FIT} \cdot P_{Grid_t^-})^2 \right) \quad (19)$$

The total charging cost is the sum of the cost of electricity drawn from the grid minus the electricity feed back to the grid. Electricity costs are taken into consideration with $P_{Grid_t^+}$, which is multiplied by the variable electricity price λ_{Grid_t} . Electricity delivered back to the grid is included by subtracting $P_{Grid_t^-}$ multiplied by the Feed-in-tariff λ_{FIT} . Both $P_{Grid_t^+}$ and $P_{Grid_t^-}$ are squared to allow for peak shaving. Taking the square of $P_{Grid_t^+}$ and $P_{Grid_t^-}$ is important to penalize very high peaks. The sum over time of load with a very high peak and a very low peak and a result with two medium-high peaks would result in the same cost. However, when taking the square of $P_{Grid_t^+}$ and $P_{Grid_t^-}$ the sum over time with the very high peak has a larger cost. Ultimately, motivating the optimization model to pick the flatter load profile.

Bilinear and linear

The term introduced in Equation 8, although initially seeming to be a linear term introduces non-linear characteristics in the optimization problem. It can be considered a bi-linear term, which is caused by multiplications of two decision variables (Conrad, 2008). This results in the solution of the model being non-convex. Therefore, to find an optimum a non-linear solver is required. This can result in long computational times in some edge cases, or when there is a large amount of input data.

Therefore, in the revised algebraic model, the bi-linear term is removed from the model. The variables P_{Grid^+} and P_{Grid^-} are not used, removed from the cost function and Equations 8, 9 and are removed. This results in the following cost function:

$$C_{tot} = \left(\sum_{t=1}^T (\lambda_{Grid_t} \cdot P_{Grid_t})^2 \right) \quad (20)$$

4. Methods

Penalty function

According to Apostolaki-Iosifidou et al. (2017), charging at lower charging rates can result in higher charging costs. The charging efficiency increases with increasing charging current. However, the current cost function does not make a distinction between charging two EVs at a lower current or alternating charging between two EVs at a higher current. This is undesirable because charging with lower values can result in lower efficiency, as reported by Apostolaki-Iosifidou et al. (2017). To prevent the model from dividing the maximum charging current, resulting in lower charging currents, a penalty function is added. This results in the final cost functions as presented in Equation 21 and Equation 22, for the bi-linear and linear cost functions, respectively:

$$C_{tot} = \left(\sum_{t=1}^T (\lambda_{Grid_t} \cdot P_{Grid_t^+})^2 - \sum_{t=1}^T (\lambda_{FIT} \cdot P_{Grid_t^-})^2 \right. \\ \left. - \lambda_{Weight} \cdot \sum_{t=1}^T \sum_{i=1}^N \left(\frac{1}{1 + \lambda_{Grid_t}} \cdot P_{Charge_{t,i}} \right)^2 \right) \quad (21)$$

$$C_{tot} = \left(\sum_{t=1}^T (\lambda_{Grid_t} \cdot P_{Grid_t})^2 - \lambda_{Weight} \cdot \sum_{t=1}^T \sum_{i=1}^N \left(\frac{1}{1 + \lambda_{Grid_t}} \cdot P_{Charge_{t,i}} \right)^2 \right) \quad (22)$$

The added term increases for high values for $P_{Charge_{t,i}}$ and low values for the price λ_{Grid_t} . Ultimately, resulting in a lower value for the total cost. This causes the model to prefer charging at higher charging power for each EV. To allow for adjusting the penalty function the variable λ_{Weight} is added to the cost function. Various values for this variable are tested and compared in Section 5.2.

The performance of all three cost functions, presented in Equations 20, 21 and 22 are compared in section 5.2. In total this results in the following variations of optimization models that are simulated, presented in Table 4.4:

Table 4.4 Tested optimization models and their specifications.

Optimization model	Time sample (Ts)	Weight factor (λ_{Weight})
Bi-linear	15 min	-
	5 min	-
Linear	15 min	-
	5 min	-
Bi-linear w/ Penalty function	15 min	1
	5 min	1
Linear w/ Penalty function	15 min	1
		0.6
		0.4
	5 min	1
		0.6
		0.4

The models are formatted as [model]_[timesample]_[weight].

4. Methods

4.5. Optimization model

The optimization model is programmed in python using the Pyomo package. The optimization model is solved using the iPOPT solver. This solver is chosen since it allows for solving non-linear optimization problems (Kawajir et al., 2023). This is useful since the initial optimization problem includes a bilinear function, making it non-linear.

Hardware

The simulations are run within the Jupyter notebook using the Python 3 IPykernel. The hardware specifications of the computer used for the simulations are the following:

Table 4.5 Hardware specifications of the simulation computer

Central processing unit (CPU)	Intel i7 11800-H @ 2.30 Hz
Graphics processing unit (GPU)	Nvidia Geforce RTX 3080 (Laptop)
Memory	32 GB 3200 MHz DDR4
Drive	Samsung PM9A1 M.2 SSD

Computational times

For all the different optimization models the computational times are collected for later comparison. These computational times are received directly from iPOPT. It is called the “Total CPU secs in IPOPT (w/o function evaluations)”. For each case, the optimization models are run 3 times, collecting the computational time each time. Finally, the computational times are averaged.

PHIL-testbed

A PHIL-testbed is used in the project to emulate EV charging with hardware. This testing was performed at Avans Smart Energy Lab. The testbed allows for running simulations with the use of real hardware components. The components on the PHIL-testbed include a bidirectional DC EV charger, an EV emulator, a multimeter, measuring grid voltages and currents and a host computer. The hardware is presented below in Table 4.6.

Table 4.6: The hardware on the PHIL-testbed

EV emulator	Delta Elektronika SM15k (PSU)
DC EV charger	PRE Power Developers 10 kW V2G charger module V2



Figure 4.3: The PHIL testbed at Avans SEND Lab

4. Methods

The PHIL-testbed is controlled from MATLAB Simulink. Simulink loads the optimal current values as calculated by the optimization model in Python. These current values are then used as input for an EV battery model in Simulink. The EV battery model calculates voltage values for the EV emulator based on SOC. Since this is unknown, various values for the SOC should be tested when running the PHIL simulations. The current values are directly sent to the EV charger. Finally, the testbed measurements are sent back to Simulink and stored. A diagram of the PHIL simulation process in Simulink is presented in Figure 4.4.

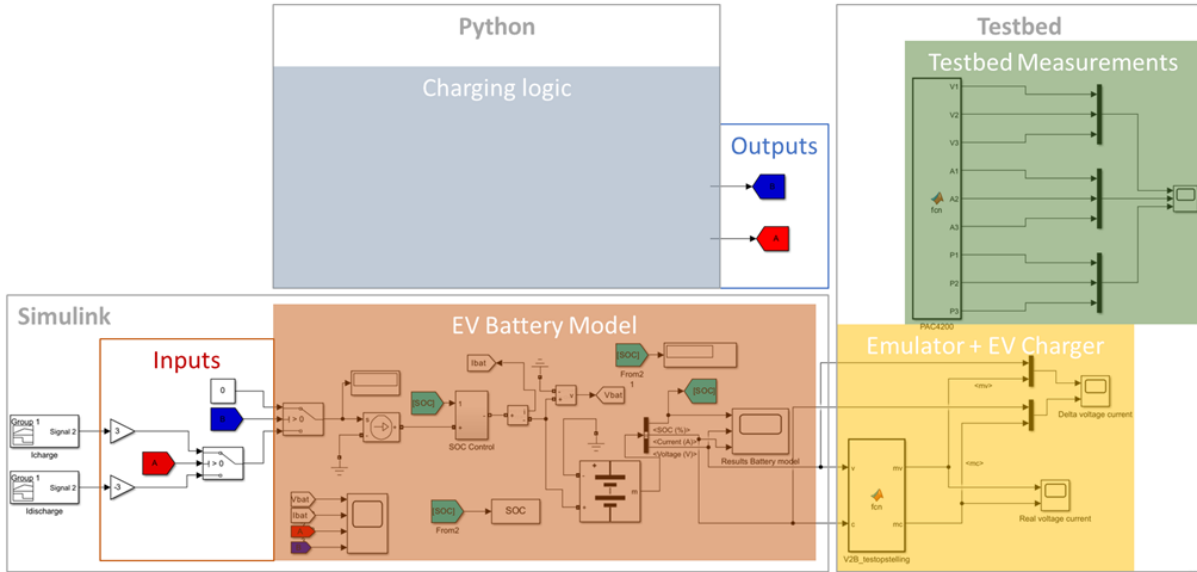


Figure 4.4: Diagram showing the PHIL simulation process in Simulink

By using the PHIL-testbed it is possible to increase the accuracy of the optimization model. This starts by measuring the energy charged by the EV emulator and the energy drawn from the grid. By dividing the energy charged by the EV emulator and the energy drawn from the grid the total charging efficiency can be calculated. This efficiency can then be used as input for the optimization model. Afterwards, the simulation can be rerun. Comparing the values calculated by the model to the values measured at the EV emulator and on the grid. This can give an insight into how accurate the optimization model is.

4.6. Simulation scenarios

Increased PV-generated electricity

Apart from running the optimization model on historic data, the model is tested on several simulation scenarios. The first scenario is an increase in PV-generated electricity. For example, taking into account that the number of solar panels can increase in the future. On the roof of the office of Kropman Breda, 65 solar panels are installed with a combined capacity of 16.9 kW. According to Google Earth the roof is approximately 556m². At the moment, about 70 to 100 m² of the roof is not used for solar panels. As visible in Figure 4.5, when comparing an area of 5 by 5 solar panels to the free space available, it is assumed that approximately 25 to 32 panels can be placed in the available space. This yields an increase in PV-generated electricity of 1.38 to 1.49, respectively.



Figure 4.5: The roof of the office with an area of approximately 70m² in red

Increased number of EVs

As the number of EVs continuously grows in the Netherlands, there is a large possibility that the number of EVs charging at the office will increase as well. Therefore, EV data sets are created with 10 to 20 EVs for simulating optimization modelling with a larger EV fleet. The datasets are created by combining historic EV data from various days in one table. The datasets can be found in Appendix A.

5. Results

5.1. Data analysis

During the equinox, in March, there is the largest potential for peak shaving and valley-filling. The amount of daylight is approximately equal to the amount of darkness (NOAA's National Weather Service, n.d.). This results in a relatively high amount of PV-generated electricity. However, the outdoor temperatures are still relatively low, with an average of 7.3 °C in 2022 (KNMI & de Wijs, 2022). Therefore, there is a high heating demand, which depends greatly on the internal solar gain. This can result in a fluctuating building load, as visible in Figure 5.1 on Tuesday. Figure 5.1 was drawn for the days of 21st to 24th March.

When looking at the graphs of Wednesday the 23rd of March (in Figure 5.1), EV charging took place largely in the morning. Even though there was more PV-generated electricity available in the afternoon. This resulted in a large power peak in the morning and a valley in the afternoon. Furthermore, on Tuesday no EV charging took place. However, when looking at the building load, if EV charging did take place there would be a potential for efficiently planning EV charging.

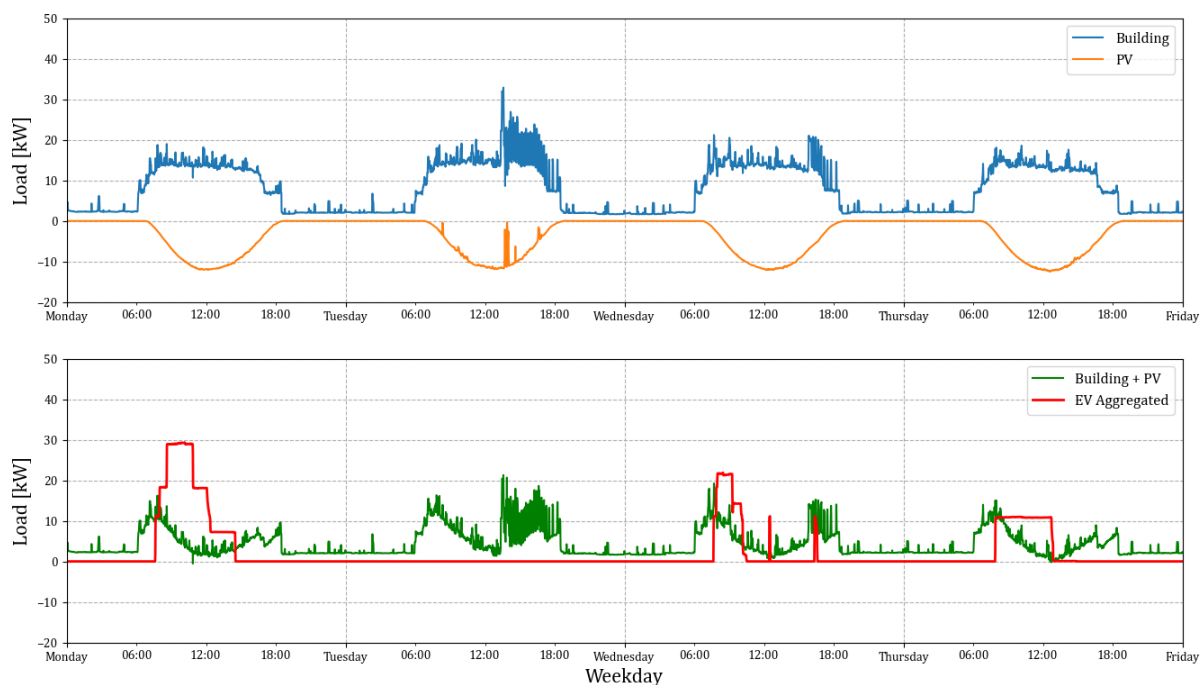


Figure 5.1: Valley-filling and peak-shaving potential in March

When looking at the graphs in Figure 5.2 for the week of June 19th to June 24th, the smart charging potential is less obvious. The amount of PV-generated electricity is high, and the building load is low on most days, compared to March and December. Furthermore, the EV load profiles have lower power peaks and are more spread out during the day. However, the EV loads on Monday and Wednesday could have been shifted to when the building load was lower and PV-generated electricity is available, assuming the idle time to be longer than the charging time on those days.

5. Results

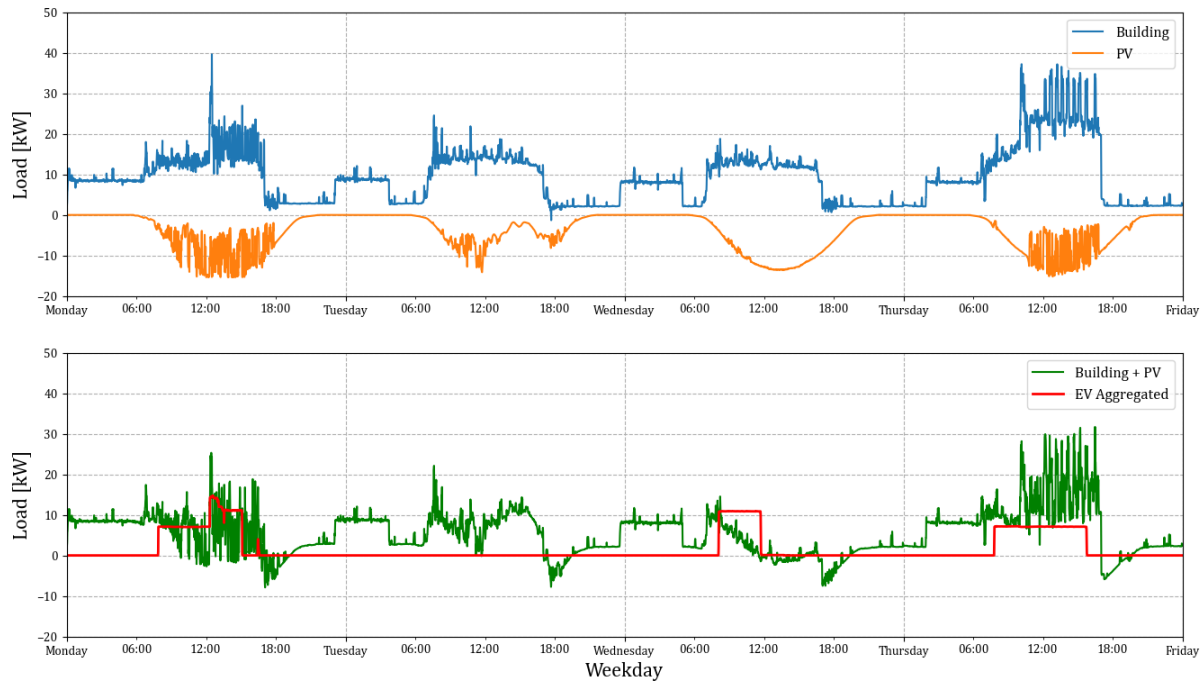


Figure 5.2: Valley-filling and peak-shaving potential in June

The amount of PV-generated electricity in the winter is very low compared to the building load. Nonetheless, as visible in Figure 5.3, there is a potential for peak shaving and valley-filling. In the building load, there are both peaks and valleys which can be flattened by re-distributing the EV loads.



Figure 5.3: Valley-filling and peak-shaving potential in December

5. Results

5.2. Optimization models

In this section, the performance of the different optimization models, described in Section 4.4, is presented.

5.2.1. Computational times

Table 5.1, Table 5.2 and

Table 5.3 show that, overall, the linear optimization models have a shorter computational time compared to the bi-linear optimization models. Decreasing the time resolution from 15 to 5 minutes increases the computational times of both the bilinear and linear optimization models. When looking at the computation times for all three dates, the computational times do not necessarily increase more for the bi-linear optimization models compared to the linear optimization models. However, since the linear optimization models have a lower computational time in general when the computational time increases due to a larger amount of input data, the bi-linear optimization model has a significantly longer computation time. In some cases, the bi-linear model can take more than 40 times longer to compute compared to linear models. For example, when comparing the bi-linear to the linear optimization models with a time resolution of 5 minutes in Table 5.1 and

Table 5.3. Next to the computational times, the difference Δ and the increase x in computational time compared to the baseline bilinear and linear optimization model are presented.

Table 5.1 Computational times of different optimization models for March 21st

Optimization model	Computational time (Tc) [s]	Δ	x
Bilinear_15min (baseline)	0.74	-	-
Bilinear_5min	41.05	40.31	55.47
Bilinear_penalty_15min	0.97	0.23	1.31
Bilinear_penalty_5min	41.37	40.63	55.91
Linear_15min (baseline)	0.06	-	-
Linear_5min	0.06	0.00	1.00
Linear_penalty_15min	0.26	0.20	4.41
Linear_penalty_5min	0.92	0.86	15.58

5. Results

Table 5.2 Computational times of different optimization models for June 20th

Optimization model	Computational time (Tc) [s]	Δ	x
Bilinear_15min (baseline)	0.25	-	-
	3.85	3.60	15.41
	0.30	0.05	1.20
	4.00	3.75	16.00
Linear_15min (baseline)	0.02	-	-
	0.07	0.04	3.00
	0.05	0.03	2.18
	0.27	0.25	12.45

Table 5.3 Computational times of different optimization models for December 12th

Optimization model	Computational time (Tc) [s]	Δ	x
Bilinear_15min (baseline)	0.94	-	-
	37.93	36.99	40.35
	1.26	0.32	1.34
	40.09	39.15	42.65
Linear_15min (baseline)	0.03	-	-
	0.08	0.05	3.12
	0.21	0.18	8.28
	0.66	0.64	26.48

The optimization models with and without the penalty function, have similar computational times. When looking at Table 5.1 and

Table 5.3, only for the linear optimization models with a time resolution of 5 minutes there is a significant increase in the computational time when adding a penalty function. However, the computational times are still low compared to the bi-linear computational models with a penalty function.

5.2.2. Control performance

As discussed earlier in Section 4.4, the optimization model initially showed unwanted behaviour when calculating the current for each EV. An example can be seen in Figure 5.4. The model charges multiple EVs at once. The second graph in Figure 5.4. shows that low currents are calculated for some of the EVs. For one of the EVs, the current is around 20 A for a long time and lower than 20 A for a shorter time.

5. Results

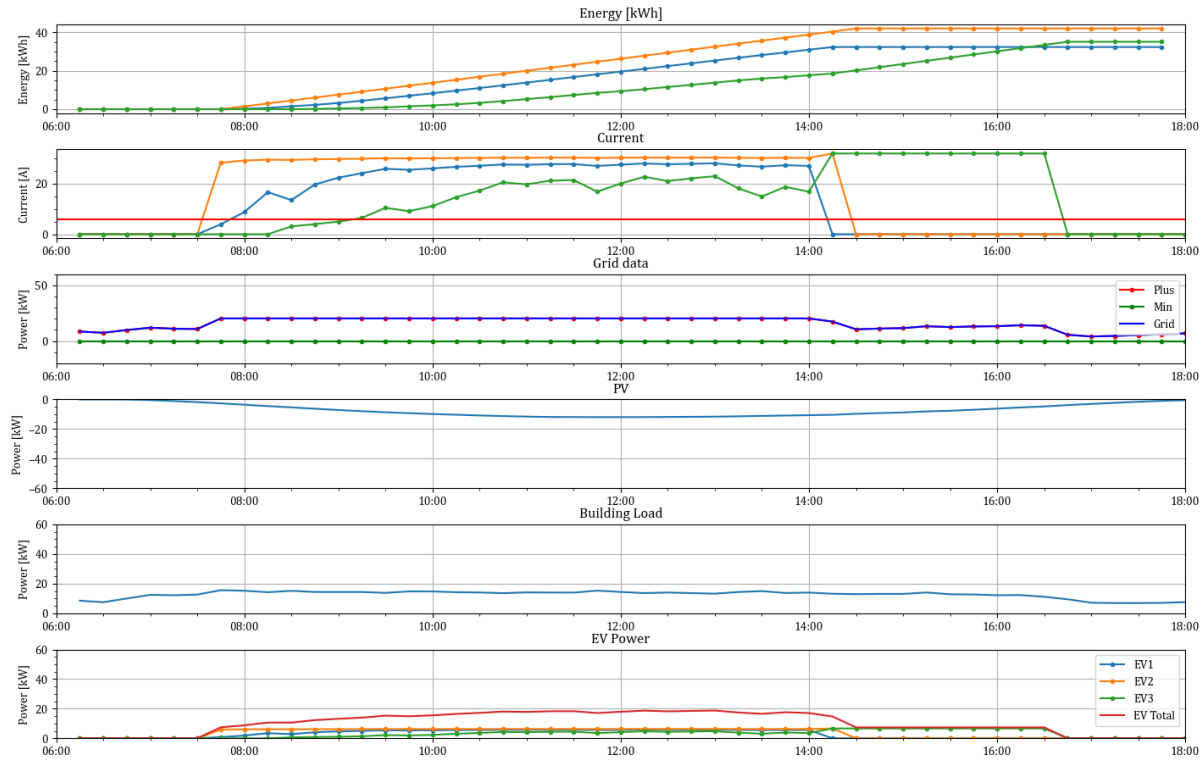


Figure 5.4: EV data on March 21st for bi-linear_15 min optimization model (in the second top graph the red line indicates the minimum of 6A)

In this section only the results of March 21st for the bi-linear optimization model are presented. However, this behaviour is seen on all three test dates for both the bi-linear and linear optimization models. The figures with the EV data graphs for all test dates and both models can be found in Appendix B.

Penalty function

Adding a penalty function to the optimization objective results in higher current output values for the EVs. In Figure 5.5, for all three EVs higher current values, around 32 A, are calculated. Charging of the three EVs takes place alternately rather than at the same time. However, for one of the EVs at one time step a current of 6 A is calculated, which is the minimum charging current possible.

The control performance is improved on all test dates for both models. All the EV data graphs can be found in Appendix B.

The time resolution of 5 minutes

As shown in Figure 5.5, when lowering the time resolution from 15 minutes to 5 minutes the optimization model continues to calculate high current values.

5. Results

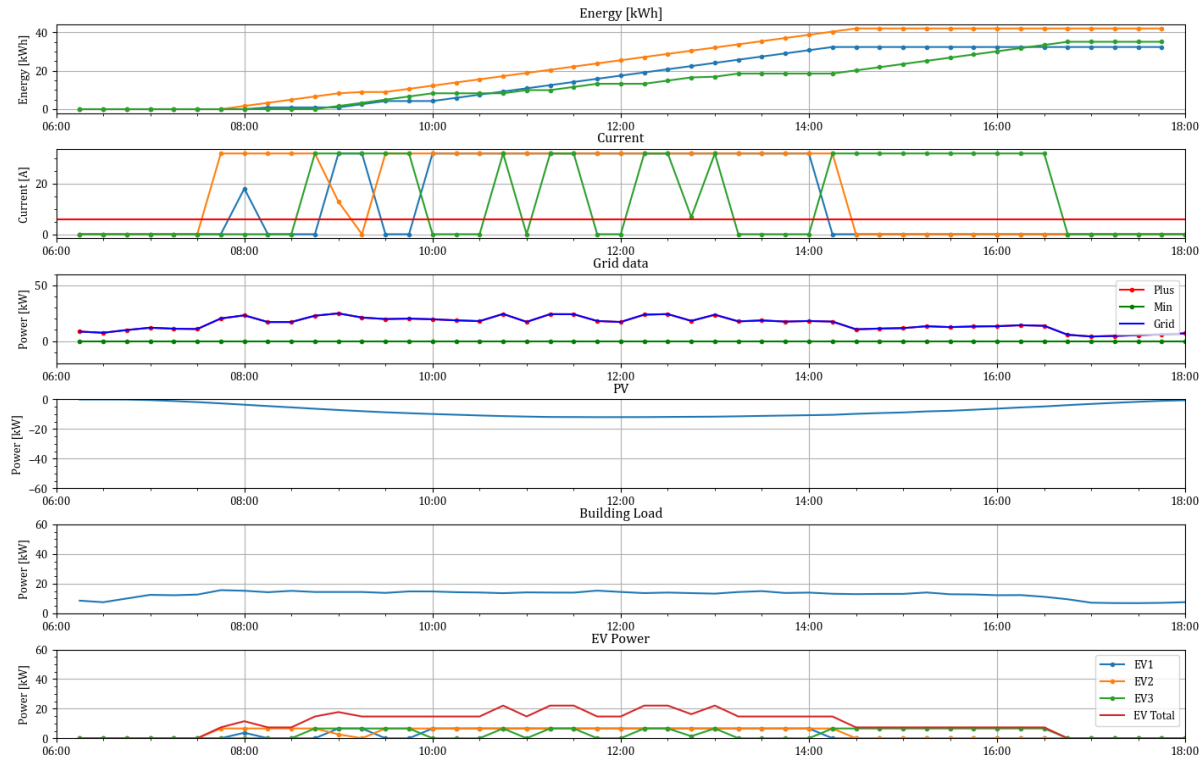


Figure 5.5: EV data on March 21st for bilinear_penalty_15min optimization model

5.2.3. KPIs

When comparing the bi-linear optimization model with the penalty function to its linear counterpart, the performance is not significantly different. From the information in Table 5.4, it follows that the SS and SC, all optimization models perform the same on all the simulation dates. Except on June 20th, where there is a marginal difference in SS and SC between the 15- and 5- minute resolution models.

As visible in Table 5.5, the reduced peak power value (PPR) for the bilinear and linear models without a penalty function are equal on all three simulation dates. However, there is difference in performance between the 15- and 5- minute resolution models, the latter resulting in a higher PPR in most cases. On the 20th of June, the PPR for the bilinear and linear optimization models is equal.

Furthermore, on March 21st the optimization models without a penalty function have a higher PPR compared to the models with a penalty function. Lowering the weight of the penalty function does increase the PPR for March 21st and December 12th. For March 21st this increase reaches a maximum of 1.02 kW for a weight (λ_{Weight}) of 0.6. The linear optimization models with penalty function have a higher PPR on the 12th of December compared to the bi-linear models with a penalty function.

Table 5.4: SS and SC on the three simulations dates

Optimization model	March 21 st	June 20 th	December 12 th
--------------------	------------------------	-----------------------	---------------------------

5. Results

	SS [%]	SC [%]	SS [%]	SC [%]	SS [%]	SC [%]
Historic data 15 min	31.1	100.0	37.9	96.0	15.4	100.0
Bilinear_15min	31.1	100.0	37.9	96.0	15.4	100.0
Linear_15min	31.1	100.0	37.9	96.0	15.4	100.0
Bilinear_penalty_15min	31.1	100.0	37.9	96.0	15.4	100.0
Linear_penalty_15min	31.1	100.0	37.9	96.0	15.4	100.0
Linear_penalty_15min_0.6	31.1	100.0	37.9	96.0	15.4	100.0
Linear_penalty_15min_0.4	31.1	100.0	37.9	96.0	15.4	100.0
Historic data 5 min	31.1	100.0	37.4	96.1	15.4	100.0
Bilinear_5min	31.1	100.0	37.4	96.1	15.4	100.0
Linear_5min	31.1	100.0	37.4	96.1	15.4	100.0
Bilinear_penalty_5min	31.1	100.0	37.4	96.1	15.4	100.0
Linear_penalty_5min	31.1	100.0	37.4	96.1	15.4	100.0
Linear_penalty_5min_0.6	31.1	100.0	37.4	96.1	15.4	100.0
Linear_penalty_5min_0.4	31.1	100.0	37.4	96.1	15.4	100.0

Table 5.5 PPR on the three simulation dates

Optimization model	March 21st	June 20th	December 12th
	PPR	PPR	PPR
Bilinear_15min	16.66	10.41	9.27
Bilinear_5min	16.96	14.44	10.80
Linear_15min	16.66	10.41	9.27
Linear_5min	16.96	14.44	10.80
Bilinear_penalty_15min	12.13	8.81	5.20
Linear_penalty_15min	11.75	8.81	5.32
Linear_penalty_15min_0.6	11.75	8.81	5.98
Linear_penalty_15min_0.4	12.77	8.81	6.14
Bilinear_penalty_5min	12.70	13.88	4.36
Linear_penalty_5min	12.35	13.88	5.93
Linear_penalty_5min_0.6	12.35	13.88	7.27
Linear_penalty_5min_0.4	13.15	13.88	7.87

5. Results

5.3. Simulation Scenario's

5.3.1. Historic data vs optimization data

In Figure 5.6, Figure 5.7 and Figure 5.8, the performance of the linear optimization model with a time penalty with a weight factor of 0.4 and a time resolution of 5 minutes on the three test dates is presented. When comparing the three test dates, it is visible that on March 21st there was the largest potential to shift EV loads. This can be recognized by the relatively flat EV power and grid power for the controlled data compared to the uncontrolled historic data.

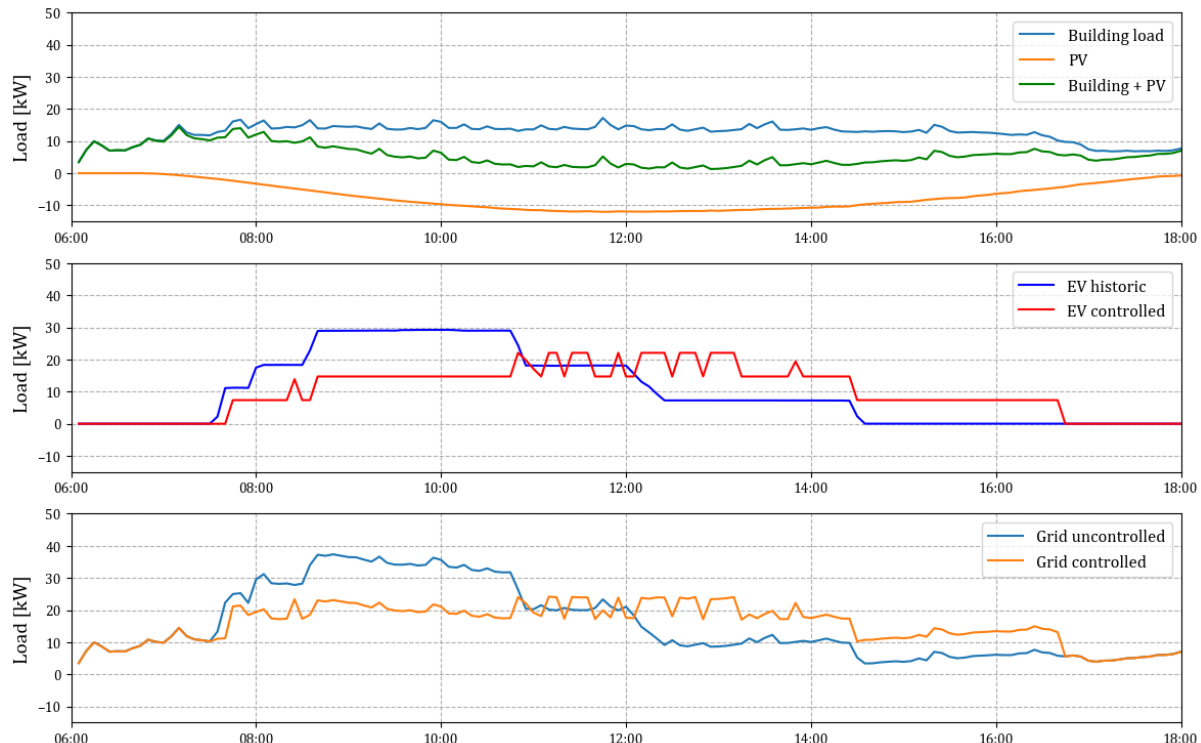


Figure 5.6: Historic data vs optimization data on March 21st for linear_penalty_5min_0.4

On June 20th and December 12th, the EV load and grid power profiles were already close to flat. This is also supported by the results for the KPIs, presented in **Error! Reference source not found.**. On March 21st the PPR is the highest of the three test dates.

5. Results

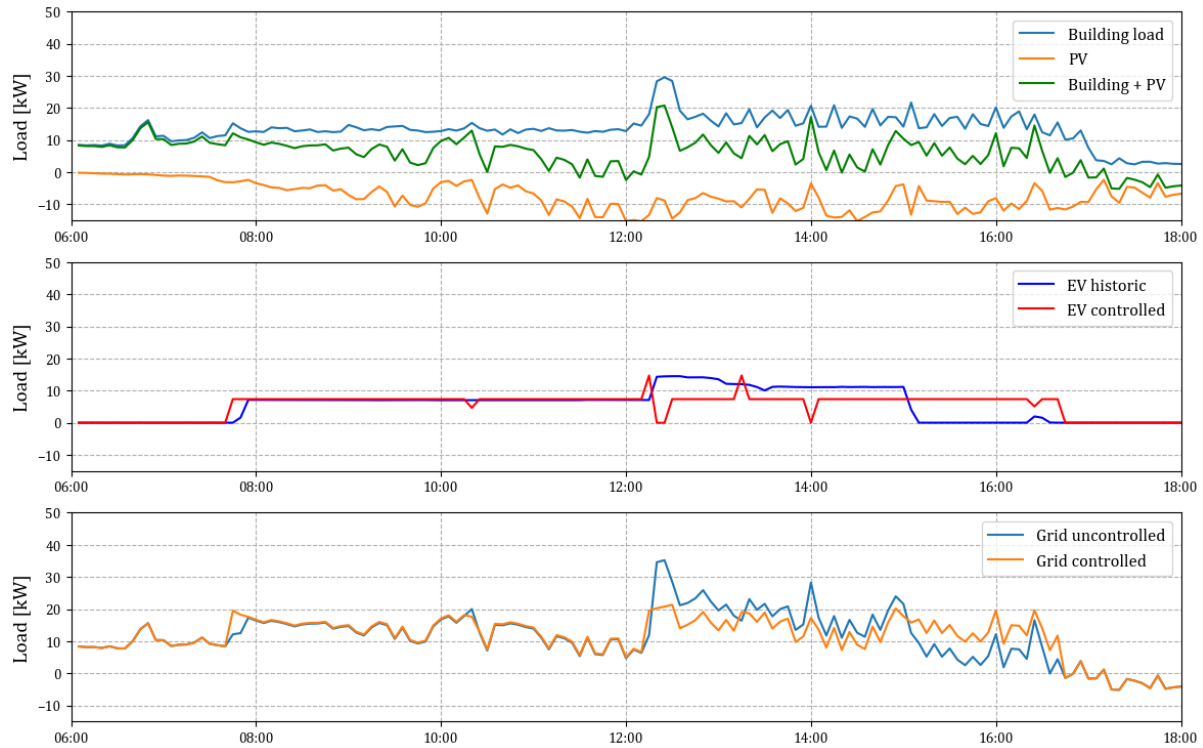


Figure 5.7: Historic data vs optimization data on June 20th for linear_penalty_5min_0.4

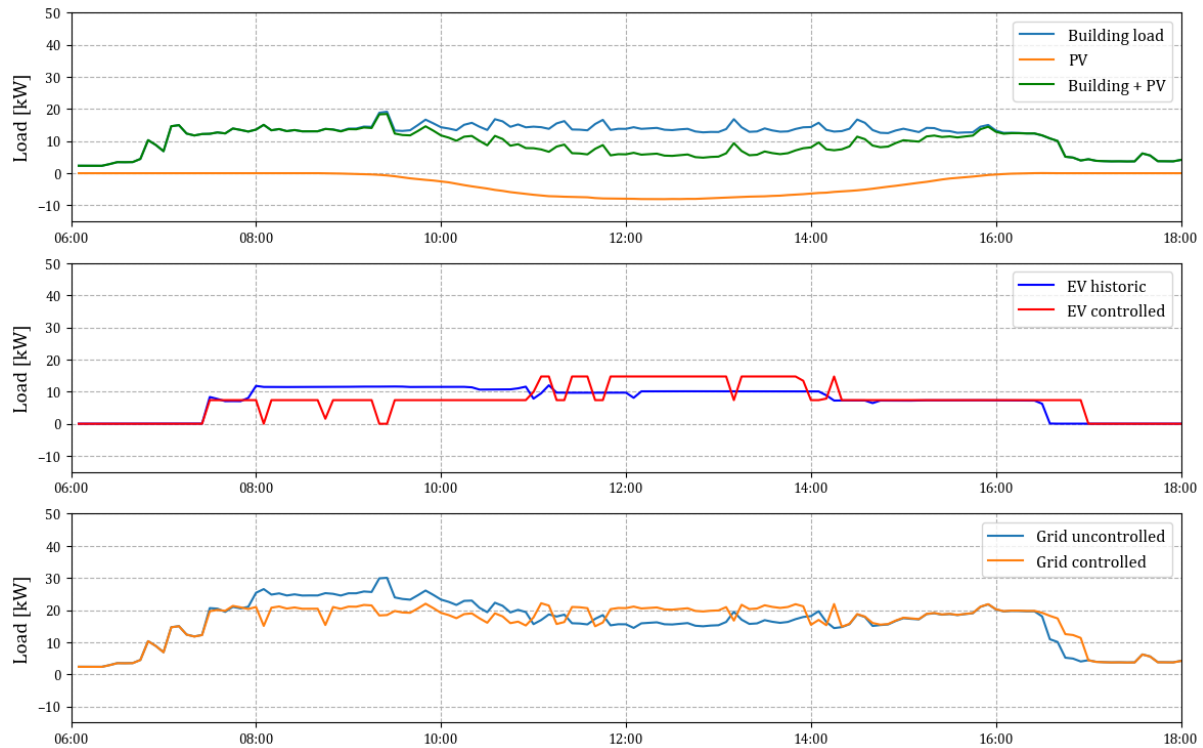


Figure 5.8: Historic data vs optimization data on December 12th for linear_penalty_5min_0.4

5. Results

For all test dates, although the redistribution of the EV load results in a PPR and peak-shaving overall, the SS and SC are not increased. However, when comparing the historic data to the optimization data on a day with a relatively low building load and high PV-generated electricity, the SS and SC values are impacted. As shown in Figure 5.9, on July 6th, the model is able to spread out the EV load over the entire day. Furthermore, since on that day, there was a surplus of PV-generated electricity, as visible in Table 5.6, there is an increase in the SS and SC when re-distributing the EV load during the day using the optimization model.

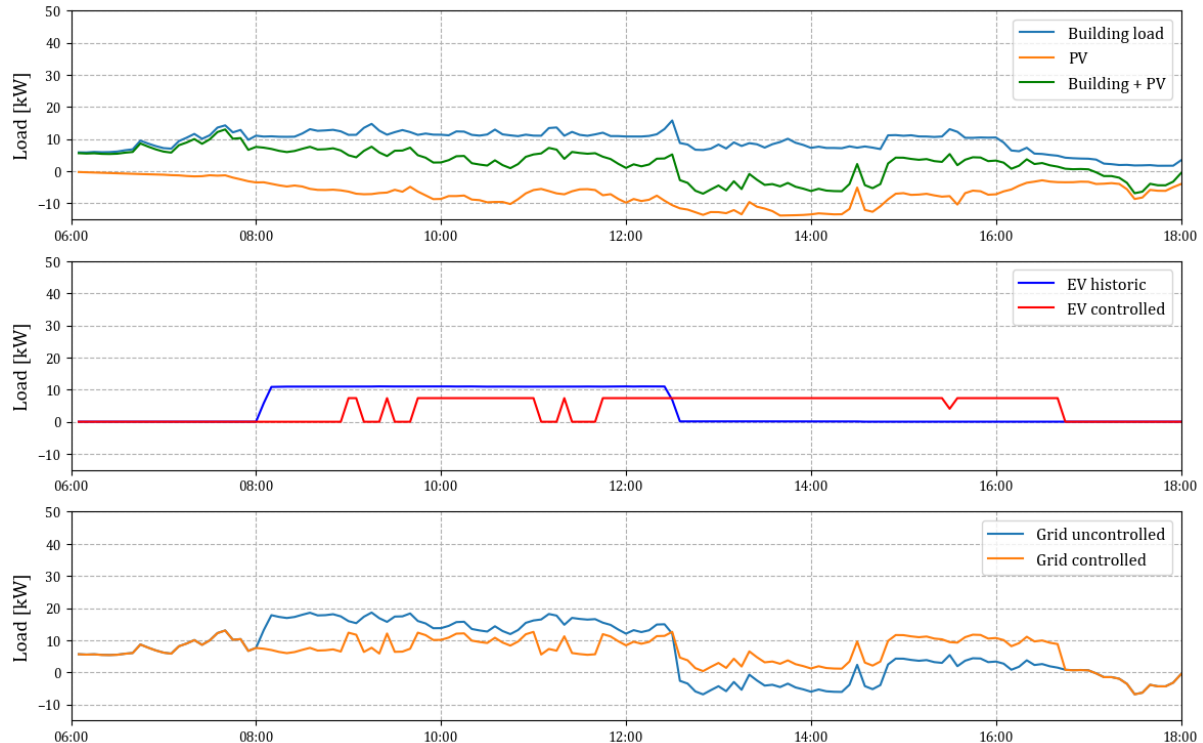


Figure 5.9: Historic data vs optimization data on July 6th for linear_penalty_5min_0.4

Table 5.6: KPIs of historic data vs optimization data on July 6th

Optimization model	PPR [kW]	SS [%]	*Δ	SC [%]	Δ
Historic data 5 min	-	42.3	-	83.6	-
Linear_penalty_5min_0.4	5.60	48.6	+6.27	96.0	+12.35

5. Results

5.3.2. Increasing the number of EVs

When comparing the second graphs in Figure 5.6 and Figure 5.10, it is visible that increasing the amount of EVs from 3 to 10 results in a larger power peak in the morning. As visible in Figure 5.10, the optimization model successfully re-distributes the EV loads during the day, flattening the load profile of the EVs. This results in peak shaving in the morning and valley-filling in the evening. Furthermore, when looking at the results in Table 5.7, it follows that the total charged energy is almost equal between the uncontrolled scenario and the optimization model, with only a deviation of around 2%.

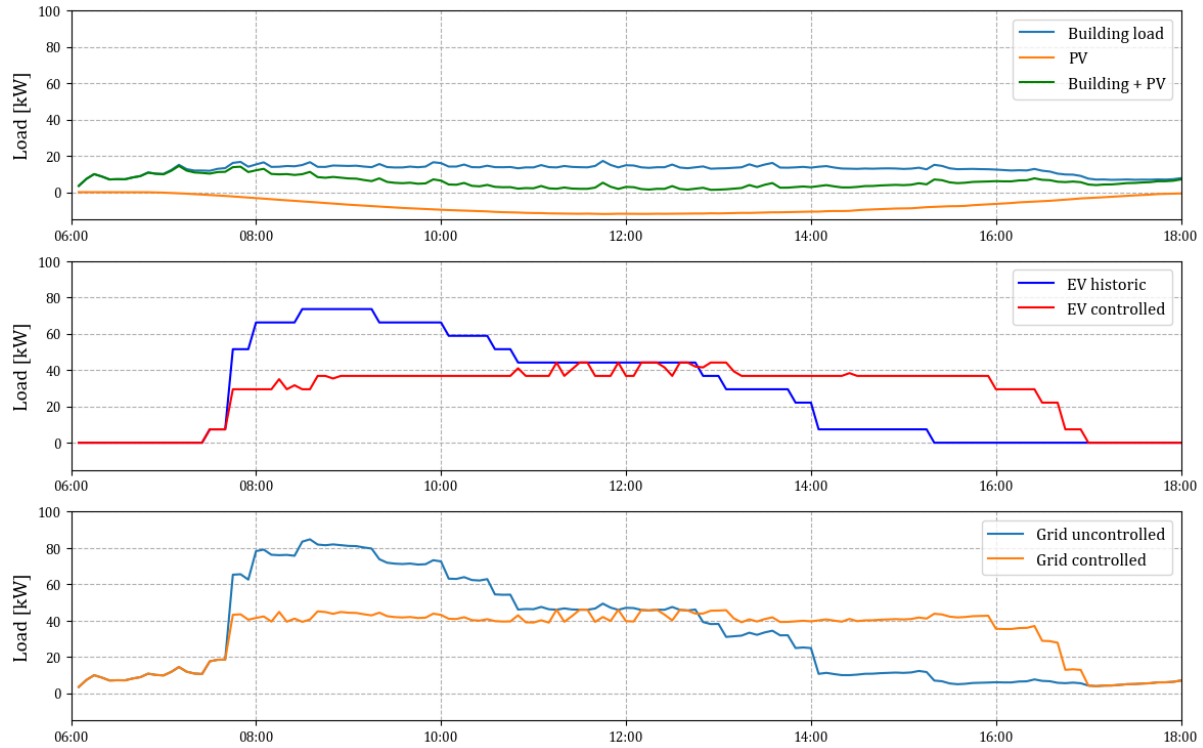


Figure 5.10: Uncontrolled charging of 10 EVs vs optimization model on March 21st

Table 5.7: Amount of energy charged for 10 EVs

Optimization model	Total EV energy [kWh]	Δ
Input data	330.86	-
*Uncontrolled	335.49	+4,63
Linear_penalty_5min_0.4	330.86	-

*Data artificially created using historic data to resemble uncontrolled charging

In Figure 5.11, the scenario with 20 EVs is presented, based on the combined EV data of various days, as explained in Section 4.6. In this case, two things are noticeable: Firstly, the power peaks are higher than compared to the uncontrolled scenario with 10 EVs. Secondly, in contrast to the scenario with 10 EVs, the EV loads are more spread out during the day. Nonetheless, the optimization model significantly flattens the EV load profile. When looking at the total charged energy, in Table 5.8, this is higher than for the uncontrolled scenario. However, the deviation is still only around 2%. In this scenario,

5. Results

the amount of energy charged by the optimization model is slightly lower than compared to the input EV data. However, this is marginal.

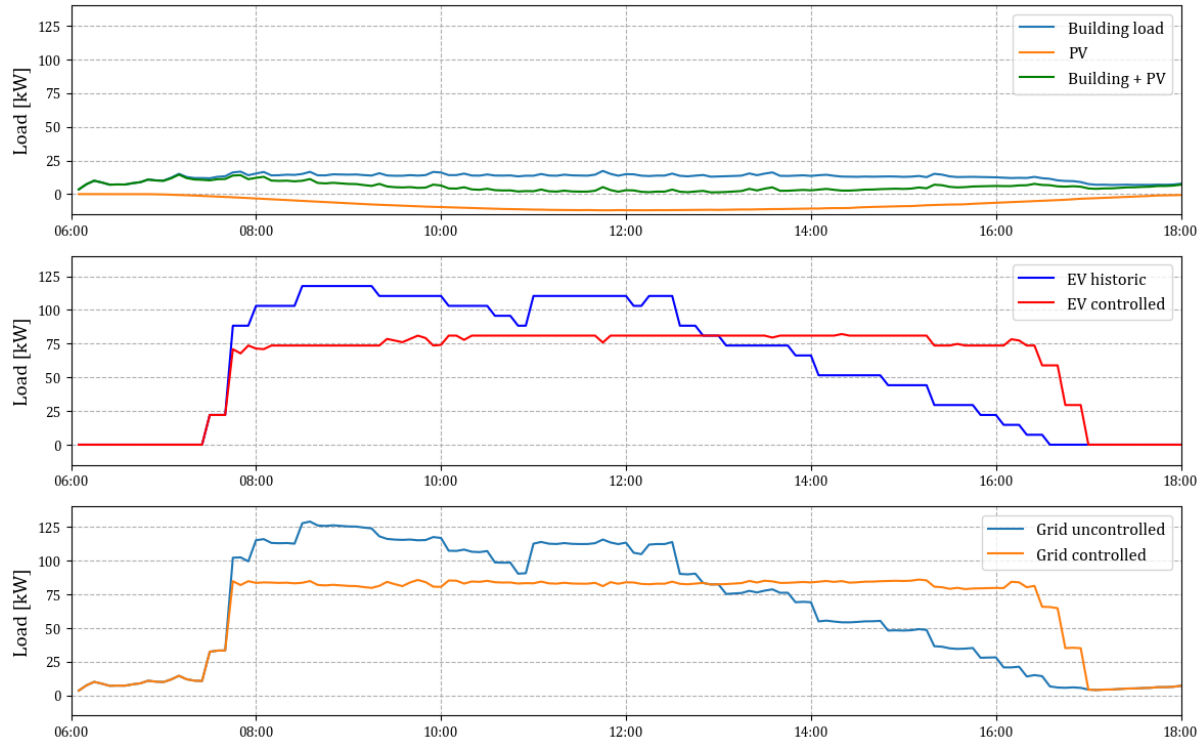


Figure 5.11: Uncontrolled charging of 20 EVs vs optimization model on March 21st

Table 5.8: Amount of energy charged for 20 EVs

Optimization model	Total EV energy [kWh]	Δ
Input data	712.13	-
*Uncontrolled	724.35	+12.22
Linear_penalty_5min_0.4	711.66	-0.47

*Data artificially created using historic data to resemble uncontrolled charging

From the information in Table 5.9, it is evident that increasing the number of EVs increases the computational time of the model. Increasing the number of EVs from 3 to 10 increases the computational time 6.4 times and from 3 to 20 EVs increases the computational time 16.2 times.

As shown in Table 5.10, when increasing the number of EVs the SS decreases. This is caused by the increasing EV load. Furthermore, the PPR increases when increasing the number of EVs for these scenarios.

Table 5.9: Computational times for different numbers of EVs on March 21st

Optimization model	Computational time (Tc) [s]	Δ	x
Linear_penalty_5min_0.4 (3 EVs)	0.970	-	-
Linear_penalty_5min_0.4 (10 EVs)	7.367	6,397	7.60

5. Results

Linear_penalty_5min_0.4 (20 EVs)		17.204	16.234	17.74
----------------------------------	--	--------	--------	-------

Table 5.10: KPIs for different numbers of EVs on March 21st

Optimization model	PPR [kW]	SS [%]	Δ	SC [%]	Δ
Historic data 5 min	-	31.1	-	100	-
Linear_penalty_5min_0.4 (3 EVs)	7.91	31.1	-	100	-
*Uncontrolled (10 EVs)		17.5	-	100	-
Linear_penalty_5min_0.4 (10 EVs)	38.74	17.6	+0.1	100	-
*Uncontrolled (20 EVs)	-	9.7	-	100	-
Linear_penalty_5min_0.4 (20 EVs)	43.07	9.9	+0.2	100	-

* Data artificially created using historic data to resemble uncontrolled charging

5.3.3. Increasing solar energy and EVs

In this section, the amount of PV-generated electricity is multiplied by the factors described in Section 4.6. As shown in Table 5.12, when increasing the PV for the test date March 21st with a factor of 1.38, the overall SS and SC increase. There is no increase in the SS and SC for the optimization data compared to the historic data. When increasing the PV by a factor of 1.49, there is only a marginal increase in the SS. With the increasing amount of PV-generated electricity, the PPR does increase with steps of around 1 kW.

Table 5.11: KPIs for different amounts of PV on March 21st

Optimization model	PPR [kW]	SS [%]	Δ	SC [%]	Δ
Historic data 5 min	-	31.1	-	100	-
Linear_penalty_5min_0.4	13.15	31.1	-	100	-
Historic data 5 min (PV x1.38)	-	42.9	-	100	-
Linear_penalty_5min_0.4 (PV x1.38)	14.81	42.9	-	100	-
Historic data 5 min (PV x1.49)	-	46.1	-	100	-
Linear_penalty_5min_0.4 (PV x1.49)	15.47	46.4	+0.3	100	-

When exploring another test data, the 6th of July, the results are different. On the 6th of July, the amount of PV-generated electricity was already relatively high compared to the building load. As visible in Table 5.12, when increasing the amount of PV-generated electricity the SS and SC increase. Contrary to the test date of March 21st, the model increases the SS and SC even further when the PV is increased. However, this increase is not significantly higher compared to the simulation without an increase in PV.

Finally, when increasing the number of EVs, the SS and SC drop both for the uncontrolled data and the optimized data. The increase in SS and SC due to the

5. Results

optimization model is reduced as well. The PPR, similarly to the results shown in Table 5.12, is increased when increasing the amount of EVs from 3 to 10.

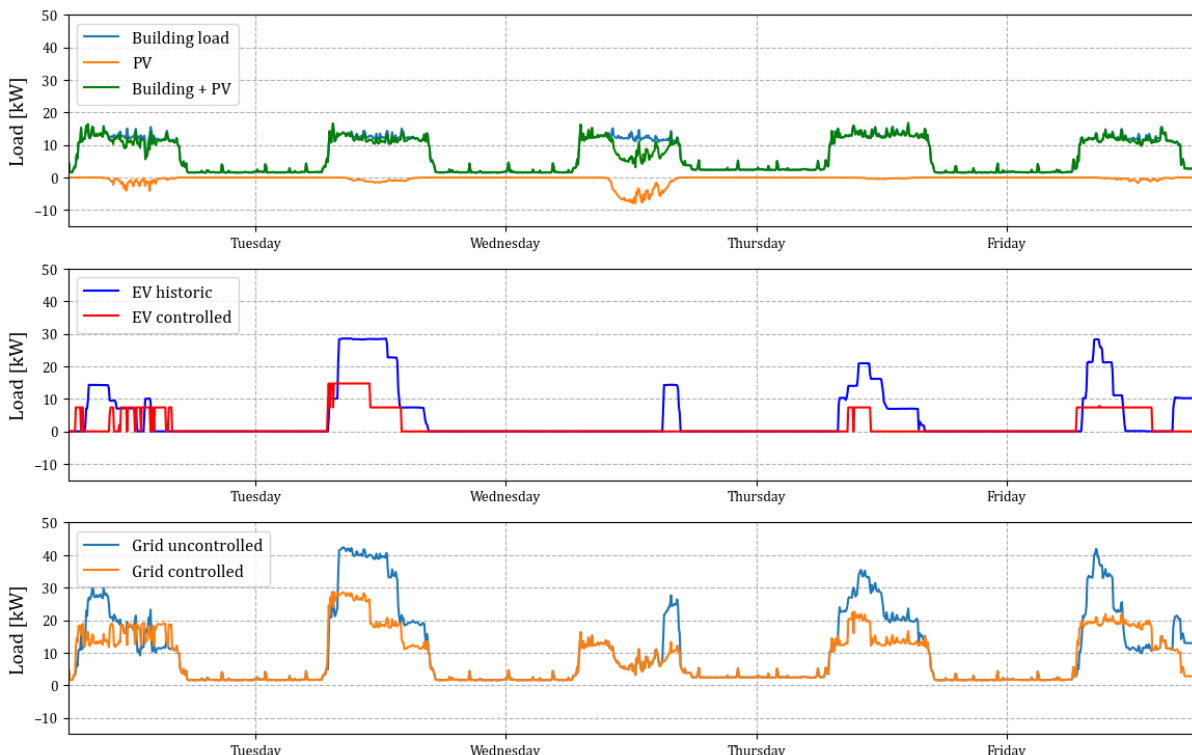
Table 5.12: KPIs for different amounts of PV and EVs on July 6th

Optimization model	PPR [kW]	SS [%]	Δ SC [%]	Δ
Historic data 5 min	-	42.3	-	83.7
Linear_penalty_5min_0.4	5.60	48.6	+6.3	96.0 +12.3
Historic data 5 min (PV x1.38)	-	53.4	-	76.5
Linear_penalty_5min_0.4 (PV x1.38)	3.95	63.3	+9.9	90.7 +14.2
Historic data 5 min (PV x1.49)	-	56.3	-	74.7
Linear_penalty_5min_0.4 (PV x1.49)	3.56	66.7	+10.4	88.4 +13.7
*Uncontrolled data 5 min (PV x1.38 & 10 EVs)	-	23.3	-	93.2
Linear_penalty_5min_0.4 (PV x1.38 & 10 EVs)	38.79	24.0	+0.7	95.2 +2.0
*Uncontrolled data 5 min (PV x1.49 & 10 EVs)	-	24.8	-	92.0
Linear_penalty_5min_0.4 (PV x1.49 & 10 EVs)	39.01	25.9	+1.1	95.0 +3.0

* Data artificially created using historic data to resemble uncontrolled charging

5.3.4. Welkom Kropman

A simulation is performed on one week of Welkom Kropman data and historic load data. As shown in Figure 5.12, on most days the EV loads in the optimization model are much lower compared to the historic data. Only on Monday, are EV loads similar.



5. Results

Figure 5.12: Historic data vs optimization model for 9 to 13 January

Below, in Table 5.13, the Welkom Kropman EV data as entered by the employees for that week is presented. In Table 5.14, the EV data is visible after the requested amount of energy has been checked for feasibility. Which is done as described in Section 4.1. It is visible that for some of the EVs, the requested amount of energy is greatly reduced by the check. For example, on the 13th of January, the requested energy for one of the EVs is reduced from 50 to 18.4.

Table 5.13: Welkom Kropman EV data for 9 to 13 January

ChargerId	E_requested	T_arrival	T_departure
3	38	09/01/2023 06:45	09/01/2023 16:00
1	54	10/01/2023 06:55	10/01/2023 14:00
4	64	10/01/2023 07:00	10/01/2023 11:00
0	50	12/01/2023 08:50	12/01/2023 11:00
1	35	13/01/2023 06:45	13/01/2023 14:00
4	50	13/01/2023 07:25	13/01/2023 10:00
3	38	09/01/2023 06:45	09/01/2023 16:00

Table 5.14: EV data for 9 to 13 January after the feasibility check

ChargerId	E_requested	T_arrival	T_departure
3	38	09/01/2023 06:45	09/01/2023 16:00
1	51.52	10/01/2023 06:55	10/01/2023 14:00
4	28.83	10/01/2023 07:00	10/01/2023 11:00
0	15.33	12/01/2023 08:50	12/01/2023 11:00
1	35	13/01/2023 06:45	13/01/2023 14:00
4	18.4	13/01/2023 07:25	13/01/2023 10:00
3	38	09/01/2023 06:45	09/01/2023 16:00

5. Results

5.4. PHIL-testbed

A test run is performed using the PHIL testbed. For three dates, the amount of energy charged in different stages of the test run is presented in Table 5.15. On the 21st of March and 20th of June the amount of energy going into the EV, calculated by the optimization model, is higher than the input data. Furthermore, the actual energy as measured by the EV emulator is even higher than the energy calculated by the optimization model. On December 12th, both the energy going into the EV emulator and the energy calculated by the optimization model are lower than the requested amount of energy. When looking at Figure 5.13, the test run on the date of December 12th, resulted in less current values and charged energy for the EV emulator compared to calculated in the model.

Table 5.15: Amount of energy charged at different stages in the PHIL-testbed simulation

Date	Energy EV emulator [kWh]	Energy optimization model [kWh]	Input data energy [kWh]
21-03-2022	3.689	3.418	3.325
20-06-2022	2.462	2.279	2.217
12-12-2022	3.170	4.178	4.680

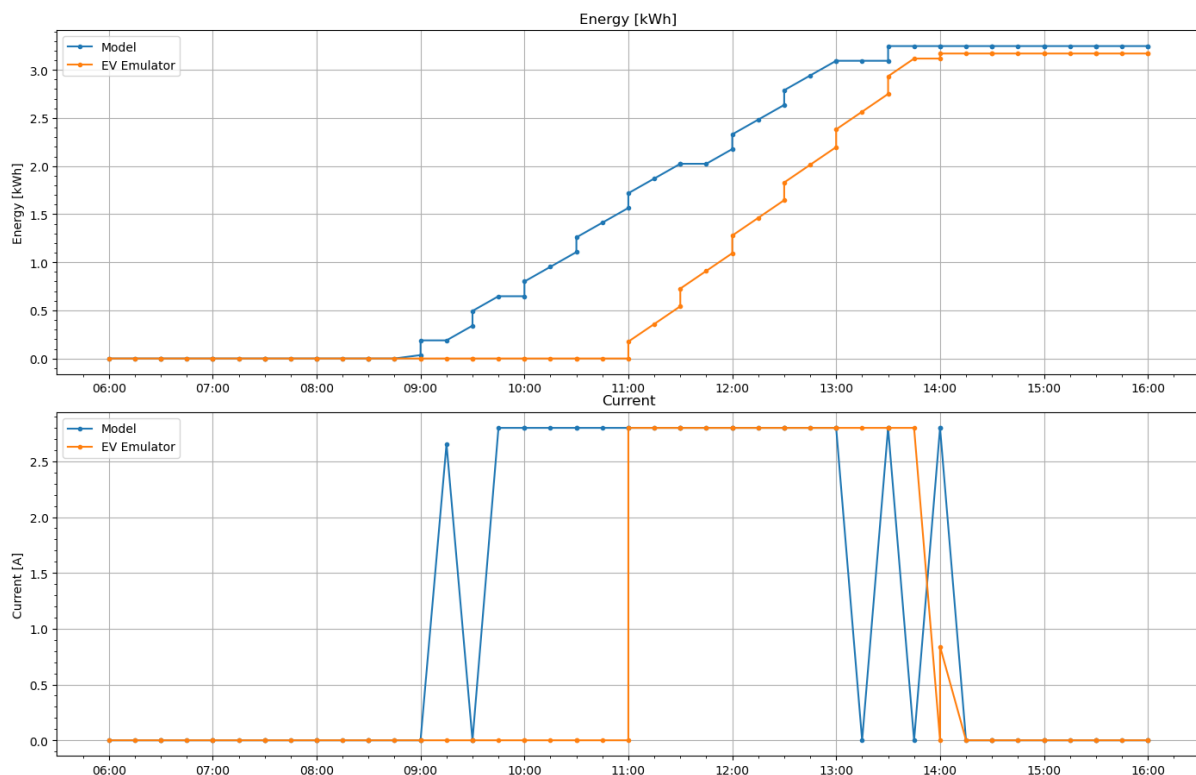


Figure 5.13: Charging on December 12th in the optimization model vs EV emulator.

6. Discussion

6.1. Optimization models

Compared to linear optimization models, bilinear optimization models generally have higher computational times. This can be attributed to the presence of the bilinear function, as discussed in Section 5.2.1. When increasing the time resolution of the optimization model, the computational time of the bilinear models increases significantly compared to that of the linear models. However, despite the longer computational time, the performance of the bilinear and linear optimization models, as assessed by the KPIs, is very similar.

The addition of a penalty function to the cost model results in improved control performance of the optimization models. This is evidenced by the model calculating higher current values for each EV, alternating charging, as opposed to charging EVs simultaneously with lower current values. This improvement applies to all optimization models. However, in most cases, the PPR decreases when the penalty function is added. This may be caused by the optimization model now prioritizing high current values over reducing power peaks.

Overall, all optimization models perform similarly on SS and SC for all three test dates, with only the PPR varying per optimization model. The models with a time resolution of 5 minutes generally have a higher PPR than those with a time resolution of 15 minutes. However, this can be caused by the data being resampled to 15 minutes. Since in that case the power peaks are reduced due to averaging the power values. The PPR is generally lower for models with a penalty function. Reducing the weight of the penalty function (λ_{Weight}) helps increase the PPR for two of the test dates. For linear models, increasing the time resolution is feasible. Computational times remain around 1 to 20 seconds, even when the number of EVs is increased to 20, which is well below the 5-minute interval.

Adding a penalty function to the cost function of the optimization model is crucial since charging with lower values results in lower efficiency (Apostolaki-Iosifidou et al., 2017). When considering computational times and KPIs, the linear optimization model with a time resolution of 5 minutes and a weight factor of 0.4 shows the best performance among models with a penalty function.

6.2. Simulation Scenario's

When comparing the historical data with the data from the optimization model, several observations can be made. For all three test dates, the SS and SC do not change. However, there is a significant increase in the PPR on all test dates. Of the three test dates, the largest PPR is observed on March 21st. On June 20th and December 12th, the PPR by the optimization model is less. However, when analyzing the impact of the model on July 6th, a day with relatively high PV-generated electricity and low building load, the SS and SC significantly improve as well.

Increasing the number of EVs results in a longer computation time, taking approximately 7 and 17 times longer for 10 and 20 EVs, respectively. As expected, the SS decreases with increasing EV load. The data from the optimization model does not

6. Discussion

show an increase in the SS. Furthermore, the SC remains at 100% as well. However, there is a significant increase in the PPR. Due to the increasing number of EVs, the power peaks significantly increase as most EVs charge in the morning. The optimization redistributes the EV load during the day, resulting in an increased PPR for each increment in EV.

When increasing the PV generated electricity on March 21st, the SS and SC increased according to the historic data. The further increase due to redistributing loads by the optimization model is marginal. The PPR increases by 1 to 2 kW when increasing the amount of PV and using the optimization model.

An increase of PV on July 6th, results in an increase of SS and SC for both a factor of 1.38 and 1.49. Using the optimization model the SS is increased by 9.9% and 10.3% for a factor of 1.38 and 1.49, respectively. This is a further increase of 3.7% and 4.1% compared to the initial increase of 6.3%. The SC does show a further increase of 1.3%, and 1.8% compared to the initial increase of 12.4% for a factor of 1.38 and 1.49, respectively. When increasing the number of EVs as well, the SS and SC increase for both PV factors. The influence of the optimization model on the key performance indicators (KPIs) is less in this scenario. Compared to the test date of March 21st, the PPR is similar for 10 EVs on July 6th.

Simulation on the week from 9 to 13 January, using the Kropman EV data as input, shows a large difference in the amount of energy charged between the historic data and the optimization data. When looking at the amount of energy entered in the form by employees and as input for the model there is a significant difference. The feasibility check reduces the requested amounts of energy on several days, such as on the 10th, 12th and 13th of January. Furthermore, on Wednesday the 11th of January, there is an EV load present in the historic data and no EV data from the Welkom Kropman form.

6.3. PHIL-testbed

The results of PHIL-testing showed that a higher amount of energy was charged by the EV emulator, compared to both the input energy data and the energy calculated by the optimization model. However, on December 12th, both the energy charged by the EV emulator and the calculated energy by the optimization model was lower than the input energy data. This was since the EV emulator did not receive the same current values as those calculated in the optimization model, resulting in lower current values.

The lower amount of energy calculated by the optimization model may have been caused by a flaw in the model, where one charging iteration was lost, leading to less energy being calculated than expected from the input data. This issue has been resolved in the current model, but it was not fixed during the PHIL testing. Further testing is needed with the PHIL-testbed.

6.4. User Feedback

When looking at the impact on user convenience of the EV form, the form needs some work. Based on the data, not on all days the EV data was collected correctly when compared to historic data. Furthermore, employees have reported that filling in the form can be tedious every day.

7. Conclusion

How to implement smart charging to shift EV loads, increase the self-use of PV and reduce peak loads, without the use of SOC values and EV load predictions?

The charging controller designed in this research offers a solution to the ever-growing peak power loads due to uncontrolled EV charging. Peak power loads due to uncontrolled EV charging can be reduced by utilizing an online form for EV charging, which collects EV data and can be used as input for an optimization model along with building load and PV power data. Since user-specific information is collected through an online form, SOC values are not necessary for redistributing EV loads more efficiently.

What method of smart charging is best applicable to solve the research problem?

The smart charging method used in this research, optimization modelling, has proven successful for planning and controlling EV charging during a workday. By testing different variations of the optimization model, the performance has improved. Firstly, linear optimization models perform better than bilinear optimization models in terms of computational time. If less powerful hardware is used for running the optimization models, the computational time is potentially longer. Therefore, it may be better to choose the linear optimization model, which has a much lower computational time.

Furthermore, for the linear optimization models, the computational time remained relatively low. Reducing the time resolution allows for running the optimization model more often, reducing the time for new EVs to be detected and building load and PV data to be updated.

Secondly, adding a penalty function to the cost function greatly improves the control performance. This results in the optimization model alternating charging at higher current values compared to without a penalty function. This is preferred since charging at higher current results in higher charging efficiency.

To what extent does the smart charging solution improve energy flexibility, PV self-use and decrease peak loads?

Simulation with the final variant of the optimization model showed the following: on the main simulation days (the 21st of March, 20th of June, and 12th of December), the PPR is significant. If the number of EVs increases at the office in the future, the PPR is potentially even greater. If, in the future, the number of EVs increases at the office, the PPR is potentially even greater. The SS and SC do not increase on the three main simulation days for this case study since the PV production is not changed. However, when simulating for a day with higher PV-generated electricity and a lower building load, an increase in SS and SC is perceived as well. Therefore, it can be concluded that the optimization model allows for peak-shaving and valley-filling.

Furthermore, the optimization model is versatile. By changing the parameters, such as the total charging efficiency, the maximum voltage, power, and current, the model can be used for different EV chargers, both for the level 2 AC chargers used at the office of Kropman and the DC charger on the PHIL-testbed.

7. Conclusion

In conclusion, this research presents a versatile smart charging controller design based on optimization modelling, which successfully redistributes EV loads to allow for peak-shaving and valley-filling.

7.2. Recommendations

Initially, the goal of this research was to test the smart charging controller on the PHIL testbed and implement it at the office. However, due to the complexity of the optimization problem and practical implementation complications, this was not possible. The next step in the research is to run the smart charging controller in real time on the PHIL testbed, which will be conducted as a continuation of this work by another student.

The results of the optimization model can be further improved by supplying the model with more data. For example, the maximum charging current, maximum power draw, and SOC values of the vehicle can be added as input. The maximum current is especially useful, as it allows EVs that support higher charging speeds to charge faster than currently assumed. This increases the flexibility of the EVs, as both long and short charging times are available. Furthermore, it allows for using more power for charging to increase the self-consumption of PV-generated electricity when available. The SOC values are also useful for providing the model with information when an EV is full, for instance when the requested energy content is higher than the remaining empty battery capacity. This can shorten the calculated charging time of an EV, increasing flexibility.

An option for collecting the maximum power draw and charging current is by measuring the power output of uncontrolled charging at the beginning of a charging session. The maximum charging current and power can then be added to the individual EV data as input for the model.

Additionally, post-processing of the output current values is desired. At the moment, current values that are too low are still included in the output values. This can be solved by removing current values that are too low and compensating for them.

Lastly, user behaviour is not taken into consideration in the current model. When a user decides to leave earlier than initially entered in the form, it can occur that the EV has not been charged at all yet. By prioritizing giving each EV a certain percentage of the respective requested amount of energy, the number of occasions where an EV leaves without a charge can be reduced. Furthermore, a solution to reducing the tediousness of filling in the EV charging form for the Kropman employees can be storing the previously entered data. This can potentially reduce the number of inputs to multiple clicks.

References

- Apostolaki-Iosifidou, E., Codani, P., & Kempton, W. (2017). Measurement of power loss during electric vehicle charging and discharging. *Energy*, 127, 730–742.
<https://doi.org/10.1016/J.ENERGY.2017.03.015>
- Bons, P. C., Buatois, A., Lighart, G., Geerts, F., Piersma, N., & van den Hoed, R. (2019). *Impact of Smart Charging for Consumers in a Real World Pilot*. 19–22.
<https://doi.org/10.3390/wevj11010021>
- Bons, P. C., Buatois, A., Schuring, F., Geerts, F., & van den Hoed, R. (2021). Flexible charging of electric vehicles: Results of a large-scale smart charging demonstration. *World Electric Vehicle Journal*, 12(2). <https://doi.org/10.3390/WEVJ12020082>
- Boyd, S. P., & Vandenberghe, L. (2004). *Convex optimization*. Cambridge University Press.
- Chadha, S., Jain, V., & Singh, H. R. (2022). A review on Smart Charging impacts of Electric Vehicles on Grid. *Materials Today: Proceedings*, 63, 751–755.
<https://doi.org/10.1016/J.MATPR.2022.05.122>
- Conrad, K. (2008). *Bilinear forms* (pp. 11–38). <https://doi.org/10.1090/coll/056/02>
- de Bont, K. (2019). *Smart-Charging SG-BEMS Breda*. www.kropman.nl
- De Herdt, L. (2020). *Hardware-in-the-Loop Simulation of Controlled and Uncontrolled EV Charging in a Distribution Grid*. <http://repository.tudelft.nl/>.
- Egerer, J., Gerbaulet, C., & Lorenz, C. (2013). *European Electricity Grid Infrastructure Expansion in a 2050 Context*. <http://www.diw.de/discussionpapers>
- European Commission, & Directorate-General for Mobility and Transport. (2022). *EU transport in figures : statistical pocketbook 2022*. Publications Office of the European Union. <https://data.europa.eu/doi/10.2832/216553>
- European Environment Agency. (2022). *New registrations of electric vehicles in Europe*. <https://www.eea.europa.eu/ims/new-registrations-of-electric-vehicles>
- Fachrizal, R., Shepero, M., van der Meer, D., Munkhammar, J., & Widén, J. (2020). Smart charging of electric vehicles considering photovoltaic power production and electricity consumption: A review. *ETransportation*, 4.
<https://doi.org/10.1016/J.ETRAN.2020.100056>
- Fridgen, G., Thimmel, M., Weibelzahl, M., & Wolf, L. (2021). Smarter charging: Power allocation accounting for travel time of electric vehicle drivers. *Transportation Research Part D: Transport and Environment*, 97.
<https://doi.org/10.1016/j.trd.2021.102916>
- Gschwendtner, C., Sinsel, S. R., & Stephan, A. (2021). Vehicle-to-X (V2X) implementation: An overview of predominate trial configurations and technical, social and regulatory challenges. *Renewable and Sustainable Energy Reviews*, 145.
<https://doi.org/10.1016/J.RSER.2021.110977>

References

- He, Z., Khazaei, J., & Freihaut, J. D. (2022). Optimal integration of Vehicle to Building (V2B) and Building to Vehicle (B2V) technologies for commercial buildings. *Sustainable Energy, Grids and Networks*, 32, 100921.
<https://doi.org/10.1016/J.SEGAN.2022.100921>
- Heilmann, C., & Wozabal, D. (2021). How much smart charging is smart? *Applied Energy*, 291. <https://doi.org/10.1016/J.APENERGY.2021.116813>
- Heredia, W. B., Chaudhari, K., Meintz, A., Jun, M., & Pless, S. (2020). Evaluation of smart charging for electric vehicle-to-building integration: A case study. *Applied Energy*, 266. <https://doi.org/10.1016/J.APENERGY.2020.114803>
- International Renewable Energy Agency, T. (2019). *ELECTRIC-VEHICLE SMART CHARGING INNOVATION LANDSCAPE BRIEF*. www.irena.org
- Kallrath, J. (2009). Modeling difficult optimization problemsModeling Difficult Optimization Problems. In P. M. Floudas Christodoulos A. and Pardalos (Ed.), *Encyclopedia of Optimization* (pp. 2284–2297). Springer US.
https://doi.org/10.1007/978-0-387-74759-0_398
- Kawajir, Y., Laird, C., Vigerske, S., & Wächter, A. (2023). *Ipopt Documentation*.
<https://coin-or.github.io/Ipopt/index.html>
- Lee, Z. J., Chang, D., Jin, C., Lee, G. S., Lee, R., Lee, T., & Low, S. H. (2018). Large-Scale Adaptive Electric Vehicle Charging. *2018 IEEE Global Conference on Signal and Information Processing (GlobalSIP)*, 863–864.
<https://doi.org/10.1109/GlobalSIP.2018.8646472>
- Li, H., Wang, Z., Hong, T., & Piette, M. A. (2021). Energy flexibility of residential buildings: A systematic review of characterization and quantification methods and applications. *Advances in Applied Energy*, 3.
<https://doi.org/10.1016/J.ADAPEN.2021.100054>
- Mangipinto, A., Lombardi, F., Sanvito, F. D., Pavičević, M., Quoilin, S., & Colombo, E. (2022). Impact of mass-scale deployment of electric vehicles and benefits of smart charging across all European countries. *Applied Energy*, 312.
<https://doi.org/10.1016/J.APENERGY.2022.118676>
- Miyazaki, K., Kobayashi, K., Azuma, S., Yamaguchi, N., & Yamashita, Y. (2019). Design and Value Evaluation of Demand Response Based on Model Predictive Control. *IEEE Transactions on Industrial Informatics*, 15(8), 4809–4818.
<https://doi.org/10.1109/TII.2019.2920373>
- Netherlands Enterprise Agency. (2022). *Electric Vehicles Statistics in the Netherlands*.
- Ramos Muñoz, E., & Jabbari, F. (2020). A decentralized, non-iterative smart protocol for workplace charging of battery electric vehicles. *Applied Energy*, 272.
<https://doi.org/10.1016/J.APENERGY.2020.115187>

References

- Reinders, K. J. H. (2022). *Model Predictive Controller for a Battery Energy Storage System to reshape the energy demand curve of an office. Case study: office in the Netherlands.*
- Sadeghian, O., Oshnoei, A., Mohammadi-ivatloo, B., Vahidinasab, V., & Anvari-Moghaddam, A. (2022). A comprehensive review on electric vehicles smart charging: Solutions, strategies, technologies, and challenges. In *Journal of Energy Storage* (Vol. 54). Elsevier Ltd. <https://doi.org/10.1016/j.est.2022.105241>
- Sadeghianpourhamami, N., Refa, N., Strobbe, M., & Develder, C. (2018). Quantitive analysis of electric vehicle flexibility: A data-driven approach. *International Journal of Electrical Power and Energy Systems*, 95, 451–462. <https://doi.org/10.1016/J.IJEPES.2017.09.007>
- Sears, J., Roberts, D., & Glitman, K. (2014). A comparison of electric vehicle Level 1 and Level 2 charging efficiency. *2014 IEEE Conference on Technologies for Sustainability, SusTech 2014*, 255–258. <https://doi.org/10.1109/SUSTECH.2014.7046253>
- Somers, W. (2022). *Forecasting individual and aggregated electric vehicle charging loads at offices with machine learning 7LS2M0-Master project Research B.*
- Spencer, S. I., Fu, Z., Apostolaki-Iosifidou, E., & Lipman, T. E. (2021). Evaluating smart charging strategies using real-world data from optimized plugin electric vehicles. *Transportation Research Part D: Transport and Environment*, 100. <https://doi.org/10.1016/J.TRD.2021.103023>
- Tüzes, K., & van Barlingen, W. (2022). *Dynamic load balancing explained.* <https://blog.evbox.com/dynamic-load-balancing>
- United Nations Framework Convention on Climate Change (UNFCCC). (2016). *THE PARIS AGREEMENT.* https://treaties.un.org/Pages/ViewDetails.aspx?src=TREATY&mtdsg_no=XXVII-7-1
- Van Der Meer, D., Mouli, G. R. C., Mouli, G. M. E., Elizondo, L. R., & Bauer, P. (2018). Energy Management System with PV Power Forecast to Optimally Charge EVs at the Workplace. *IEEE Transactions on Industrial Informatics*, 14(1), 311–320. <https://doi.org/10.1109/TII.2016.2634624>
- Wang, G. C., Ratnam, E., Haghi, H. V., & Kleissl, J. (2019). Corrective receding horizon EV charge scheduling using short-term solar forecasting. *Renewable Energy*, 130, 1146–1158. <https://doi.org/10.1016/j.renene.2018.08.056>
- Wei, H., Zhang, Y., Wang, Y., Hua, W., Jing, R., & Zhou, Y. (2022). Planning integrated energy systems coupling V2G as a flexible storage. *Energy*, 239, 122215. <https://doi.org/10.1016/J.ENERGY.2021.122215>

Appendices

A. Appendix A: Simulation scenario test data

Table A.1: Simulation EV data for 10 EVs

ChargerId	E_requested	T_arrival	T_departure
0	40.83	21/03/2022 07:30	21/03/2022 15:15
2	36	21/03/2022 07:45	21/03/2022 14:15
0	46.74	21/03/2022 07:45	21/03/2022 14:30
2	16.41	21/03/2022 07:45	21/03/2022 13:00
3	10.92	21/03/2022 07:45	21/03/2022 16:30
0	19.81	21/03/2022 07:45	21/03/2022 13:00
0	46.82	21/03/2022 07:45	21/03/2022 16:00
0	20.63	21/03/2022 08:00	21/03/2022 17:00
0	53.67	21/03/2022 08:00	21/03/2022 16:45
3	39.03	21/03/2022 08:30	21/03/2022 16:45

Table A.2: Simulation EV data for 20 EVs

ChargerId	E_requested	T_arrival	T_departure
0	33.0723	21/03/2022 07:30	21/03/2022 15:15
2	46.5345	21/03/2022 07:30	21/03/2022 17:00
2	29.8404	21/03/2022 07:30	21/03/2022 17:00
1	27.6372	21/03/2022 07:45	21/03/2022 13:45
0	37.8594	21/03/2022 07:45	21/03/2022 14:30
0	25.1748	21/03/2022 07:45	21/03/2022 17:00
2	28.1799	21/03/2022 07:45	21/03/2022 15:15
2	29.16	21/03/2022 07:45	21/03/2022 14:15
0	37.9242	21/03/2022 07:45	21/03/2022 16:00
0	16.0461	21/03/2022 07:45	21/03/2022 13:00
3	8.8452	21/03/2022 07:45	21/03/2022 16:30
2	13.2921	21/03/2022 07:45	21/03/2022 13:00
0	43.4727	21/03/2022 08:00	21/03/2022 16:45
0	16.7103	21/03/2022 08:00	21/03/2022 17:00
3	31.6143	21/03/2022 08:30	21/03/2022 16:45
0	45.5787	21/03/2022 08:30	21/03/2022 16:45
1	29.808	21/03/2022 11:00	21/03/2022 16:00
0	28.3986	21/03/2022 11:00	21/03/2022 16:30
0	22.113	21/03/2022 11:00	21/03/2022 16:30
0	25.1829	21/03/2022 12:15	21/03/2022 16:45

B. Appendix B: Control performance

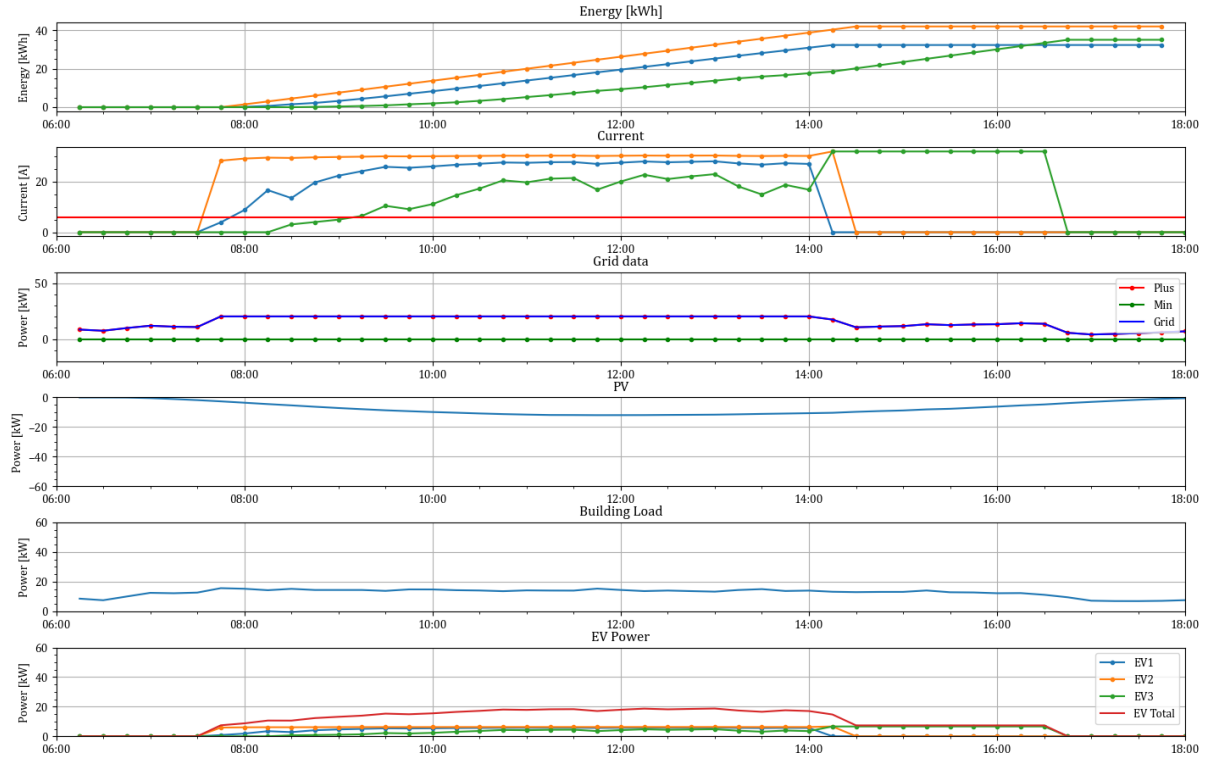


Figure B.1: EV data on March 21st for bi-linear_15min optimization model

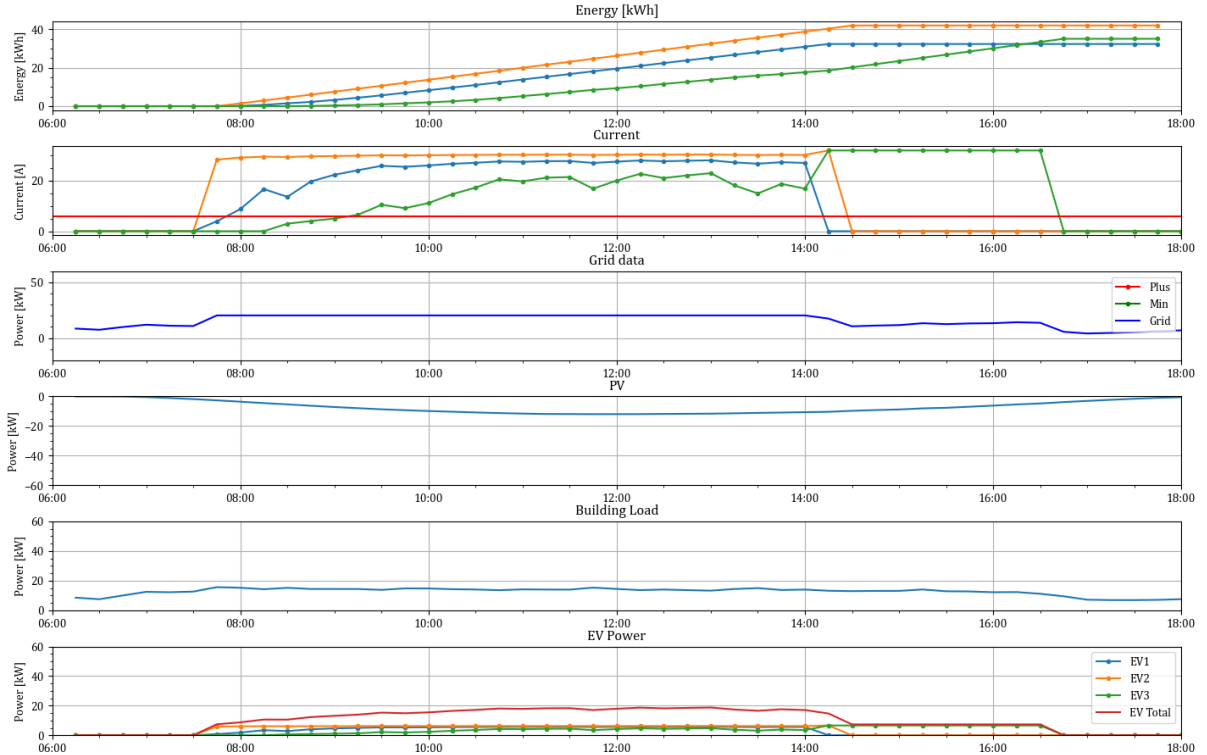


Figure B.2: EV data on March 21st for linear_15min optimization model

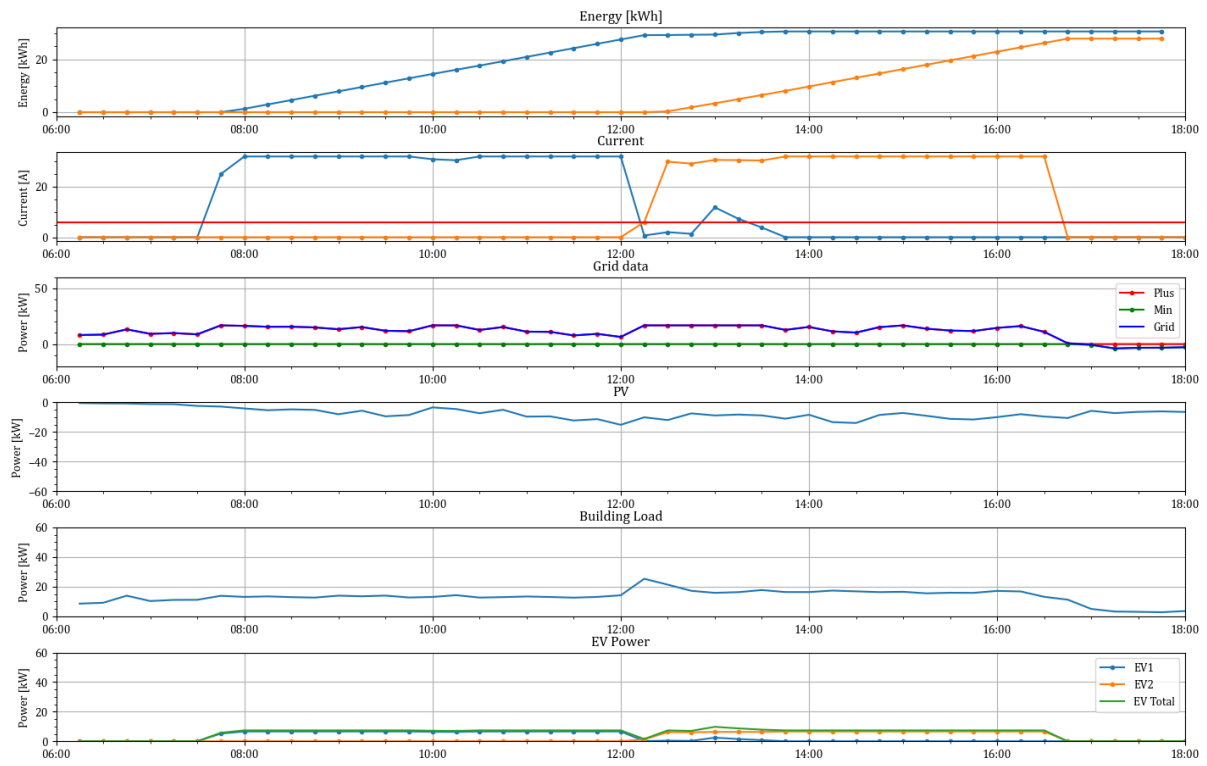


Figure B.3: EV data on June 20th for bi-linear_15min optimization model

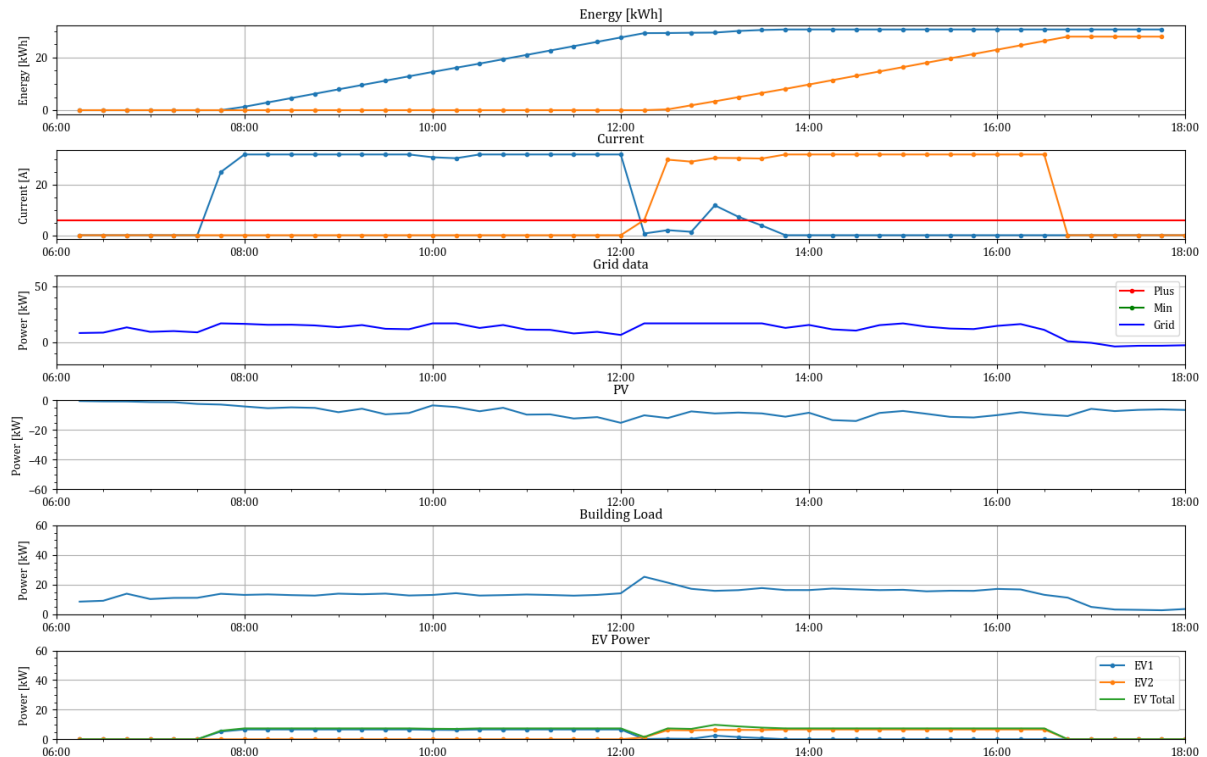


Figure B.4: EV data on June 20th for linear_15min optimization model

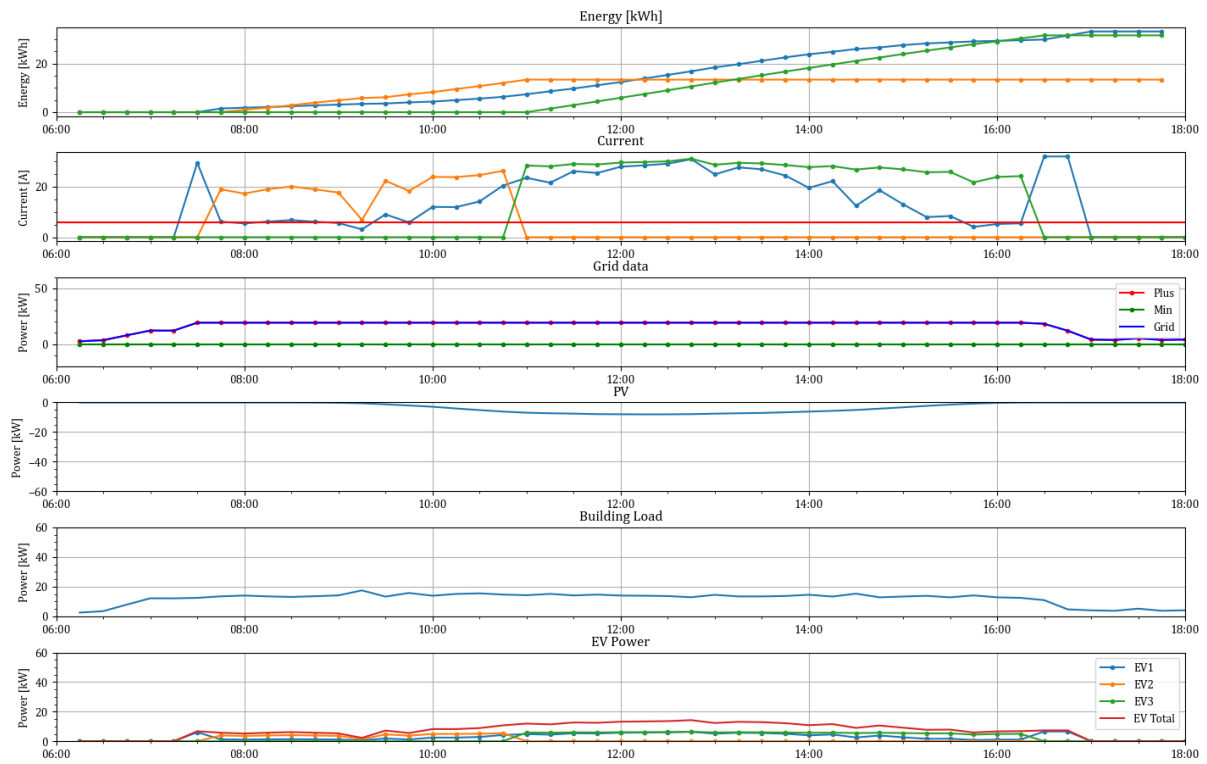


Figure B.5: EV data on December 12th for bi-linear_15min optimization model

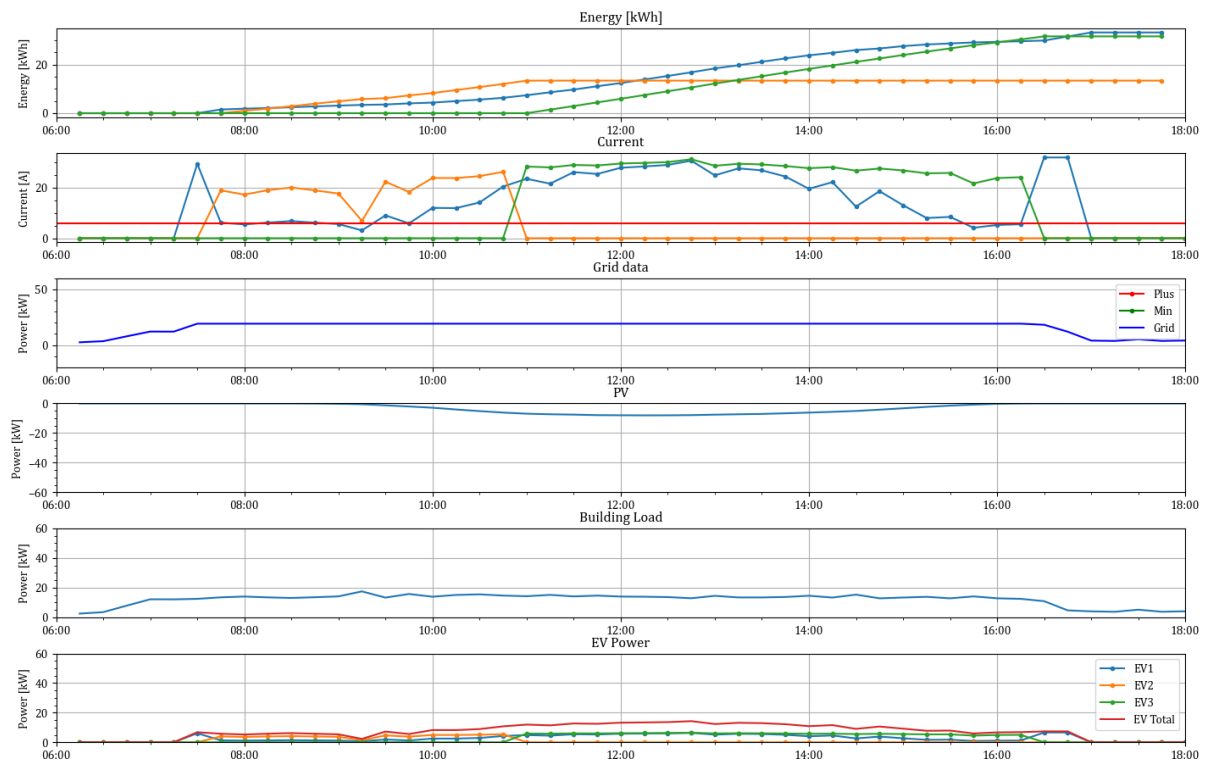


Figure B.6: EV data on December 12th for linear_15min optimization model

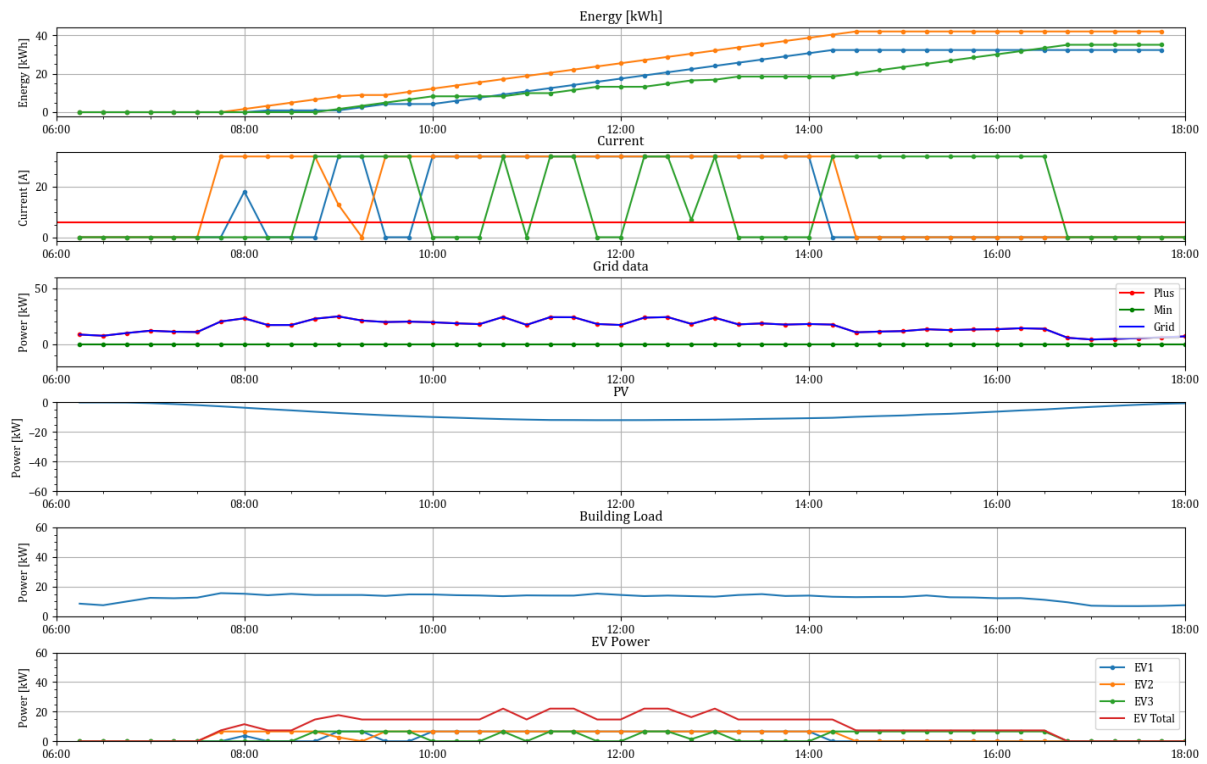


Figure B.7: EV data on March 21st for bi-linear_penalty_15min optimization model

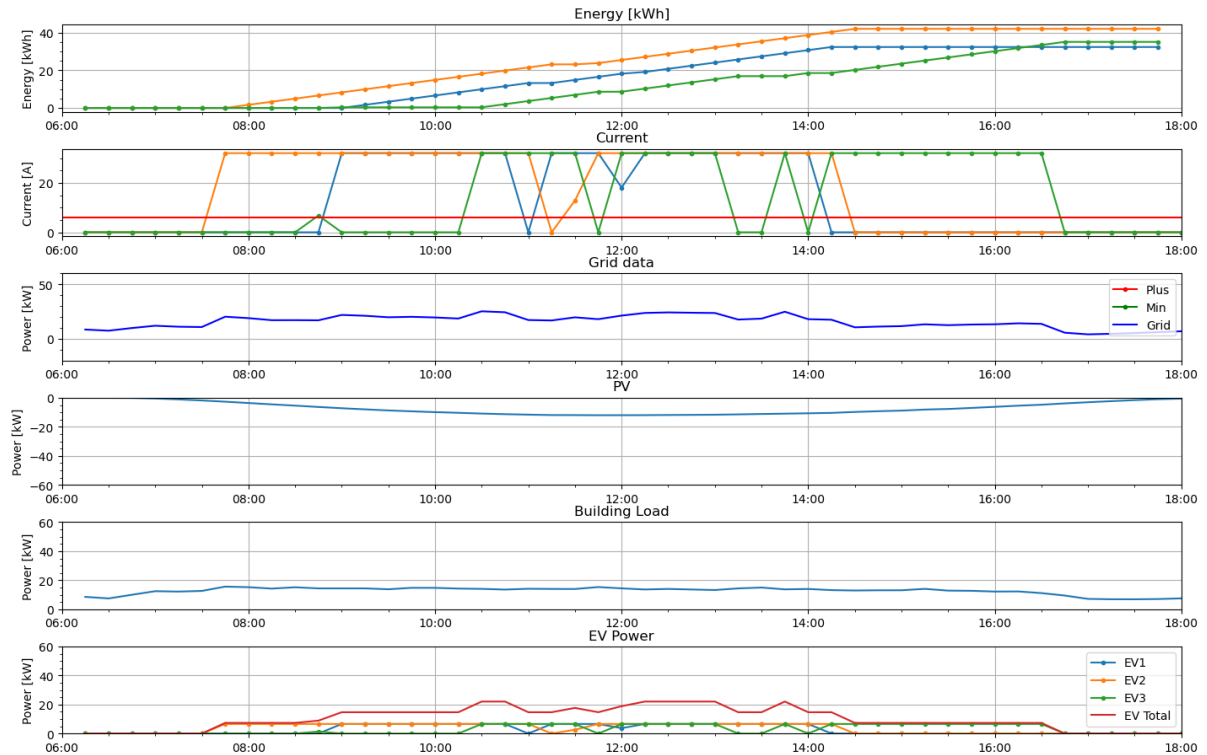


Figure B.8: EV data on March 21st for linear_penalty_15min optimization model

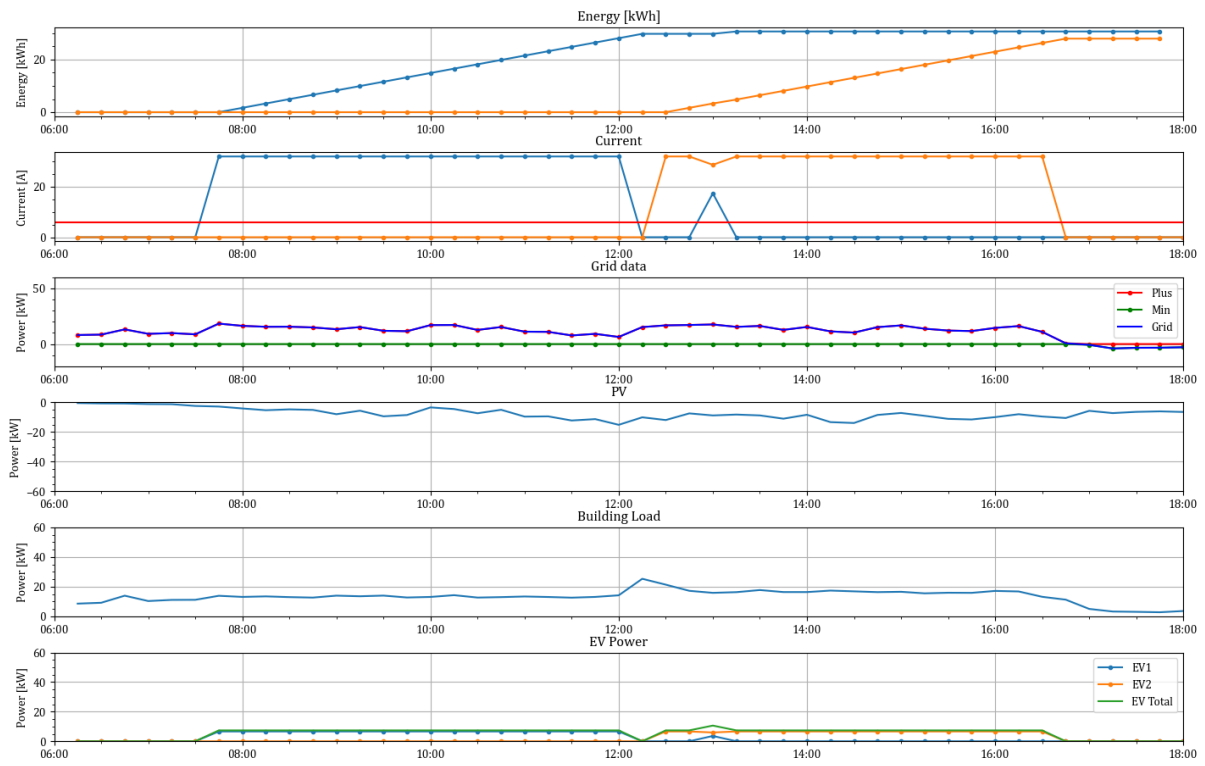


Figure B.9: EV data on June 20th for bi-linear_penalty_15min optimization model

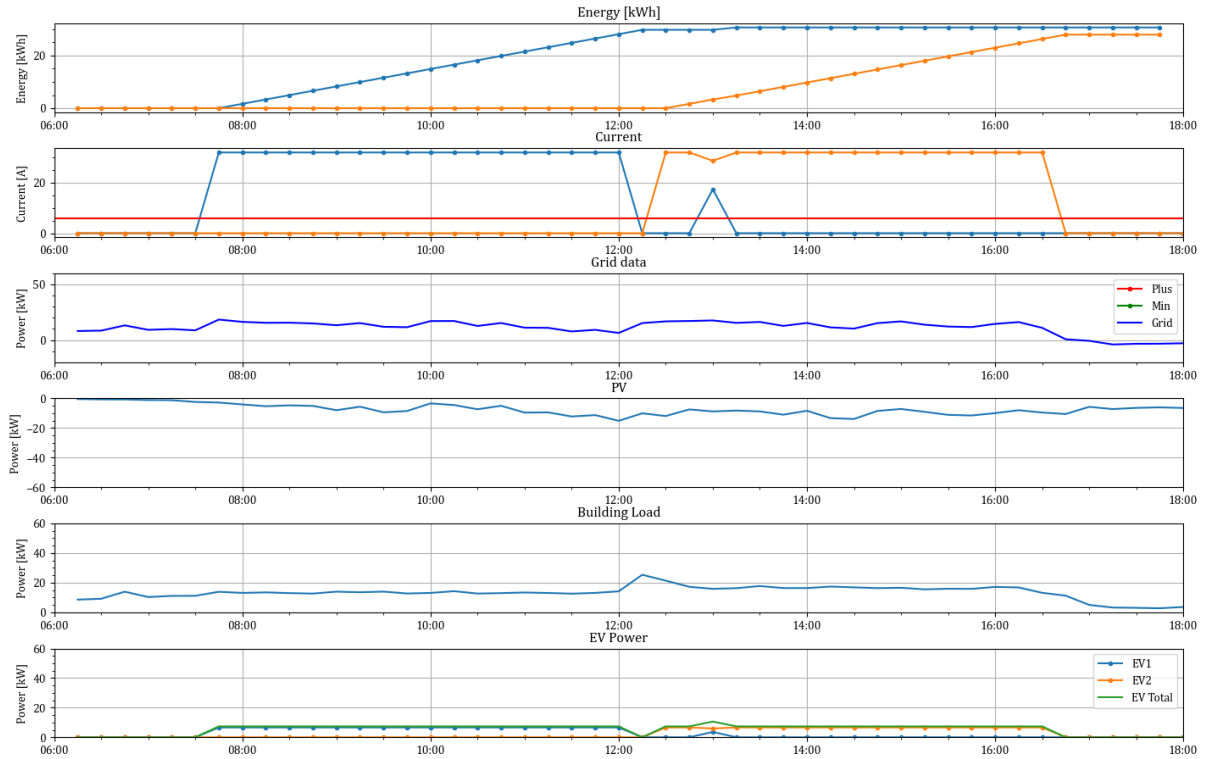


Figure B.10: EV data on June 20th for linear_penalty_15min optimization model

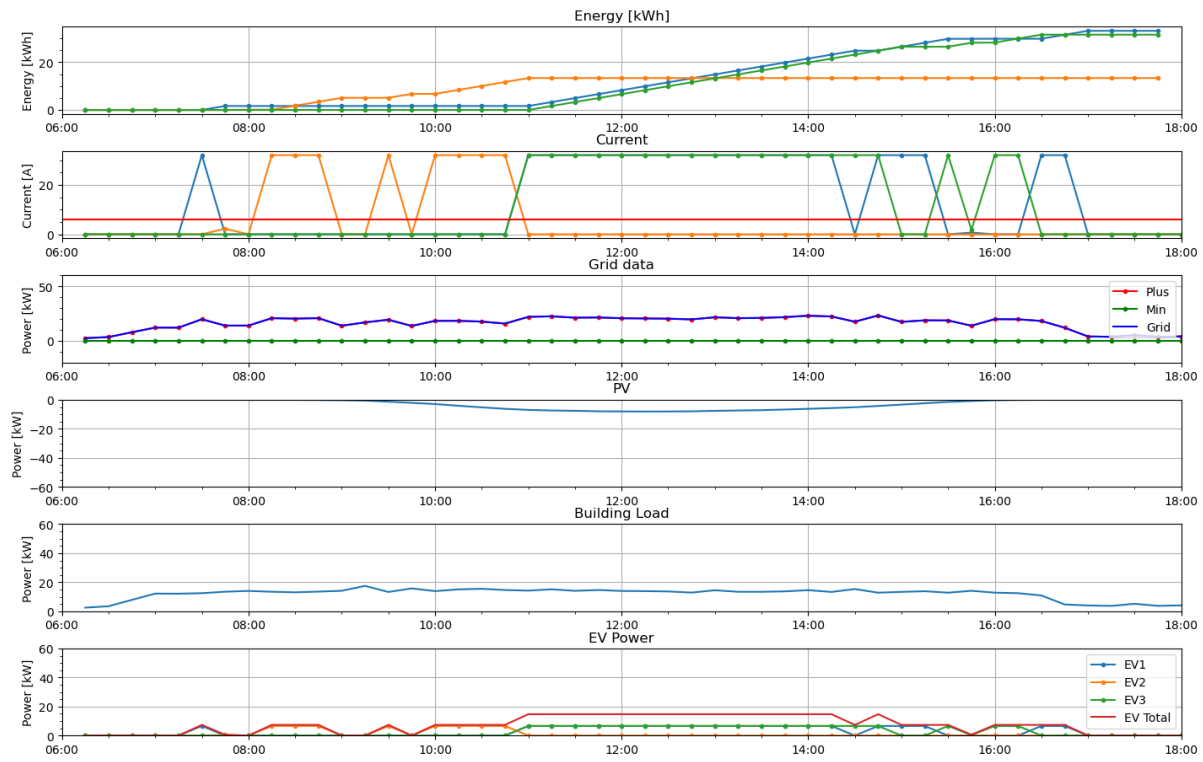


Figure B.11: EV data on December 12th for bi-linear_penalty_15min optimization model

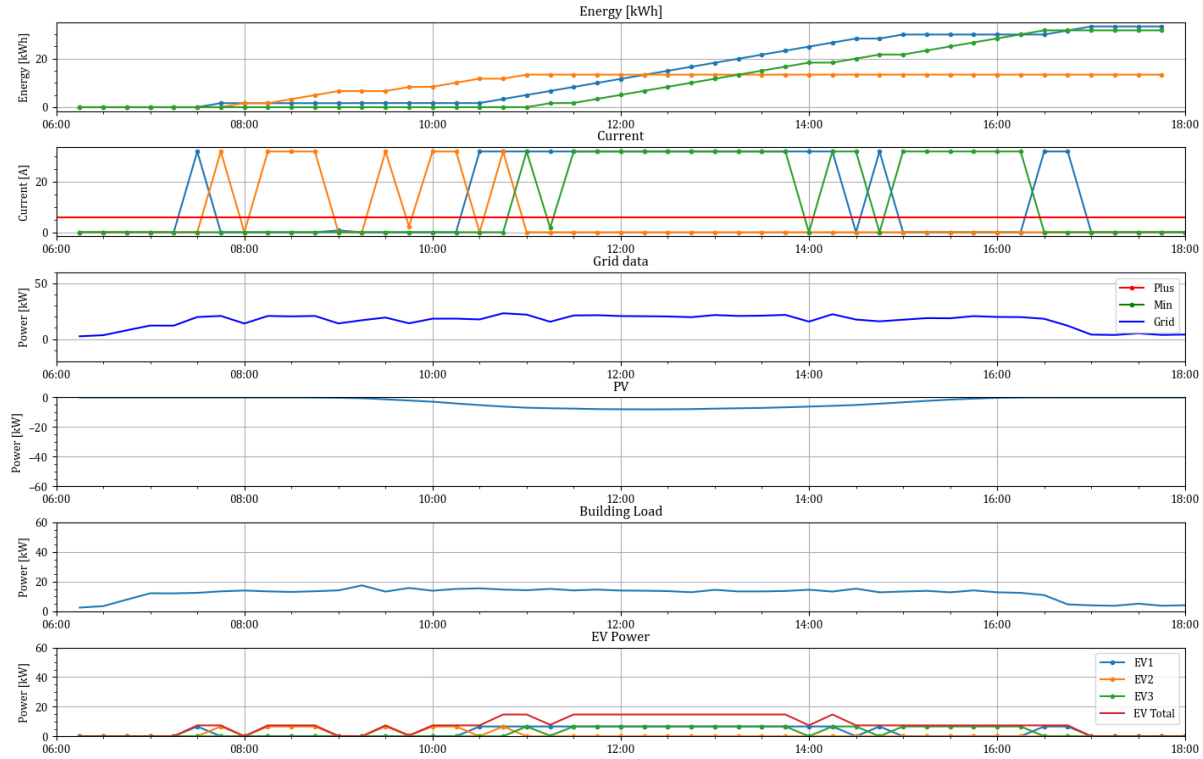


Figure B.12: EV data on December 12th for linear_penalty_15min optimization model

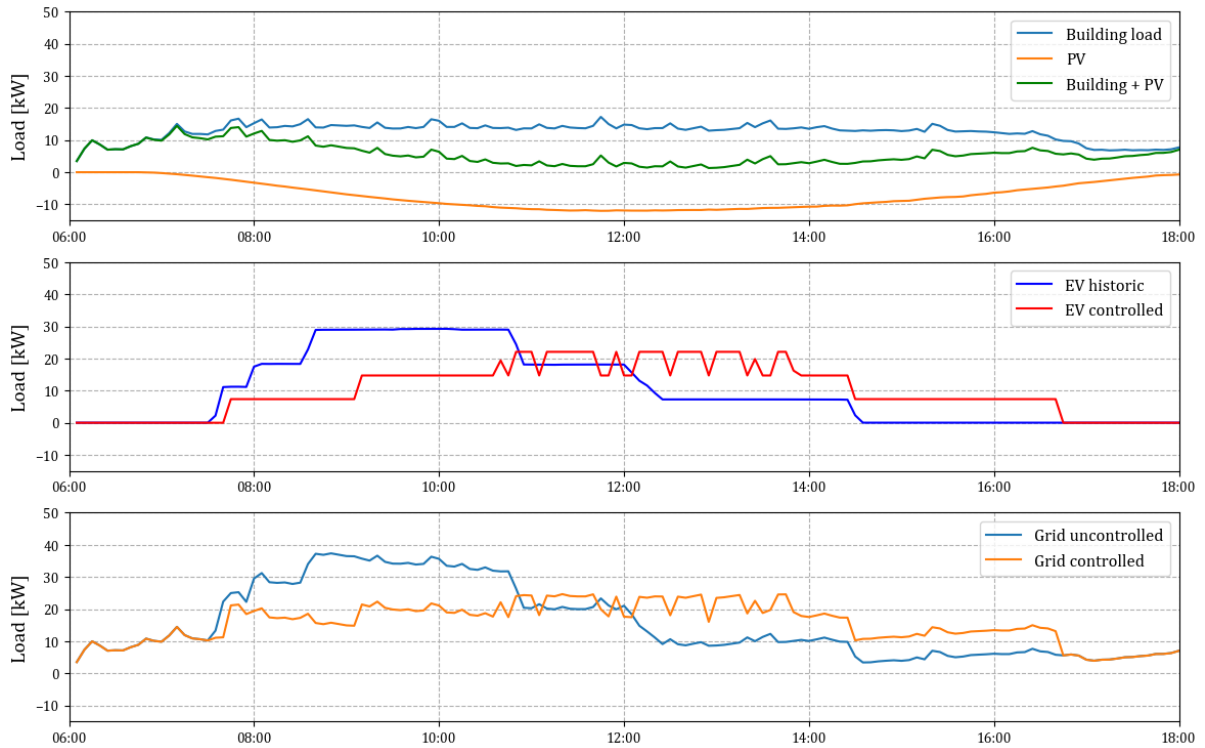


Figure B.13: EV data on March 21st for bi-linear_penalty_5min optimization model

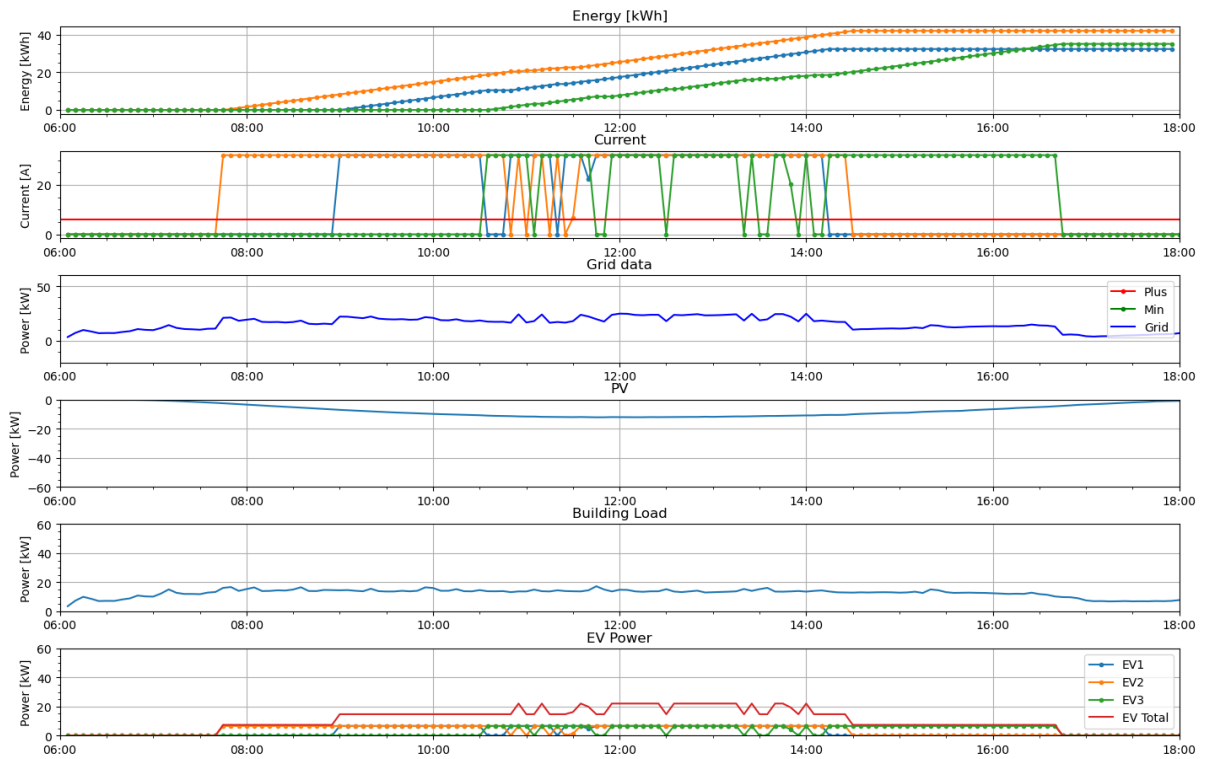


Figure B.14: EV data on March 21st for linear_penalty_5min optimization model

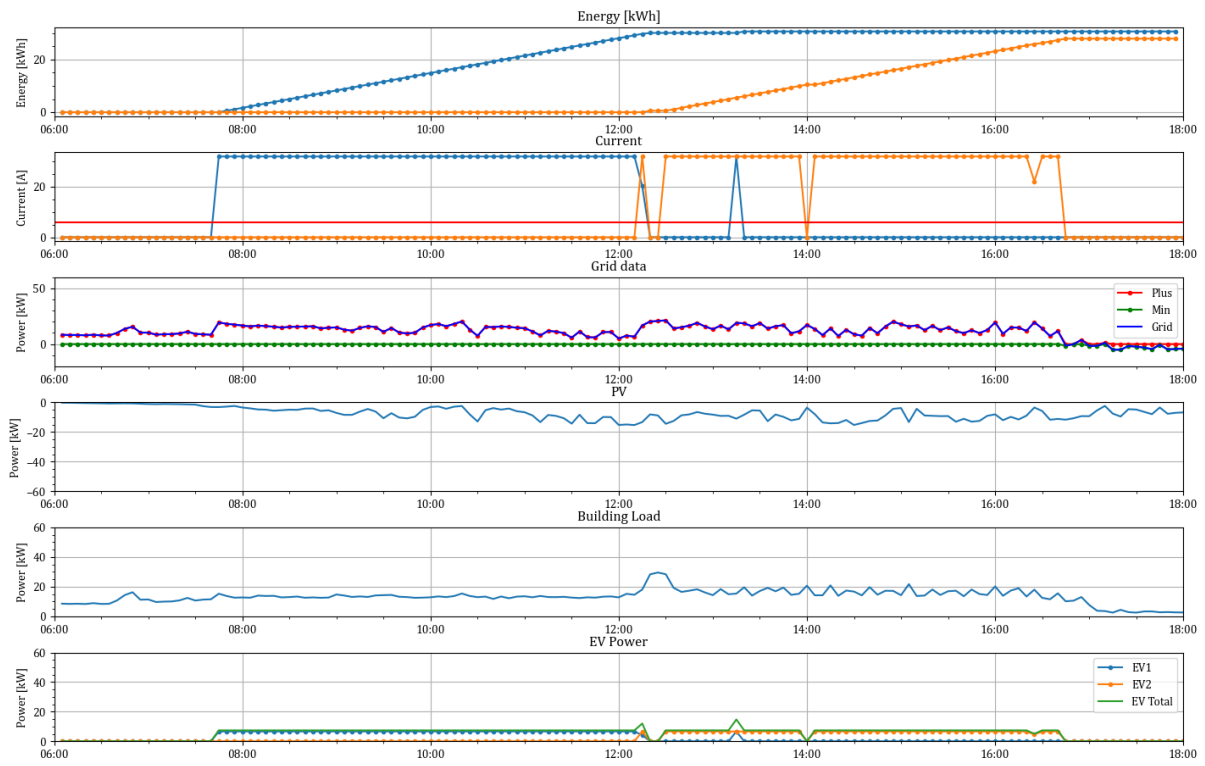


Figure B.15: EV data on June 20th for bi-linear_penalty_5min optimization model

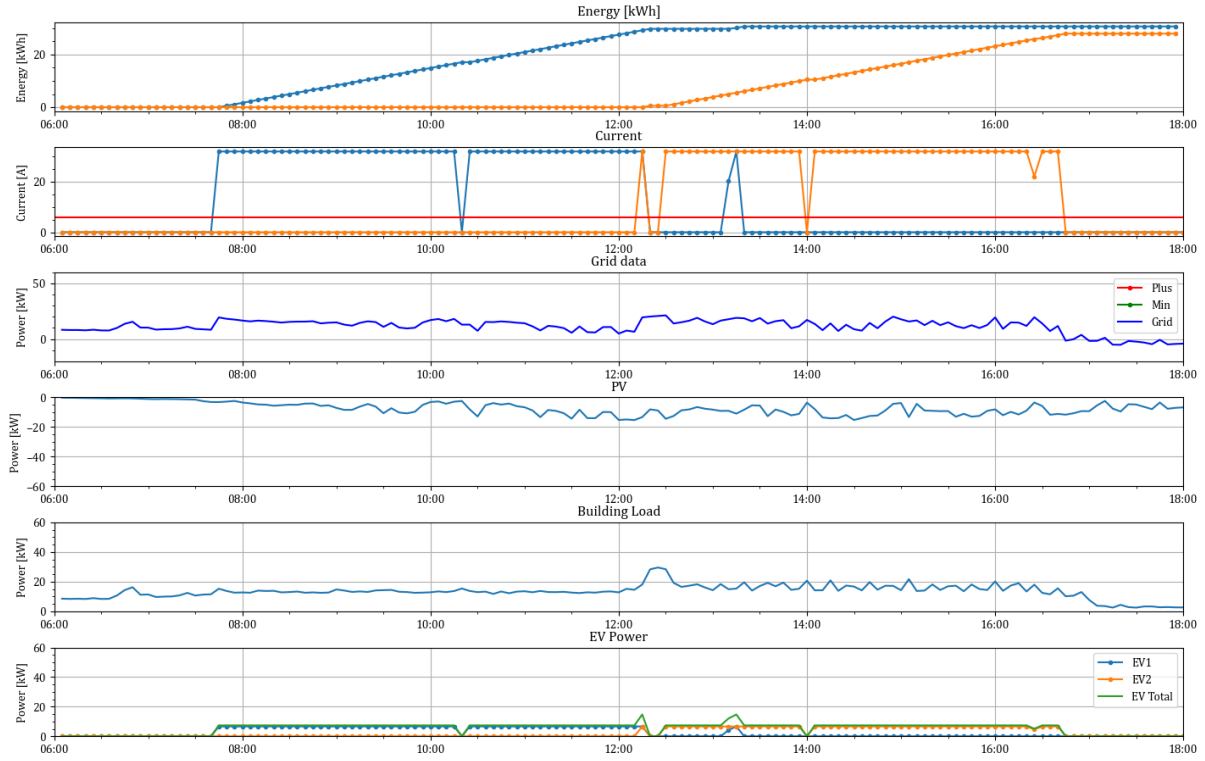


Figure B.16: EV data on June 20th for bi-linear_penalty_5min optimization model

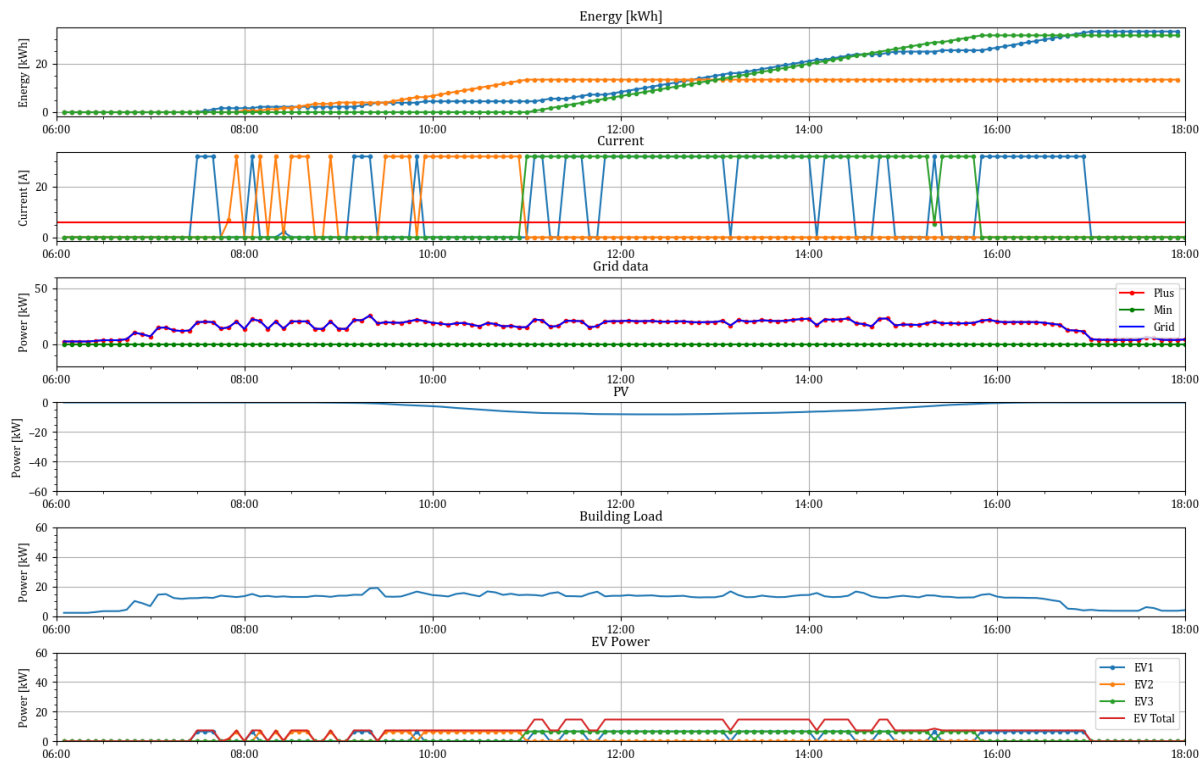


Figure B.17: EV data on December 12th for bi-linear_penalty_5min optimization model

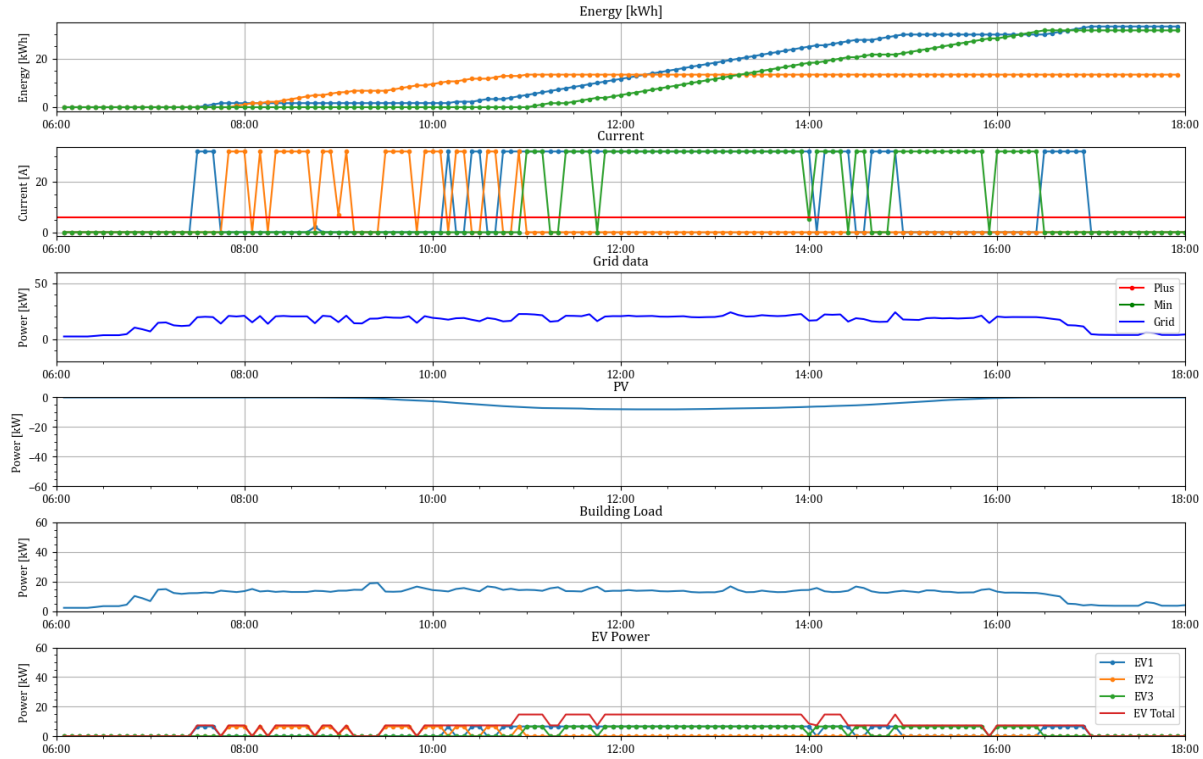


Figure B.18: EV data on December 12th for linear_penalty_15min optimization model

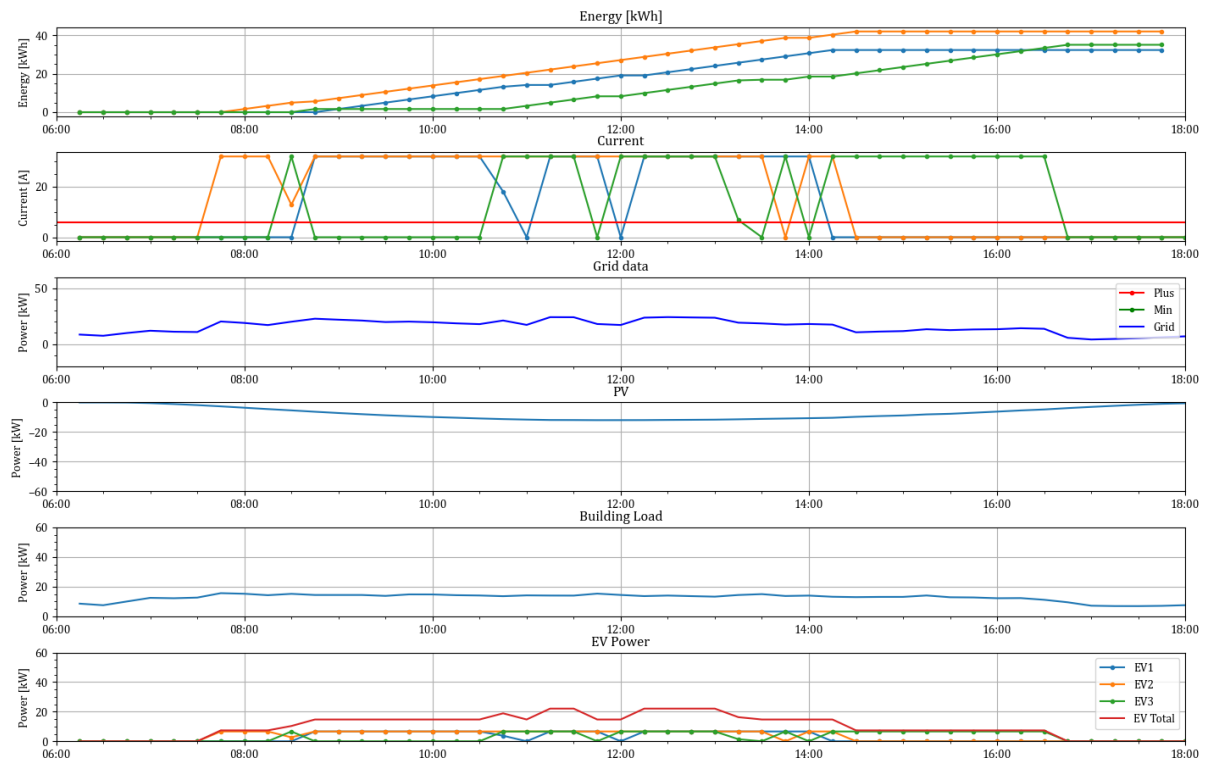


Figure B.19: EV data on March 21st for linear_penalty_15min_0.4 optimization model

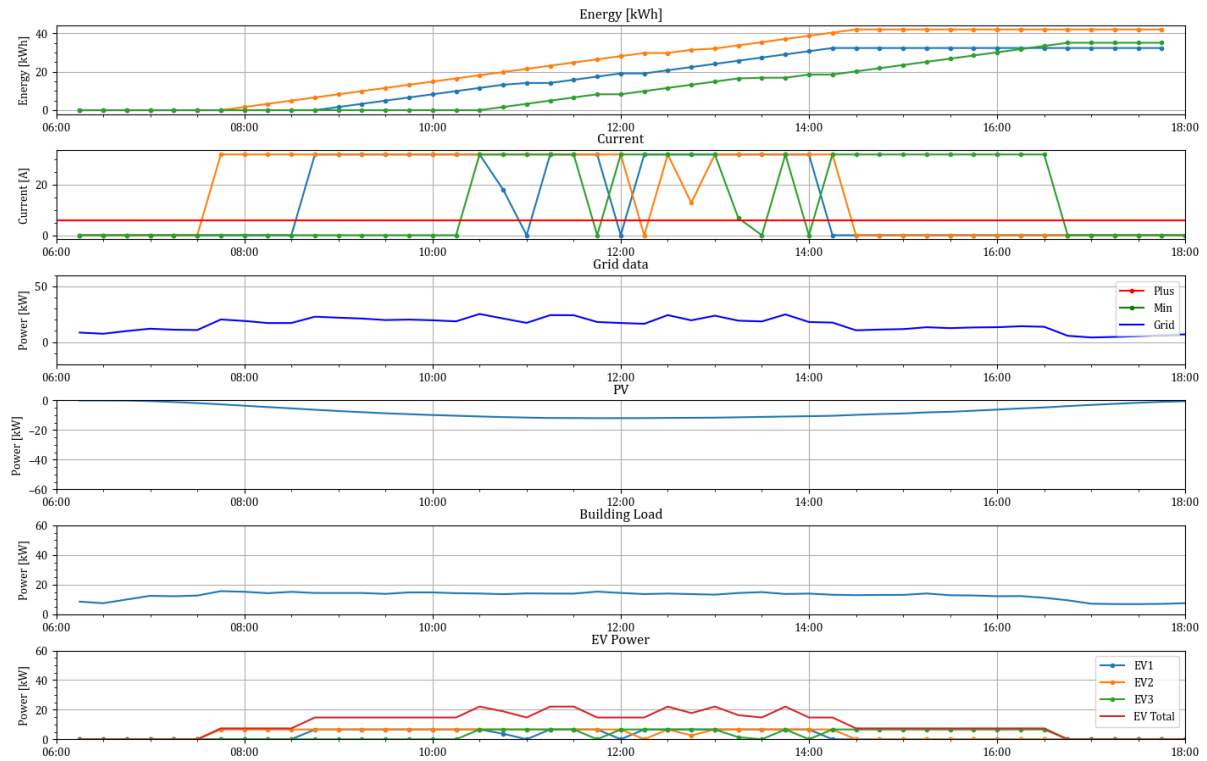


Figure B.20: EV data on March 21st for linear_penalty_15min_0.6 optimization model

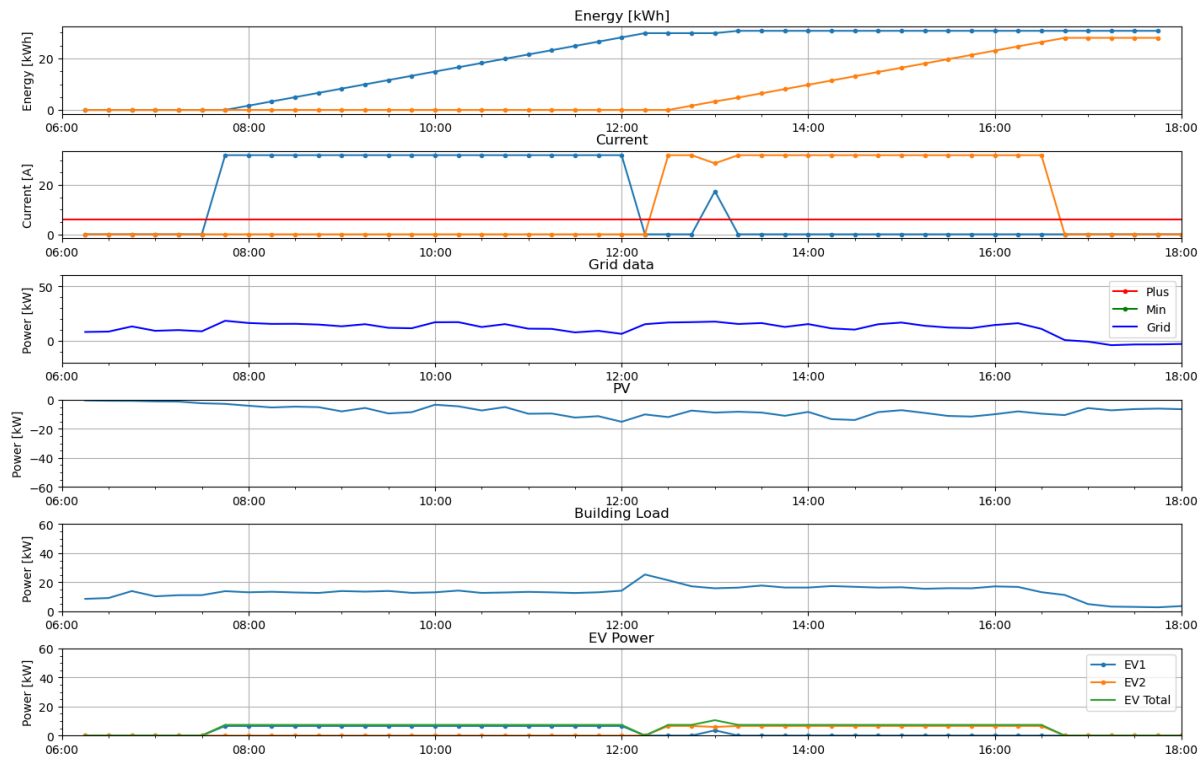


Figure B.21: EV data on June 20th for linear_penalty_15min_0.4 optimization model

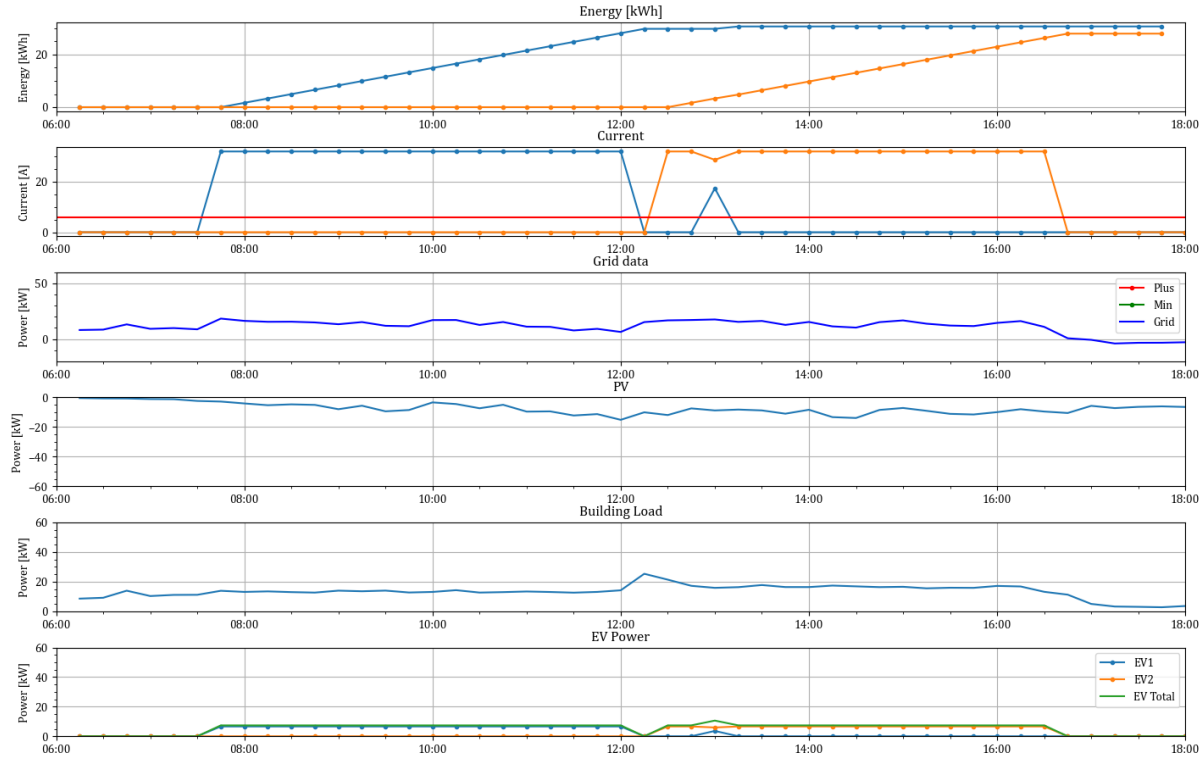


Figure B.22: EV data on June 20th for linear_penalty_15min_0.6 optimization model

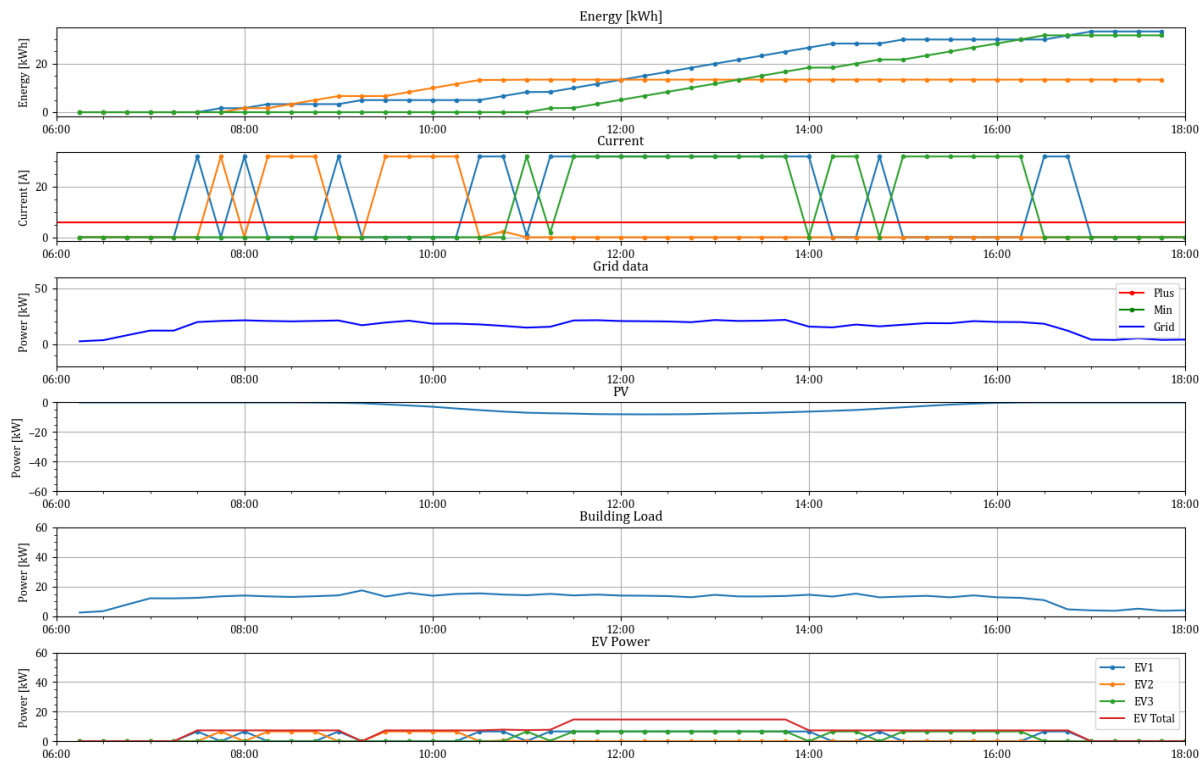


Figure B.23: EV data on December 12th for linear_penalty_15min_0.4 optimization model

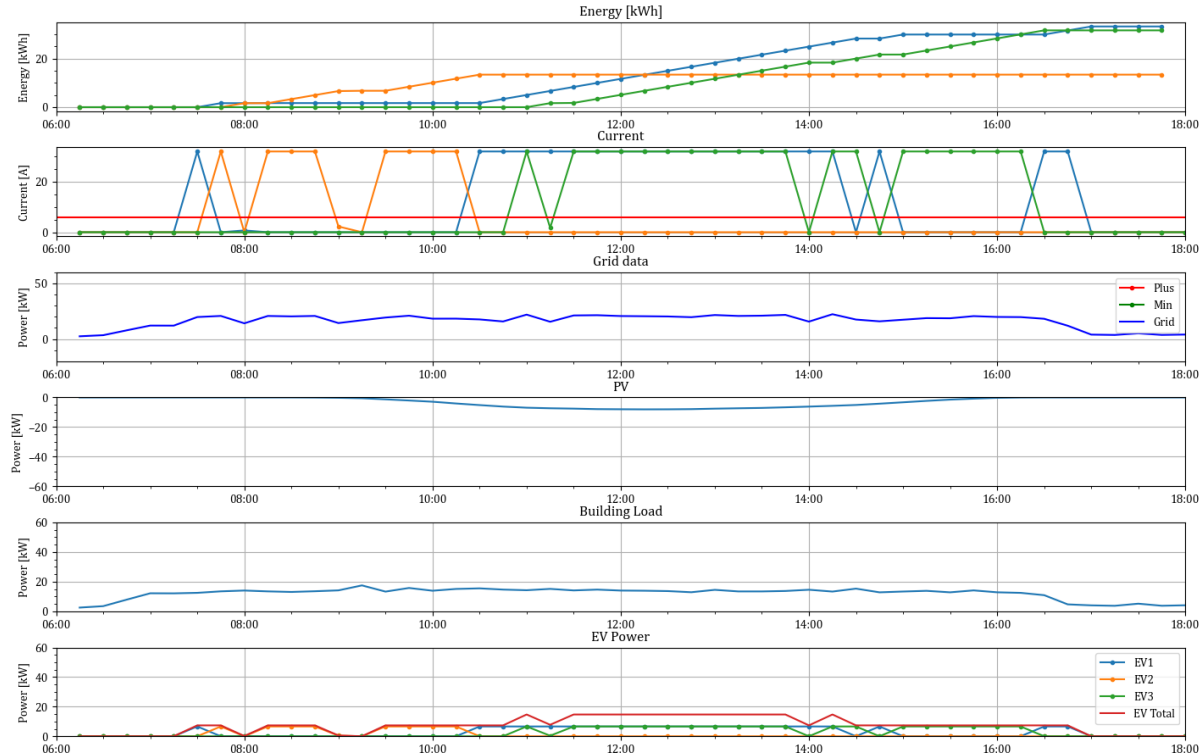


Figure B.24: EV data on December 12th for linear_penalty_15min_0.6 optimization model

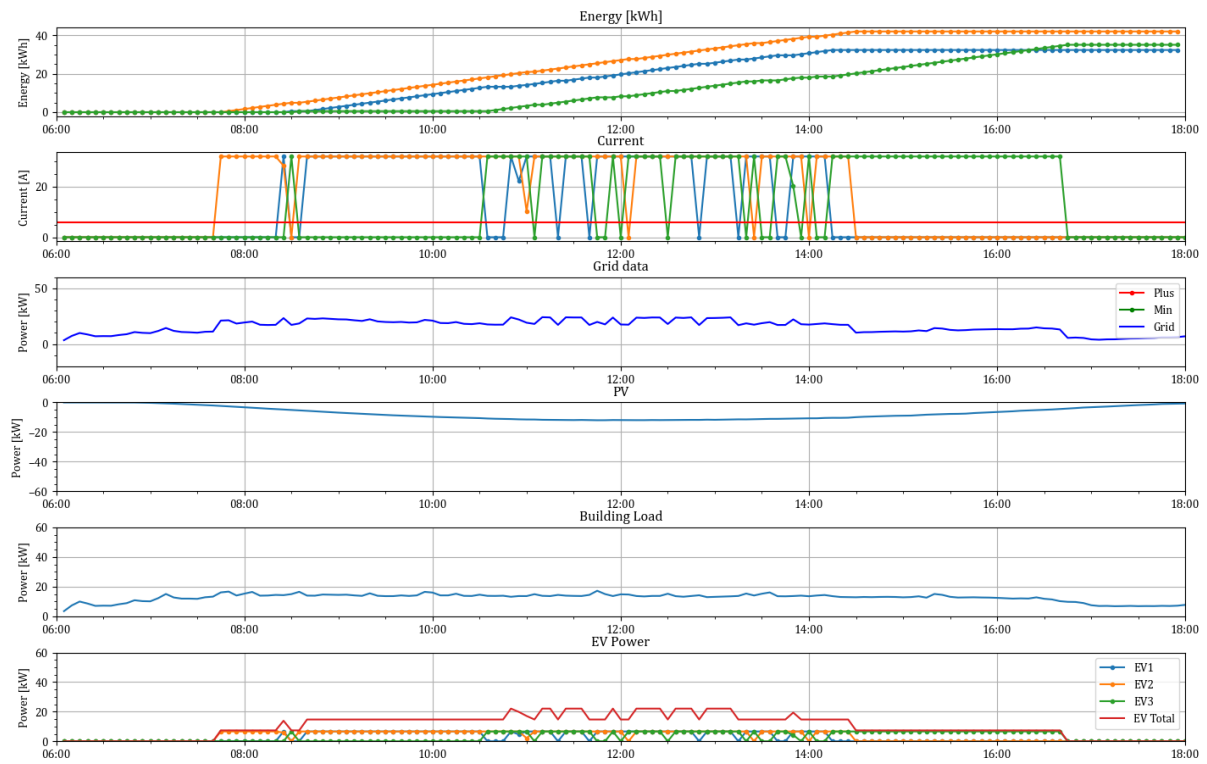


Figure B.25: EV data on March 21st for linear_penalty_5min_0.4 optimization model

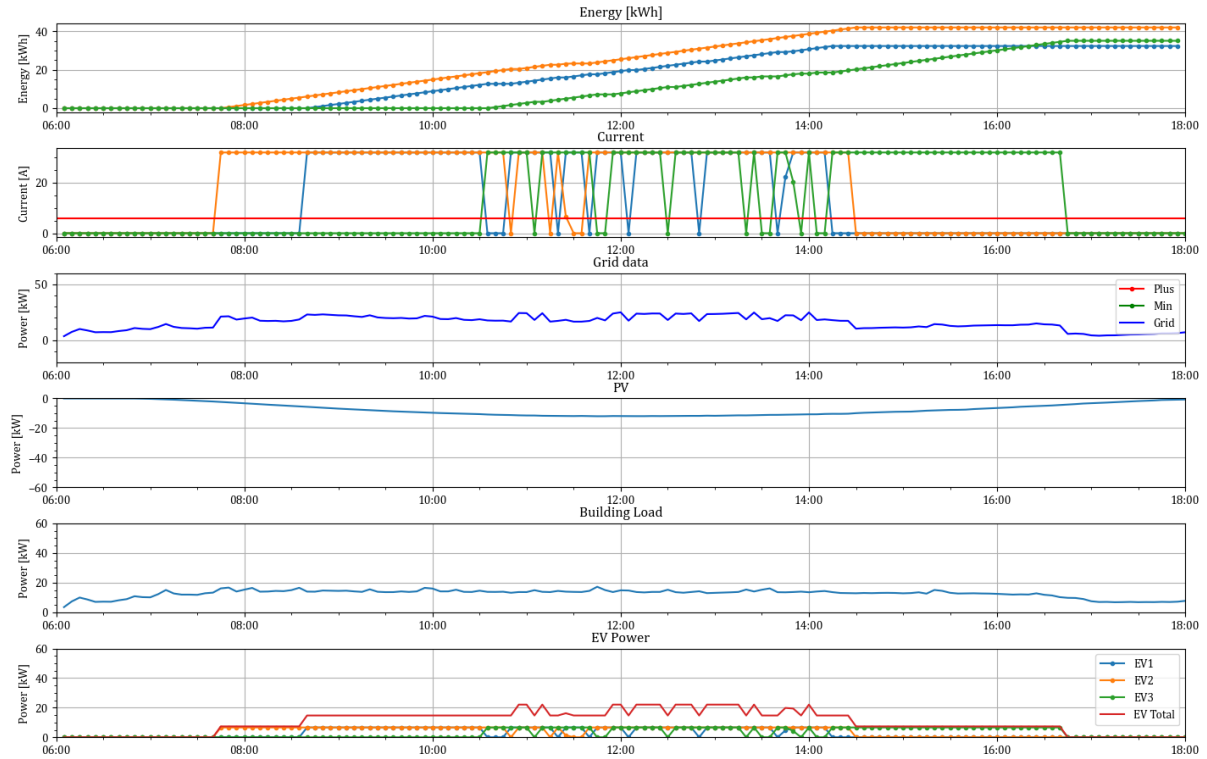


Figure B.26: EV data on March 21st for linear_penalty_5min_0.6 optimization model

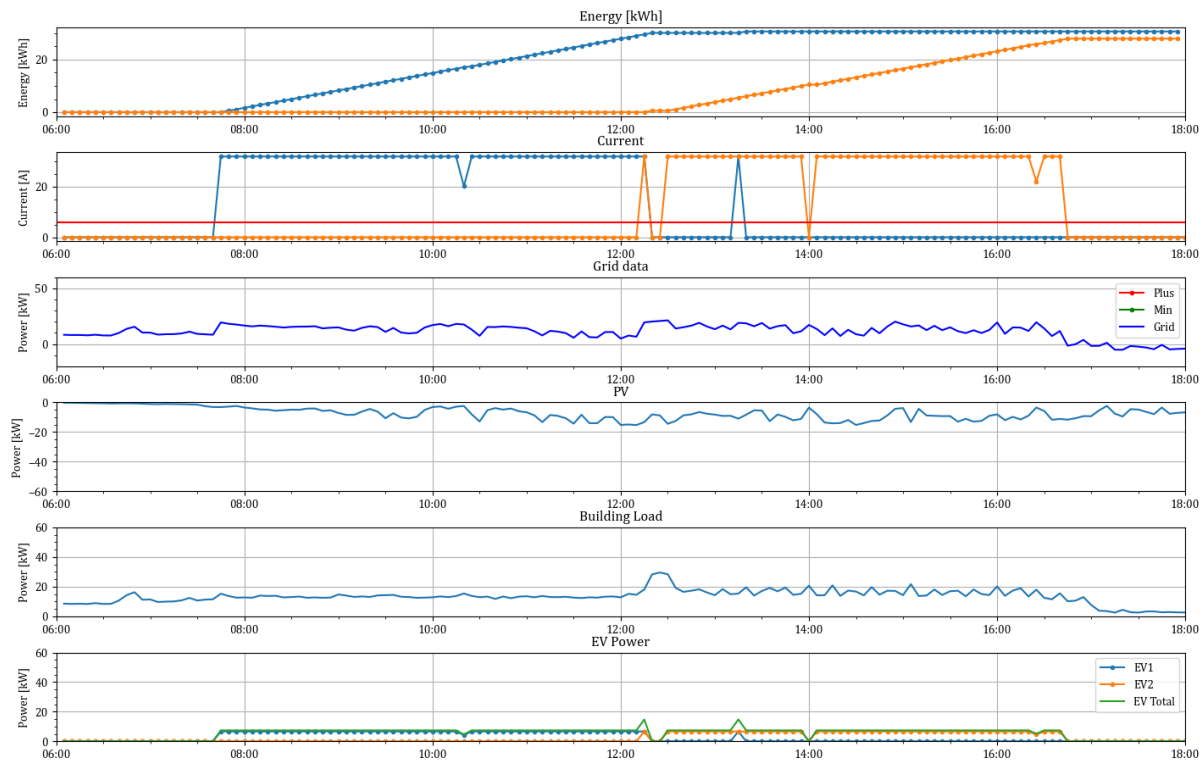


Figure B.27: EV data on June 20th for bi-linear_penalty_5min_0.4 optimization model

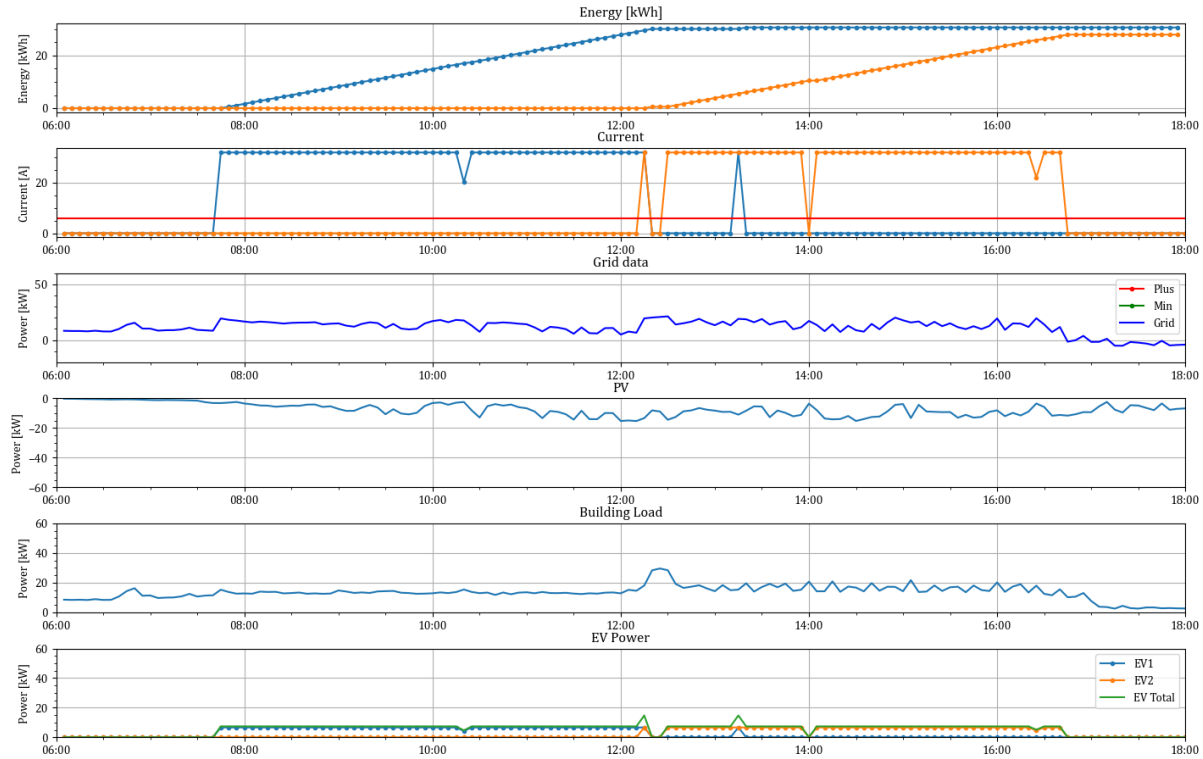


Figure B.28: EV data on March 21st for linear_penalty_5min_0.6 optimization model

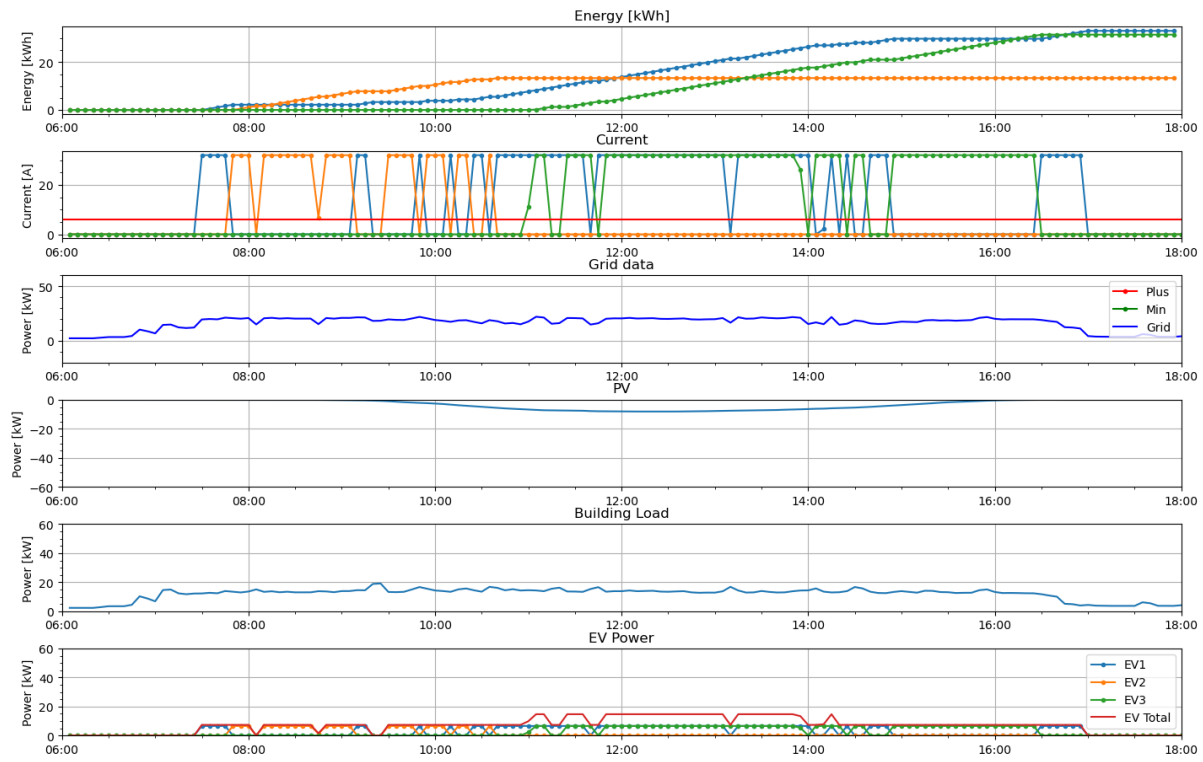


Figure B.29: EV data on December 12th for linear_penalty_5min_0.4 optimization model

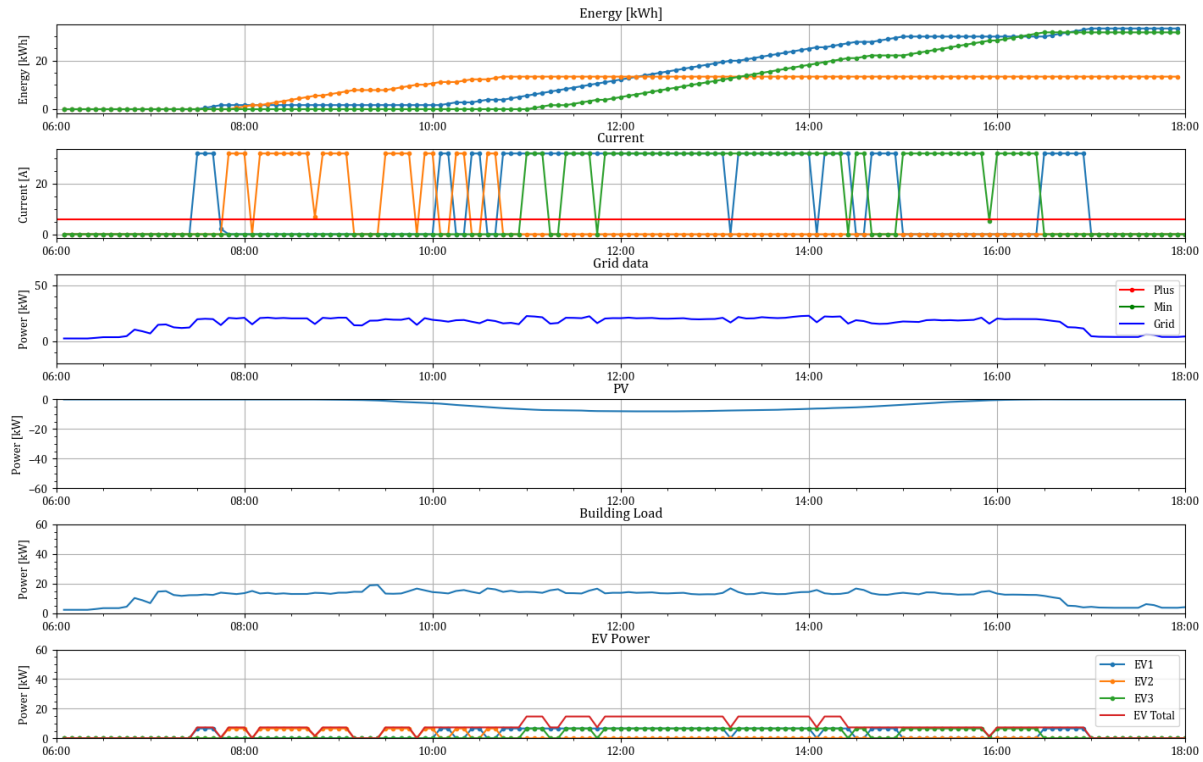


Figure B.30: EV data on December 12th for linear_penalty_5min_0.6 optimization model